MODELING, CONTROL AND TECHNO-ECONOMIC ANALYSIS OF KARABUK UNIVERSITY MICROGRID

Nuri Almargani ALI ALMAGRAHI

2020
PhD THESIS
ELECTRICAL-ELECTRONICS ENGINEERING

Thesis Advisor
Assoc. Prof. Dr. Ziyodulla YUSUPOV

MODELING, CONTROL AND TECHNO-ECONOMIC ANALYSIS OF KARABUK UNIVERSITY MICROGRID

Nuri Almargani Ali ALMAGRAHI

T.C
Karabuk University
Institute of Graduate Programs
Department of Electrical-Electronics Engineering
Prepared as PhD Thesis

Thesis Advisor
Assoc. Prof. Dr. Ziyodulla YUSUPOV

KARABUK
April 2020

I certify that in my opinion the thesis submitted by Nuri Almargrani Ali ALMAGRAHI titled "MODELING, CONTROL AND TECHNO-ECONOMIC ANALYSIS OF KARABUK UNIVERSITY MICROGRID" is fully adequate in scope and in quality as a thesis for the degree of PhD.

Assoc. Prof. Dr. Ziyodulla YUSUPOV .....
Thesis Advisor, Department of Electrical-Electronics Engineering

This thesis is accepted by the examining committee with a unanimous vote in the Department of Electrical-Electronics Engineering as a PhD thesis. April 29, 2020

Examining Committee Members (Institutions)	Signature
Chairman : Prof. Dr. Necmi S. TEZEL (KBU)	.....
Member : Assoc. Prof. Dr. Ziyodulla YUSUPOV (KBU)	.....
Member : Assoc. Prof. Dr. Selami SAĞIROĞLU (KBU)	.....
Member : Assoc. Prof. Dr. Metin VARAN (SUBU)	.....
Member : Assist. Prof. Dr. Adem DALCALI (BANU)	.....

The degree of PhD by the thesis submitted is approved by the Administrative Board of the Institute of Graduate Programs, Karabuk University.

Prof. Dr. Hasan SOLMAZ .....
Director of the Institute of Graduate Programs

"I declare that all the information within this thesis has been gathered and presented in accordance with academic regulations and ethical principles and I have according to the requirements of these regulations and principles cited all those which do not originate in this work as well."

Nuri Almargrani Ali ALMAGRAHI

ABSTRACT

Ph.D. Thesis

MODELING, CONTROL AND TECHNO-ECONOMIC ANALYSIS OF KARABUK UNIVERSITY MICROGRID

Nuri Almargani Ali ALMAGRAHI

Karabuk University
Institute of Graduate Programs
Department of Electrical-Electronics Engineering

Thesis Advisor:
Assoc. Prof. Dr. Ziyodulla YUSUPOV
April 2020, 168 pages

Microgrid defines as collection of distributed energy resources and loads that operates as single system by providing power and heat. In last decades, the developing of power electronic is to provide the flexibility operation of power system integrated with microsources as a single aggregated system.

Variety sources of distributed generation and loads are a reason of high nonlinearities, changing dynamics, and uncertainties. For example, some renewable energy sources such as solar PV and wind turbines work under unpredictable environmental conditions and turbulent. To solve these issues, it requires to develop intelligent control strategies, and thereby to increase reliability and performance of power systems. And thus, microgrids performance strongly depend on the applied control strategies. Therefore, collaboration of microgrid and electric grid are required to provide reliability, security and stable operation of the power system. Based on these

considerations, in this work, the modeling and simulation of Karabuk university microgrid are developed, considered operation in both grid-connected and island modes. Microgrid control system is designed and developed to ensure the power balance between distributed energy sources and loads along with continues energy supply during fault conditions. Fault control of microgrid system is executed. The fault control and optimal power flow control has been implemented in the microgrid system to effectively manage the energy in the system.

Techno-economic and environmental analyses are executed using HOMER Grid software tool to evaluate the effectiveness of microgrid application at Karabuk university campus.

Key Words : Microgrid, distributed energy resources, optimization, fault control.
Science Code : 90502

ÖZET

Doktora Tezi

KARABÜK ÜNİVERSİTESİ MİKRO ŞEBEKESİNİN MODELLENMESİ, KONTROLÜ VE TEKNO-EKONOMİK ANALİZİ

Nuri Almargani Ali ALMAGRAHI

Karabük Üniversitesi
Lisansüstü Eğitim Enstitüsü
Elektrik-Elektronik Mühendisliği Anabilim Dalı

Tez Danışmanı:
Doç. Dr. Ziyodulla YUSUPOV
Nisan 2020, 168 sayfa

Mikro şebeke, güç ve ısı sağlayarak tek bir sistem olarak çalışan dağıtılmış enerji kaynaklarının ve yüklerin toplanması olarak tanımlanmıştır. Son yıllarda güç elektroniğinin geliştirilmesi, güç sisteminin yenilenebilir enerji kaynaklarla esnek bir şekilde tek bir toplu sistem olarak çalışmasını sağlamaktadır.

Dağıtılmış üretim ve yüklerin çeşitli kaynakları, yüksek doğrusalsızlıkların, değişen dinamiklerin ve belirsizliklerin bir nedenidir. Örneğin, güneş PV ve rüzgâr türbinleri gibi bazı yenilenebilir enerji kaynakları, öngörülemeyen çevre koşulları ve türbülans altında çalışır. Bu sorunları çözmek için akıllı kontrol stratejileri geliştirmek ve böylece güç sistemlerinin güvenilirliğini ve performansını arttırmak gerekir. Mikro şebekelerin performansı büyük ölçüde uygulanan kontrol stratejilerine bağlıdır. Bu nedenle, güç sisteminin dayanaklığını, güvenliğini ve istikrarlı çalışmasını sağlamak için mikro şebeke ve elektrik şebekesinin uygun çalışması gerekmektedir. Bu

düşüncelere dayanarak, bu çalışmada hem şebekeye bağlı hem de özerk tarzda çalışan Karabük Üniversitesi mikro şebekesinin modellenmesi ve simülasyonu geliştirilmiştir. Microgrid kontrol sistemi, dağıtılmış enerji kaynakları ve yükler arasındaki güç dengesini sağlamak ve arıza koşullarında devam eden enerji tedarikini sağlamak için tasarlanmış ve geliştirilmiştir. Mikro şebeke sisteminin arıza kontrolü yapılmıştır. Arıza kontrolü ve optimum güç akışı kontrolü, sistemdeki enerjiyi etkin bir şekilde yönetmek için mikro şebeke sistemine uygulanmıştır.

Karabük Üniversitesi'nde mikro şebeke uygulamasının etkinliğini değerlendirmek için HOMER Grid yazılımını kullanılarak teknolojik-ekonomik ve çevresel analizler yapılmıştır.

Anahtar Kelimeler : Mikro şebeke, dağıtılmış enerji kaynakları, optimizasyon, arıza kontrolü.

Bilim Kodu : 90502

ACKNOWLEDGMENT

After sincerely thanking Allah for all blessings and bounties.

First, I express to give thanks to my advisor, Assoc. Prof. Dr. Ziyodulla YUSUPOV, for his guidance and assistance in preparation of my dissertation thesis.

I would like also to acknowledge the assistance of many people who provided help, support, and encouragement, enabling me to complete my Ph.D. dissertation. In particular, I would like to extend my thanks to the Prof. Dr. Necmi Serkan TEZEL and Assoc. Prof. Dr. Selami SAĞIROĞLU for their support.

I wish to express my love to my wife, and my children for their love, support and encouragement.

I also would like to thank all my friends and colleagues who helped me in many other ways. I will not forget the special help and financial support provided to me by my government (Libya), which made it possible for me, and gave me the best chance, to attend this Ph.D. education program to equip me to be able to contribute the development of my country.

CONTENTS

Page

APPROVAL ii
ABSTRACT iv
ÖZET vi
ACKNOWLEDGMENT viii
CONTENTS ix
LIST OF FIGURES xiii
LIST OF TABLES xvi
SYMBOLS AND ABBREVITIONS INDEX xvii

PART 1 1
INTRODUCTION 1
1.1. PROBLEM STATEMENT AND MOTIVATION OF THE THESIS 2
1.2. RESEARCH OBJECTIVES 3
1.3. METHODOLOGY 4
1.4. LITERATURE REVIEW 6

PART 2 12
MICROGRIDS ARCHITECTURE 12
2.2. MICROGRID OPERATION MODES 16
2.3. MICROGRID TYPES 19
2.3.1. DC Microgrid 20
2.3.2. AC Microgrid 22
2.3.2.1. Line-Frequency AC Microgrid 24
2.3.2.2. High-Frequency AC Microgrid 25
2.3.3. Hybrid Microgrid 26
2.4. STANDARDS FOR MICROGRIDS 27
2.4.1. 1547 Series of Standards 30

Page

PART 3 35
CONTROL STRATEGIES OF MICROGRID 35
3.1. PRIMARY CONTROL 37
3.1.1. Grid-feeding Controls 38
3.1.2. Grid-forming Control 39
3.1.2.1. Control Methods With Communication Link 40
3.1.2.2. Control Methods Without Communication Link 41
3.2. SECONDARY CONTROL 47
3.2.1. Centralized Control 48
3.2.2. Decentralized Control 51
3.2.2.1. Distributed Secondary Control 53
3.2.2.2. Decentralized Secondary Control 56
3.3. TERTIARY CONTROL 56
3.3.1. Centralized Tertiary Control 57
3.3.2. Distributed Tertiary Control 58

PART 4 59
MICROGRID MODELING AND DYNAMICS 59
4.1. STUDIED SYSTEM CHARACTERISTICS 60
4.2. CONNECTION MODELING BETWEEN THE MAIN GRID AND THE KBU MICROGRID 66
4.2.1. Modeling of the Medium Voltage Transmission Lines 66
4.2.2. Modeling of Medium Voltage Transmission Lines 68
4.2.3. Passive Load Modeling 69
4.2.4. Modeling of Relevant Buses 70
4.2.5. Grid Bus 71
4.2.6. MV Bus 72
4.3. GRID-CONNECTED KBU MICROGRID 73
4.3.1. Microgrid Bus 73
4.3.2. Overall Microgrid Architecture 74
4.4. KBU MICROGRID ARCHITECTURE IN ISLANDED MODE 75
4.5. MODELING OF KBU MICROGRID COMPONENTS 76

Page

4.5.1. Modeling a Diesel Generator 77
4.5.2. PV Panels 82
4.5.3. Modeling MPPT with Boost Converter 85
4.5.4. Modeling of battery storage system 88
4.5.5. Modeling Voltage Source Inverter 90
4.5.6. Static Transfer Switch 91

PART 5 93
LOAD SHARING AND FAULT CONTROL OF MICROGRID SYSTEM 93
5.1. INTRODUCTION 93
5.2. MODELING AND SIMULATION OF KBU MICROGRID 94
5.3. MATLAB SIMULATIONS OF KBU MICROGRID 96
5.4. SIMULATION RESULTS AND DISCUSSION 100

PART 6 114
TECHNO-ECONOMIC ANALYSIS OF MICROGRID IMPACT TO KARABUK UNIVERSITY CAMPUS 114
6.1. INTRODUCTION 114
6.2. METHODOLOGY OF TECHNO-ECONOMIC ASSESSMENT 115
6.3. LOAD PROFILES 117
6.3.1. Critical and Non-critical Loads Profile 118
6.3.2. PV -System and Diesel Generator Load Profiles 120
6.3.3. Solar Resource 121
6.4. OPTIMIZATION ANALYSIS 122
6.5. SENSITIVITY ANALYSIS 125
6.6. DEMAND RESPONSE 126
6.7. SIMULATION RESULTS AND DISCUSSION 127

PART 7 134
CONCLUSION AND FUTURE WORKS 134
7.1. GENERAL CONCLUSIONS 134
7.2. SPECIFIC CONTRIBUTIONS OF THE THESIS 135

Page

7.3. RECOMMENDATION FOR FUTURE WORKS 137

REFERENCES 138

APPENDIX A. TECHNICAL SPECIFICATIONS OF KBU SUBSTATION AND DISTRIBUTION CENTER TRANSFORMERS 153

APPENDIX B. TECHNICAL CHARACTERISTICS OF PV SYSTEM, BATTERY AND DIESEL GENERATOR 155

APPENDIX C. LOAD PROFILE OF ENGINEERING FACULTY 159

APPENDIX D. CRITICAL LOADS OF ENGINEERING FACULTY 162

APPENDIX E. UTILITY MONTHLY SUMMARY COMPARISON 164

APPENDIX F. PUBLISHED PAPERS 166

RESUME 168

LIST OF FIGURES

Page

Figure 1.1. Methodology flow chart of the thesis. 5
Figure 2.1. Typical Microgrid structure 15
Figure 2.2. Power exchange between distribution network and MG. 17
Figure 2.3. Schematic diagram of Microgrid. 18
Figure 2.4. MG interconnection with a distribution network. 19
Figure 2.5. Classification of MGs based on operational frequency. 20
Figure 2.6. DC Microgrid system 21
Figure 2.7. DC Microgrid system 23
Figure 2.8. Typical structure of LFAC MG. 24
Figure 2.9. Typical schematic chart of HFAC MG. 26
Figure 2.10. Topology of Hybrid MG. 27
Figure 2.11. Common standards used for a general MG architecture 29
Figure 2.12. IEC 61850 Standard Structure. 31
Figure 3.1. Control strategies of MG and their main functions. 36
Figure 3.2. Classification of MG control strategies. 37
Figure 3.3. Equivalent circuit of connection between VSC and AC bus. 44
Figure 3.4. Conventional droop method. 45
Figure 3.5. Small-signal model (conventional active power control) 45
Figure 3.6. The principle behind the secondary control strategy in MGs 47
Figure 3.7. Centralized secondary control structure 50
Figure 3.8. Decentralized secondary control structure. 52
Figure 3.9. Distributed secondary control of MG 55
Figure 3.10. Structure of tertiary control in MGs. 57
Figure 4.1. Engineering faculty in Demir Celik Campus of Karabuk University. .. 60
Figure 4.2. Electric power supply diagram of Karabuk University. 63
Figure 4.3. Microgrid single line diagram of KBU Engineering faculty. 64
Figure 4.4. Overall structure of KBU MG in grid-connected mode. 65
Figure 4.5. One phase model of MV transmission line. 67
Figure 4.6. Block diagram of the MV transmission line. 67

Page

Figure 4.7. Single block representation of MV transmission line. 67
Figure 4.8. Block diagram of three-phase transformer. 68
Figure 4.9. Single block of transformer. 68
Figure 4.10. Model of voltage receptor load. 69
Figure 4.11. Model of current receptor load. 70
Figure 4.12. Single-line diagram of grid bus. 71
Figure 4.13. Block diagram of grid bus. 72
Figure 4.14. The single line diagram of MV bus. 72
Figure 4.15. The block diagram of MV bus. 73
Figure 4.16. Coupling MV bus. 74
Figure 4.17. Overall Microgrid architecture. 74
Figure 4.18. The overall model of KBU MG in islanded mode. 76
Figure 4.19. The model of a conventional diesel engine synchronous generator system. 77
Figure 4.20. Synchronous machine *abc* stationary frame and *0dq* rotating frame association. 78
Figure 4.21. Electrical model of a generator in the *abc* frame. 79
Figure 4.22. The model of electrical generator in the *0dq* reference frame. 82
Figure 4.23. Equivalent electric circuit of a PV cell. 83
Figure 4.24. *I* (*V*) characteristic of a PV panel. 86
Figure 4.25. Flow chart of P&O method. 88
Figure 4.26. Circuit model of a typical battery. 90
Figure 4.27. The equivalent model of three-phase inverter 90
Figure 4.28. Block diagram of VSI control loops. 91
Figure 4.29. Configuration of static switch. 92
Figure 4.30. Main grid and MG connection via static switch. 92
Figure 5.1. Flow chart of load sharing and fault control of KBU MG system. 96
Figure 5.2. Simple Microgrid system. 97
Figure 5.3. Single line diagram of Karabuk university microgrid. 98
Figure 5.4. Simulink model of fault and power flow control of MG system. 100
Figure 5.5. Simulink model of the inverter control. 101
Figure 5.6. Simulink model of the solar PV with grid connected inverter. 101
Figure 5.7. Simulink model of the battery. 102
Figure 5.8. Simulink model of the diesel generator 102

Page

Figure 5.9. Simulink model of the three-phase transformer. 103
Figure 5.10. Simulink model of the load profile. 104
Figure 5.11. Simulink model of the fault control system. 104
Figure 5.12. Load profile and circuit breaker signal for different loads. 105
Figure 5.13. Power characteristics of grid, solar PV, battery and diesel generator. 106
Figure 5.14. Fault details and fault voltage at area. 107
Figure 5.15. Critical and non-critical load profiles while the fault. 107
Figure 5.16. Grid voltage and current at the primary transformer. 108
Figure 5.17. Grid voltage and current at the secondary transformer. 109
Figure 5.18. Voltage and current of PV-battery bus. 109
Figure 5.19. Voltage and current of diesel generator. 110
Figure 5.20. Load voltage and current at diesel generator. 111
Figure 5.21. Load voltage and current at PV-battery bus. 112
Figure 5.22. Load voltage and current at secondary of the transformer. 113
Figure 5.23. Frequency response on grid-connected and island modes. 113
Figure 6.1. Flow chart of the methodology steps for KBU MG analysis. 116
Figure 6.2. System architecture of KBU MG in Homer Grid. 118
Figure 6.3. Daily profile of critical loads. 119
Figure 6.4. Seasonal profile of critical loads. 119
Figure 6.5. Daily profile of non-critical loads. 119
Figure 6.6. Seasonal profile of non-critical loads. 120
Figure 6.7. PV loads profile consumption (kW) of months with respect to hours. 120
Figure 6.8. Generator loads profile consumption of months with respect to hours. 121
Figure 6.9. Monthly temperature graphic of Karabuk province. 122
Figure 6.10. Solar global horizontal irradiation. 122
Figure 6.11. Comparison of NPC between base case and lowest cost system configuration. 130
Figure 6.12. Annual savings of the proposed (winning) system by categories 130
Figure 6.13. Monthly average electricity production for proposed system. 131
Figure 6.14. Demand reduction during DR program. 133

LIST OF TABLES

Page

Table 2.1. Advantages and drawbacks of DC MGs versus AC MGs. 22
Table 2.2. Advantages and drawbacks of AC MGs 23
Table 2.3. MG related standards developed by IEC and IEEE. 28
Table 5.1. Specification of KBU Microgrid. 99
Table 5.2. Active power sharing of KBU MG system. 106
Table 6.1. Case-wise comparison of optimization results. 128
Table 6.2. Comparison of electricity production and consumption. 129
Table 6.4. Case-wise comparison of yearly emissions. 129
Table 6.5. Generator statistics. 132
Table 6.6. Generator quantities during outage. 132
Table 6.7. Demand response and revenue. 133
Table A.1. Technical specification of the KBU substation transformer TR 6 154
Table A.2. Technical specification of the distribution center transformer 154
Table B.1. Technical specifications of PV panel CWT300-72M 156
Table B.2. Technical specification of battery MUTLU 6OPzS-300 157
Table B.3. Technical Data of Inverter ABB TRIO-50 157
Table C.1. Load profile of Engineering faculty 160
Table D.1. Critical loads list of Engineering faculty. 163
Table E.1. Utility monthly summary comparison. 163

SYMBOLS AND ABBREVITIONS INDEX

SYMBOLS

αβ : stationary reference frame

dq : synchronous reference frame

abc : natural frame

ABBREVITIONS

RES : Renewable Energy Sources

DER : Distributed Energy Resources

PV : photovoltaic

LV : low-voltage

MV : medium-voltage

DG : distributed generation

KBU : Karabuk University

MG : Microgrid

SG: : Smart Grid

CERTS : Consortium for electric reliability technology solutions

PCC : Point of common coupling

SS : Static switch

PFC : Power factor corrector

LFAC : Line-frequency alternative current

HFAC : High-frequency alternative current

UPLC : Universal power line conditioner

UPQC : Universal power quality conditioner

EPS : Electric power system

IEEE : Institute of Electrical and Electronics Engineers

IEC : International electro-technical commission

SCC : Standards coordinating committee
ACSI : Abstract communication service interface
SCSM : Specific communication service mapping
IED : Intelligent electronic device
SAS : Sub-station automation system
UAS : Utility automation system
LN : logical nodes
SCL : System configuration language
SRD : Source requirement documents
MPPT : Maximum power point tracking
PLL : Phase locked loop
ESS : Energy storage systems
VSC : Voltage source converter
VCVSI : Voltage-controlled voltage source inverter
THD : Total harmonic distortion
MGCC : Microgrid central controller
MAS : Multi-agent system
CSI : Current source inverter
VSI : Voltage source inverter
BESS : Battery energy source system
EMS : Energy management system
NREL : National renewable energy laboratory
NPC : Net present cost
COE : Cost of energy
TSMS : Turkish state meteorological service
RF : Renewable fraction
DR : Demand response

PART 1

INTRODUCTION

The energy demand is growing exponentially in the world. Hydrocarbon resources are depletable and limited in supply. It is predicted that the energy consumption in the world will increase until $216500E\times10^6$ TW in 2035 [1]. Year by year it is difficult to maintain the operation of power systems taking into account all requirements - technical, economic and environmental. To support all of these requirements, the introduction of intelligence is required in the interest of efficiency, safety and economy, thereby creating prerequisites for the emergency of "Smart Grid" concept. These problems have led to new concept of "Smart Grid".

Hydrocarbons are the main sources to generate electricity. However, the limited availability of fossil fuels, rising fuel prices and environmental pollution from burning fossil fuels have cast doubt on the future viability of human civilization, which depends on traditional energy sources. In recent year, in many countries the share of renewable energy sources (RES) in the energy generation has been increasing due to their positive impact on addressing environmental concerns as a clean energy source, low expenses for operation and maintenance, easy setup. The total renewable energy installed capacity at the world was 2356,3 GW in 2018, and energy total production of renewable energy resources was 6190948 GWh at the end of 2017 [2].

Last decades a lot of projects, research works have been focused on microgrid (MG) as it is intended to improve operation and maintenance of power system, increase the reliability and decrease carbon dioxide emissions.

Microgrid defines as collection of distributed energy resources (DER) and loads that operates as single system. In last decades, the developing of power electronics units give to equip DERs, and thereby to provide the flexibility operation of power system with integrated microsources as a single aggregated system.

Also, MG is an interconnection of distributed generation such as microturbines, wind turbines, photovoltaics (PV), and storage devices and interior loads which operate at low-voltage (LV) and/or medium-voltage (MV) distribution network. Such a single system gives a new problem, such as provide a stability while intermittency of renewable energy sources, power quality, etc. These issues should be resolved by applying advanced technologies at LV/MV distribution network of power systems.

In this work, the microgrid is planned, designed and modeled for Engineering faculty building at Karabuk university (KBU) campus. The results for simulation, technical-economic assessment of KBU Microgrid are executed by licensed HOMER Grid version 1.6.1 software tool. HOMER Grid program developed by the National Renewable Energy Laboratory (NREL) and implements the simulation, optimization, sensitivity and demand response analysis.

1.1. PROBLEM STATEMENT AND MOTIVATION OF THE THESIS

Penetration of DERs into the power system caused new area for research such as:

- the issues with reliability and efficiency of the SG system;
- how to plug in and interface storage devices to distribution networks;
- how to support the flexibility energy generation;
- digitalization of the energy system.

Conventional power systems are designed to operate radially and not considered the integration of distributed generation at LV network. The high penetration of distributed generation (DG)s to power systems disrupts smooth operation of the system and creates the following issues:

- The complexity of system control increases
- Additional protection should be provided
- Communication difficulty of distribution systems.

Therefore, there is a problem with to integrate one or a several MGs into LV/MV networks or customer sides by properly coordinating the operability of DERs, energy storage systems and neglecting their potentially negative side effects on operation and control of power systems.

Variety sources of DG and loads are a reason of high nonlinearities, changing dynamics, and uncertainties. For example, some RES such as solar PV and wind turbines work under unpredictable environmental conditions and turbulent. To solve these issues, it requires to develop intelligent control strategies, and thereby to increase reliability and performance of power systems. And thus, MGs performance strongly depend on the applied control strategies. So, the operation of power electric system and MGs are essential to provide reliability and security of the power system. Based on the foregoing, in this work, the modeling and simulation of Karabuk university microgrid are developed, considered operation modes and control strategies of microgrid.

1.2. RESEARCH OBJECTIVES

In conventional power system, the distribution network is passive, because it is designed as centralized system where generated energy transmitted power from transmission system and distribute to customers and there is no distributed generation. While the integration of distributed generation within distribution network power systems become an active with bidirectional power flows.

Main purpose of work is to design the model of MG for a one substation of KBU campus and development the control strategy for efficiently operation of a KBU microgrid. The simulation model of microgrid demonstrates the coordination strategy of DERs as an effective way of optimizing the economic operation and the reliability of MGs.

The specific objectives of this thesis are following:

- Design of microgrid for one substation of KBU electric network;
- Microgrid dynamics representation and modeling;
- Develop control strategies of microgrid;
- Simulation of microgrid in grid-connected and isolated operation modes;
- Load sharing control of distributed energy sources;
- Fault control of microgrid;
- Techno-economic and environmental analyzing of KBU microgrid.

1.3. METHODOLOGY

The integration of DERs and energy storage devices to existing power distribution network makes problems such as to provide the operating reliability and efficiency of electricity system. Therefore, precise design and modelling microgrid system with control ensure the stability of power system.

The methodology flow chart of the research is given in Figure 1.1. In methodology the problem of research has appreciated and evaluated according to the literature review. Then appropriated case study for the research work has been chose and gathered required initial data. Planning and design of KBU MG are implemented based on initial data. Dynamic and mathematical modeling of microgrid have executed as previous step to perform the simulation of KBU MG on MATLAB/Simulink. Load sharing and fault control strategy of KBU MG are developed on MATLAB/Simulink in next stage of the research. Techno-economic and environmental analyses are executed using licensed HOMER Grid version 1.6.1 software tool to evaluate the effectiveness of MG application.

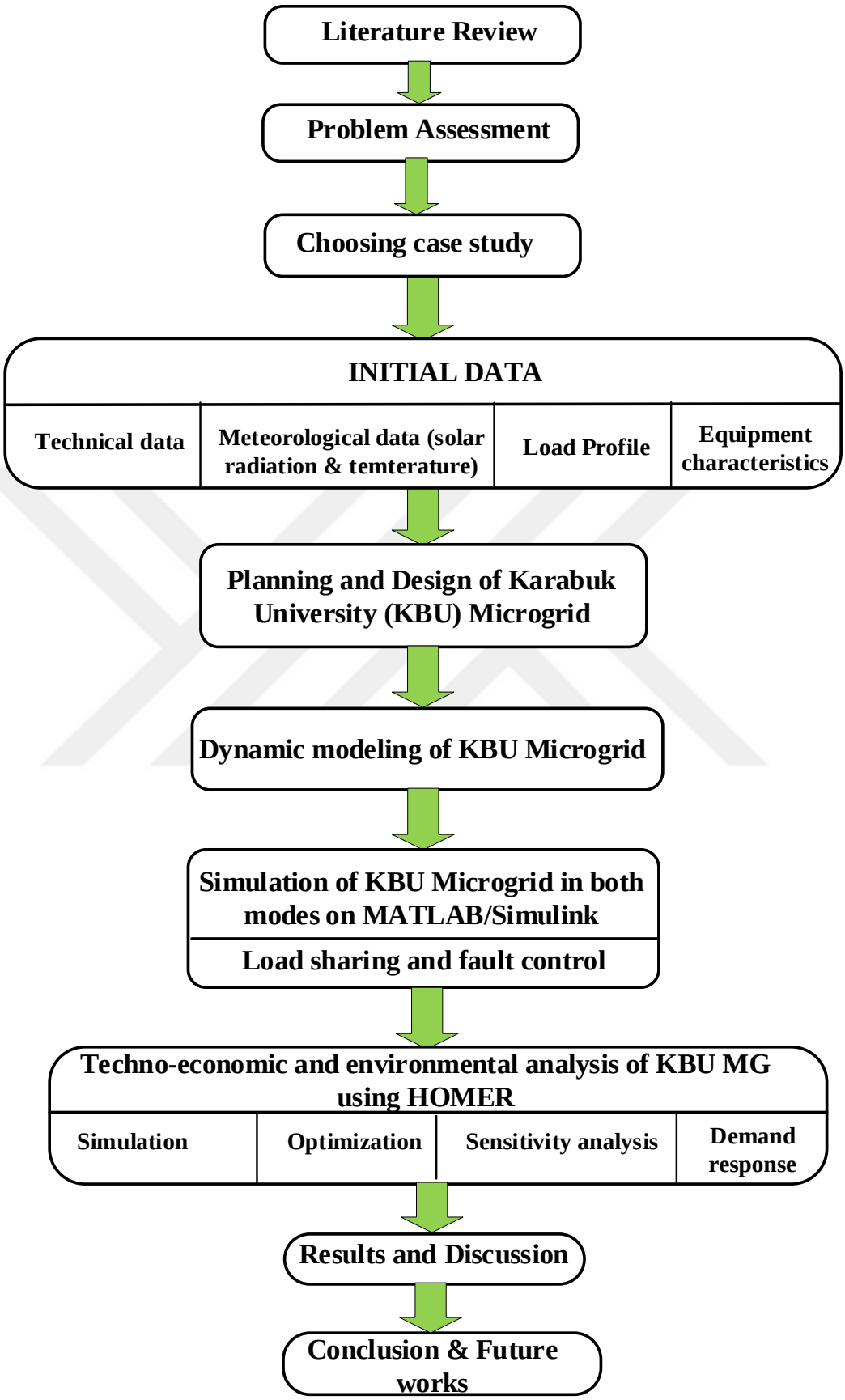

Figure 1.1. Methodology flow chart of the thesis.

1.4. LITERATURE REVIEW

The first scientific work related to microgrids was presented by *R. H. Lasseter* [3]. In the article, he describes the microgrid paradigm and gives its overview, which includes its architecture, protection, control, and energy management.

T. Ackermann et al. [4] have discussed the objectives and problems of commonly defining the concept of distributed power generation. They defined it according to the guidelines provided in the literature. Moreover, distributed resources, capacities, and utilities have been discussed. Also, this paper describes technologies for distributed generation.

R. H. Lasseter et al. [5] in their work related to research projects, published by Consortium for Electric Reliability and Technology Solutions (CERTS), which describes in detail the MG technologies for creating MGs. A major and significant feature of Microgrids is the interconnection between the Microsource Controllers. Such devices of power electronics maintain balance of energy and quality of power by means of passive plug-and-play inverter features, which help the overall operation with no fast communication and central active control.

An article by *N. Hatziargyriou et al.* [6] described the ongoing researches, developments, and show the operations of a microgrid, which is going on in United States, European countries, Canada, and Japan. MGs, which are equipped with DERs (distributed energy resources) that perform in a decentralized way, reduce the burden of control on a grid. The same article describes that every microgrid is equipped with an LV local DERs, which functions as a single producer with the grid, and they are important for power generation and energy marketing. Generally, microgrids safely and efficiently operate in a local network with islanding capability.

S. Chowdhury et al. [7] published a research that throws light on the concepts, effects, generation technologies, operations, management, and financial viability of MGs and broad perspective of their active distribution networks. They are the basic ideas behind MGs as well as their distribution networks, requirements of such networks, challenges,

technical advantages, socioeconomic impact and issues pertaining to their management and operations. The researchers have discussed the operational principles of different DERs, which are generally applied to Microgrids as well as active distribution networks, and their impact. Some microgrids show substantial effect on the operations of the main grid and its customers. The current research lists economic, technical, and environmental advantages of MGs. In this research, their protection systems, power electronic interface development, power quality, control, reliability matters, and distribution have been discussed in detail.

N.Hatziargyriou [8] provides details in his work, which deals with understanding, analyzing and justifying Microgrids as a new distribution network structure that discovers the full potential of Distributed Energy Resources (DERs), and thus, it is a basic block of smart grids, a well-thought view of the microgrid concept from the various forms of potential economic, environmental and technical benefits. This work presents results of EC-funded research projects such as "Advanced Architectures and Control Concepts for More Microgrids" and "Large Scale Integration of Micro-Generation to Low Voltage Grids," which were conducted from 1998 to 2006. That shows the role of microgrids in the power system structure focusing on their major findings specifically pertaining to primary and secondary controls, microgrid management, and multiple-microgrids. The book describes the hierarchical control levels distinguished in Microgrids' operations, the principles and main functions of centralized and decentralized control, including forecasting and state estimation. It also provides results of quantified assessment of the Microgrids benefits from economic, environmental, operational and social points of view. Finally, an overview of the basic multi-agent systems concepts and their application to decentralized control of Microgrids is provided.

In another article, which has been published [9] to review the DERs and microgrids, the authors *H. Jiayi et al.* introduced the updates on MGs and their architecture. This paper describes architecture of microgrid, MG operation modes, fault detection and safety analysis of MGs. It also throws light on the market of MGs.

In the paper published by *M. Barnes et al*. [10], global MG projects have been described. MG concept and structure are presented described by authors. Their hardware range and operational controls are also reviewed. It highlights and summarizes the operating principles, field trials, and key conclusions.

Microgrid architectures and models have been reviewed in a study by *M.S. Mahmoud et al*. [11]. In this research, the authors have reviewed various control schemes for microgrids. MGs are discussed as a "system of systems" and their applications have been highlighted.

In a paper written by *F. Martin-Martínez et al*. [12], the overall literature review has been given, which discusses MGs in detail. The authors represented basic definitions, structures and architecture of MG. In this article, exhaustive analysis of each MG's physical layer has been conducted. The physical layer has been analyzed that compares AC and DC, shows a clear physical division, and reviews DC voltage grids (Picogrids, Nanogrids, and MGs) besides comparing MG technologies.

D. Olivares et al. described microgrid control strategies [13]. Their paper highlights the major challenges faced in the microgrid controls. They have also reviewed state-of-the-art trends and control strategies. Moreover, they have given an overview of some control principles.

F. Katiraei et al. [14]cited MG structure and characteristics, DER units and MG loads. They classified control types of MG. Their article shows the main differences between huge power systems, microgrids, and provides a new controlling approach besides other microgrid operational concepts.

According to *Z.Alibhai et al.* [15], there are four major types of auction, which are used for MGs. They have presented some simulation results and techniques for managing energy sources and loads using MGs in a single community. In some situations, when there aren't many sources and loads, the auction type largely depends on the buyer's priorities. In case of several sources and loads, Dutch auctions are preferred.

P. B. Shashi et al. [16] presented a method to build MGs, which are cost-optimized and have reliability constraints. Their process determines optimal interconnection between the lead points and MS, and it is based on dynamic programming, when their possible interconnections are given.

In another article [17], *E. Ghiani et al.* explained an algorithm, which can be applied to explore the MGs optimal combination, for reconfiguring the distribution system. In search of the best combination of MGs with the most appropriate configuration, Sequential Monte Carlo simulation has been applied. The algorithm found the final structure, maximized the cost savings and minimized the service interruption cost.

Another paper [18] explains the MG architecture in a clear distinction addressing and reviewing the currently applied communication protocols. This paper culminates with a detailed and practical MG review and discussion on its key points of deploying MGs. It contributed to the existing knowledge by clearly defining the MG uses, specifically in the electric systems of the future.

A study [19] has been conducted to show the latest comprehensive literature review of DC and AC MGs in terms of distributed generation (DG) units with the help of energy storage systems (ESS), renewable energy sources (RESs), and loads. It includes a survey on the configurations of the LV alternative DG units. It also investigated the control, feasibility, and strategies to manage energy in two microgrid systems. This paper gives an introspective review of the DC and AC MGs using renewable DG units, loads, and storage devices, which are mentioned in the recent literature. It also describes the issues linked with traditional distribution systems, and MG roles and influences. It tries to address the general challenge, which is how to optimally run every MG component in optimal operating conditions.

Another study presented the state-of-the-art researches on energy management and control strategies for DC MGs [20]. This work has been broadly classified in two categories, which are based on distinguishing characteristics shown by the control strategies. This paper was written with a purpose to show an up-to-date overview of DC networks, their controls, their secondary factors, and the most common

instruments. The analysis has been performed using systematic literature review method, which helps locating and classifying the existing analysis, literature, and synthesis, which identifies the interconnection between papers to reasonably derive some useful conclusions, and they show what has been found and what is not. In both cases, the previous research and analysis is carried out, which is useful for new researchers. The authors also highlighted some interesting research questions, which experienced researchers might use for their research.

The ESS structures and technologies have been reviewed by the authors of a research paper [21], in which, they have presented their classifications, configurations, energy conversion, features, and evaluation. In addition, benefits and flipsides of ESS in MGs have been assessed in terms of energy formation, power transfer mechanism, material selection, efficiency, capacity, and cycle duration. Some reviews had critical judgments regarding some current technologies such as ESS in MGs. Even now, optimum ESS management for efficient MG operations is an issue for the latest power systems. The review highlighted some issues, key factors, and challenges giving recommendations to further develop ESS in MGs. The highlights of the current review have significantly contributed to the effort for developing an efficient and cost-effective ESS model that has a prolonged life cycle to implement sustainable MGs.

J. M. Guerrero et al. presented in their paper [22] the hierarchical controls on three different levels: primary, secondary and tertiary. These three levels applied to AC and DC microgrids. The primary control includes the use of droop method, which includes a virtual loop while the secondary control helps restoring deviations, which have emerged through primary controls. A tertiary control performs power flow management between the external distribution system and the MG. In the paper, advantages and drawbacks of each level have been explained.

A research [23] provided some recommendations and guidelines to suit the needs of researchers and designers which are helpful to address the emerging challenges while handling actual microgrids. In order to accomplish this task, a literature review was given that outlines the main design features and the main control functions, which

assure security, economy, reliability, and secure operations in different transitions and operating modes.

A paper [24] describes a research has been conducted on technologies, microgrid standards, and applications, which allow this concept's successful implementation. Basically, IEEE 1547 Standard was explained in this work. The author described the IEEE 1547 Standard approach to microgrids.

Another research was conducted on hybrid AC-DC microgrids [25], which have attracted considerable attention. It discussed the topologies for the AC/DC hybrid MGs, discussed the AC/DC interconnection, and explained some traditional power networks. After describing and analyzing each configuration, some important features were also highlighted. The future trends show that many features, including the modeling, scalability, or design need further research for integrating hybrid microgrids with an existing power network.

The researchers performed a continuous research on microgrids and reported their findings in an article [26]. This research reviews the hybrid AC-DC microgrid control strategies, which can be implemented for adequate power supply and management in both islanded and grid-connected operations. Their review mainly focuses on hierarchical controls which are part of an extended approach. They classified and elaborated it to cover three main hierarchical control strategies (mentioned as primary, secondary and tertiary in a previous part of this document). Each level was independently studied for providing comprehensive analyses.

The literature review of architecture, policy and future trends of MGs has been presented in another research paper [27]. The benefits and issues of such configurations are also mentioned in the study. RES has its own advantages and its power quality issues. The energy storage systems have certain benefits, which help developing communication systems, and assure efficient but flexible smart grid operations. Their findings are outlined along with the discussion on the policies and trends of microgrids.

PART 2

MICROGRIDS ARCHITECTURE

One of the major power systems' crises has been the conventional system's inability to deal with the mentioned issues because they require massive overhauling, which is not cost-effective. Besides, it needs intelligent command and control systems in place for connecting the power grids. Even now, such technology could not be introduced to improve the transmission systems of the existing electricity grids. This requires improved electrical grids, also termed as Smart Grid (SG), which has provided an alternative to conventional electricity transmission in the centralized networks. The evolution of the traditional power grid towards smart grid involves the grid transformation into microgrids (MG), which is a key SG component to improve power efficiency, reliability and reduce polluting emissions. Such microgrids combine storage devices (energy capacitors, batteries, and flywheels), distributed energy resources, and flexible loads. They are connected to the main power grid through switches.

2.1. MICROGRID CONCEPT AND STRUCTURE

The microgrids were first launched and introduced by the European Commission's Project on Micro-Grids and Consortium for Electric Reliability Technology Solutions (CERTS), which defined MG as follows:

CERTS [5] mentioned that a "*microgrid consists of micro-sources and a cluster of loads that operate like a single controlled system providing both heat and power. Such microgrids are electronically interfaced to enhance the quality and reliability of power supply*".

EU research projects [27] defined them as: "*Microgrids are LV distribution networks, which connect distributed energy resources (DERs) (fuel cells, microturbines, wind turbine, and PV) with storage devices including energy capacitors, flywheels, and batteries to assure flexible loads*.

MGs are mainly active distribution networks because they operate the DG systems at different distribution voltages. An MG is connectable to low-voltage distribution network. However, they also operate in the islanded mode when there are main network faults. Thus, the generators/micro-sources used the MGs generally have renewable/unconventional distributed energy resource (DERs), which are interconnected to generate power. Operationally, the microsources have power electronic controls and interfaces for providing the needed flexibility for assuring operations like a single aggregated system besides maintaining power output and quality. The controlling flexibility allows a microgrid to connect to the main system through a single control process to meet the local power requirements in a secure and reliable way.

MGs and conventional power systems are different in the following ways:

- Micro-sources have substantially lower smaller capacities as compared to conventional generators.
- The utility distribution network directly feeds on the power generated at distribution voltage.
- Micro-sources are generally placed closer to the clients' premises to efficiently supply the required heat/electric loads assuring sufficient frequency profile and voltage while minimizing the line losses.

The MGs are normally equipped with storage systems, DERs, communication systems, distribution systems, and control systems (see Figure 2.1). The MGs have the following main components:

- Distributed sources like PV panels, fuel cells, small wind turbines, gas and diesel micro-turbines

- Storage devices like super capacitors, batteries, and flywheels; and
- Critical/non-critical loads.

Since the RESs have fluctuant and intermittent availability, MG are equipped with a small hybrid power system that assures high energy security levels because of the combination of various generation systems, which generally incorporate ESSs for assuring highest possibility power supply reliability. Different hybridization types of power sources are part of an MG. As mentioned earlier, the RESs have intermittent availability, the backup power units assure high energy security levels. For instance, a micro-gas turbine, a diesel generator, and some fuel cells are used to assure interruption-less power supplies. The primary sources of renewable energy have definitive complementary benefits, such as the hybrid PV-wind systems are advisable to be used in certain areas because the solar PVs generate power only during the day; so, wind produces more power specifically if there are strong winds at night. When the energy storage devices are connected to the RESs, it assures the much needed power security and reliability, and it maximizes the gains out of renewable energy systems. Such systems optimally adjust deficits and excesses of produced energy using the energy storage units, which augments the overall energy efficiency [28].

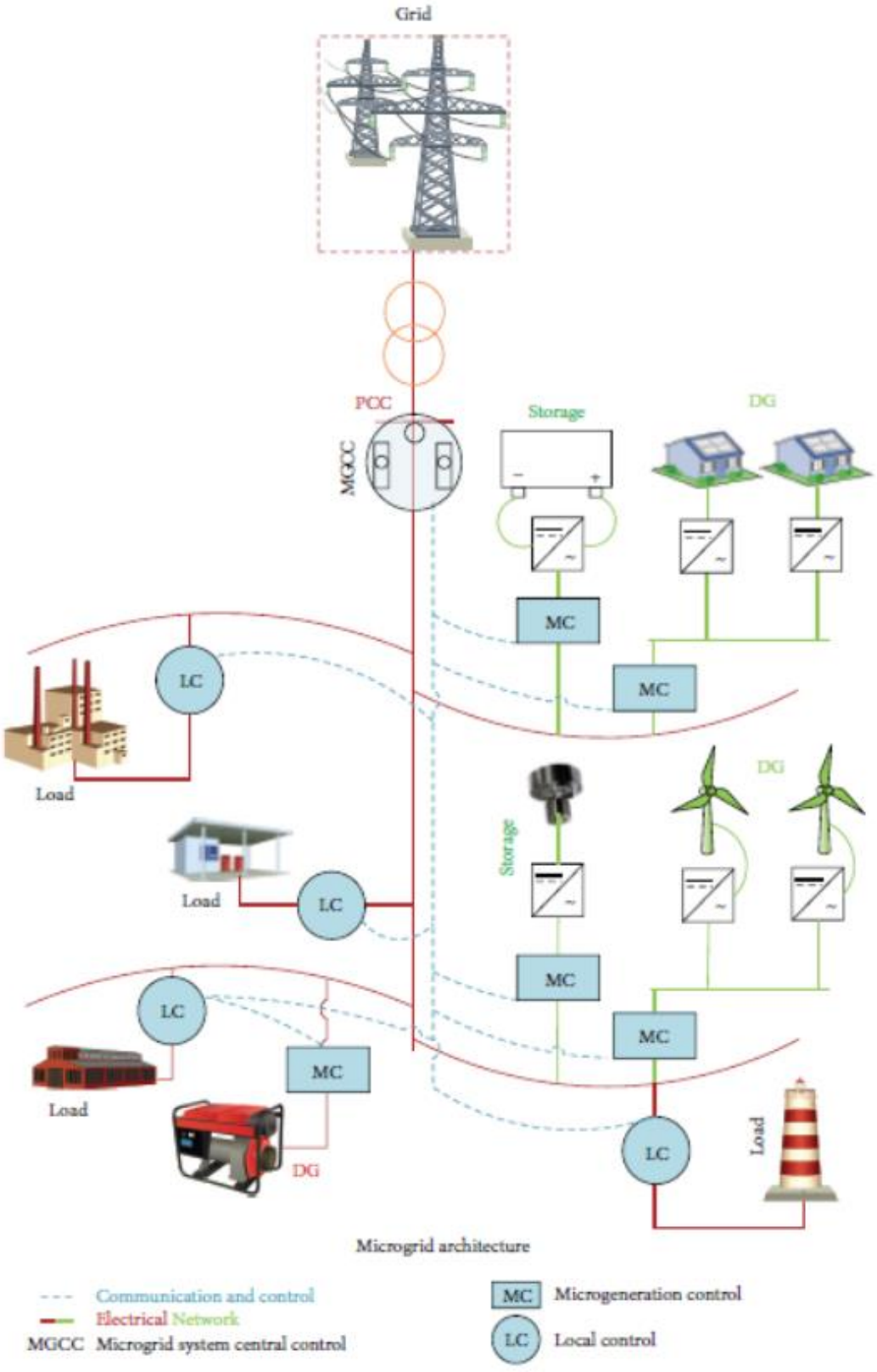

Figure 2.1. Typical Microgrid structure [29].

2.2. MICROGRID OPERATION MODES

MG is operated as follows:

- It operates autonomously in the islanded mode;
- It is connected to the main grid in grid-connected mode

When it is stand-alone, loads are provided through microsources with sufficient power, but the MG does not connect with the main grid.

When it is grid-connected, MG completely or partially connects to the MV distribution network and generates extra power for providing auxiliary services. The MG-distribution distribution network power exchange has been illustrated in Figure 2.2. The power-exchanging grid-connected mode has the following operations:

- Power-matched operations
- Power-mismatched operations

The power-matched operations involve the flow of active and reactive powers through the point of common coupling (PCC) that equals zero: $\Delta Q=0$ and $\Delta P=0$ while the current in the PCC is $I_{PCC}=0$; therefore, balance has been created among the distributed generation (DG) power flows and load powers while the operation is economic.

The power-mismatched operational mode is used when $\Delta P \neq 0$ or $\Delta Q \neq 0$; consequently, $I_{PCC} \neq 0$, which shows that power exchange takes place between the MG and the distribution network. So here, when $\Delta P < 0$, the extra DG active power is provided to the distribution networks but when $\Delta P > 0$, the DGs electricity is not sufficient to meet the local demand, which is then provided through the distribution network. In the same way, there is extra reactive power when $\Delta Q < 0$ and deficiency when $\Delta Q > 0$. These functions are normally power-mismatched [30].

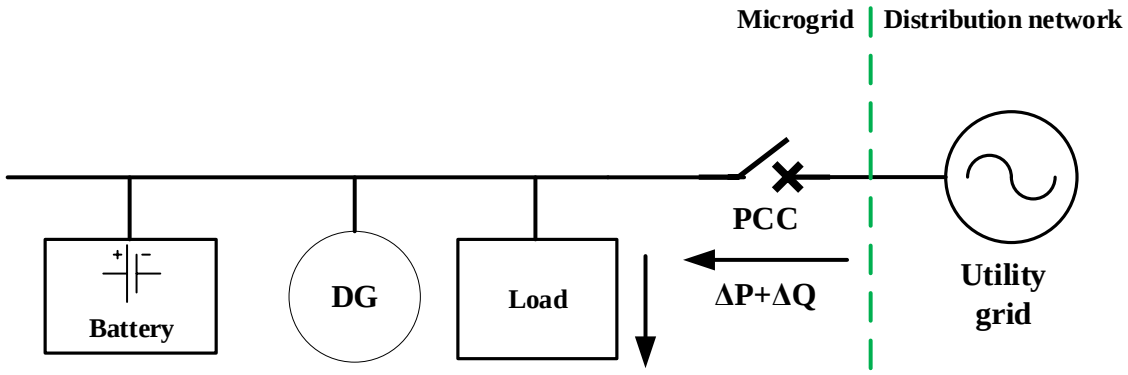

Figure 2.2. Power exchange between distribution network and MG.

The MGs general structure is capable of operating in islanded as well as connected modes, as Figure 2.3 shows. Most of the MGs have radial feeders (A, B and C) that act as parts of the distribution system architecture and supports load collection. The mentioned radial systems are linked to the distribution system at the PCC through a static switch. PCC separates the main grid from the MG, and it is on the primary side of the transformer. Every feeder is equipped with a microsource controller and a circuit breaker [31]. The local critical loads are linked to the local generation resources whereas the non-critical loads have no local generation. A static switch can perform islanding of the MG in case when the disturbances happen, or when maintenance is needed. In emergencies, such as a main grid issue, MGs are disconnected through an SS just in a single cycle, which takes place very smoothly. MG are intentionally islanded intentionally as well, and this is done for specific reasons. It is also done when no fault or disturbance occurs in the main grid. The demand-generation balance is a significant requirement of the MG management systems both in islanded and connected operational modes [32].

Different segments of the MG architecture include loads, LV network, energy storage units, controllable and uncontrollable generation, and a hierarchical control (see Figure 2.4). A communication infrastructure supports the control scheme, which monitors and controls loads and power generators. The hierarchical control system has a center, known as the MGCC. When there is low hierarchical control level, the micro-source controllers (MCs) and load controllers (LCs) exchange information with the MGCC. It manages the MG operation and provides the LCs and MCs with some set points.

Normally, MGs are centrally managed and controlled through the MGCC, which is installed at the sub-station MV/LV. MGCC performs many functions, including the cost management and control of the MG hierarchical control systems.

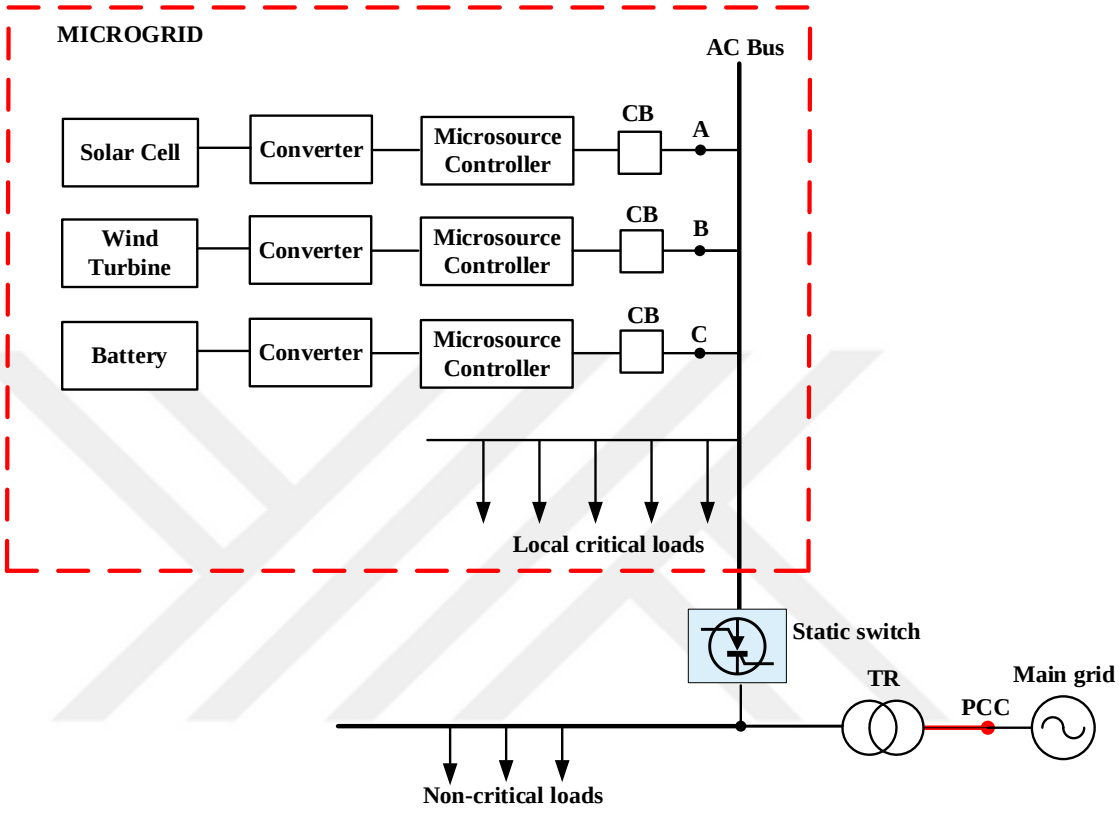

Figure 2.3. Schematic diagram of Microgrid.

When the outages or failures take place in the main grid, an MGCC synchronizes the main grid with the MG. The interfaces of power electronics connect the available DGs with the MG's electric network. When the number of MGs is high in LV sub-stations, we should expect technical benefits in the main grids because of a multi-MG operation. The MGs interconnection to the distribution power network has been shown in Figure 2.4.

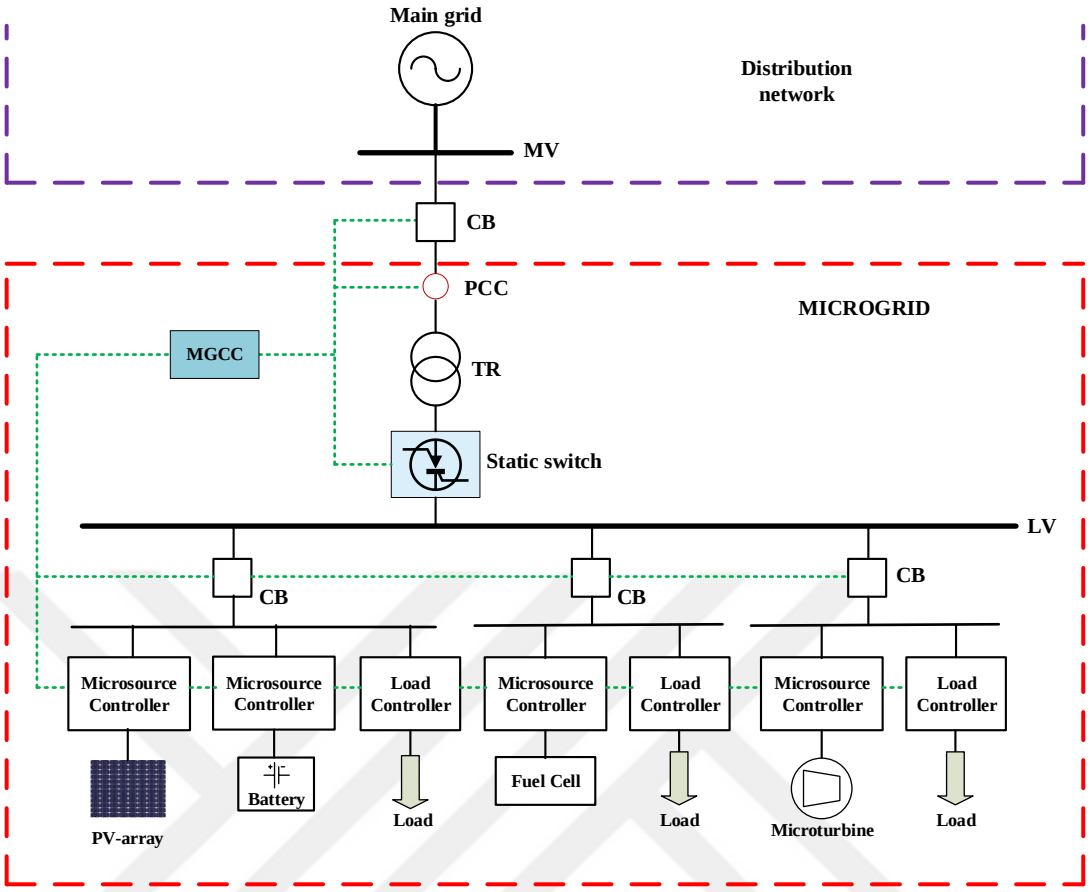

Figure 2.4. MG interconnection with a distribution network.

A distinctive feature of the MG is the MG operation in an islanded mode, i.e. MG disconnects from a main grid distribution network while the power is provided by distributed generation during the failure or outages. An MG failure might result in the rise in the ground potential when the energy sources function at the LV level; therefore, grounding of DGs and connecting the MG to a utility network through a transformer should be carefully assessed because they need developing appropriate rules. The earthing systems of the LV depend on the earthing techniques, which are on the MV/LV transformer's secondary side.

2.3. MICROGRID TYPES

The MGs according to operational frequency can be classified in the following configuration [33] (Figure 2.5):

- DC Microgrid.
- AC Microgrid.
    - Line-Frequency AC Microgrid
    - High-Frequency AC Microgrid
- Hybrid Microgrid (AC and DC coupled MG).

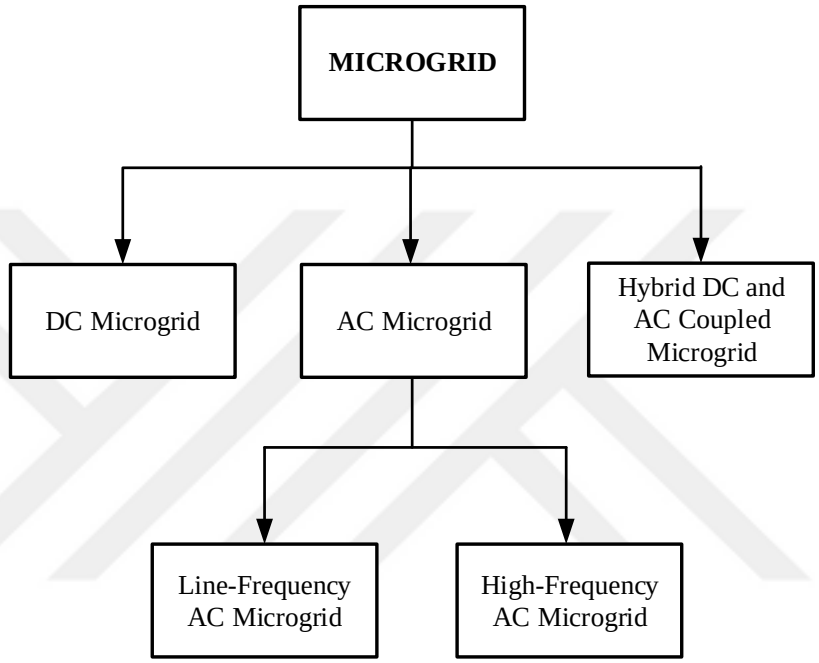

Figure 2.5. Classification of MGs based on operational frequency [33].

2.3.1. DC Microgrid

In DC microgrids, there is interconnection between large percentage of the sources, energy storage, through a single or a few DC busses. Normally, DERs produce DC power, which no power quality issue. Figure 2.6 shows a DC MG configuration system. DC MGs certainly have certain advantages over AC MGs [12,34,35]. Table 2.1 shows benefits and issues of DC MGs versus AC MGs. DC MGs have a great benefit of lower line losses because the power factor correction circuit are unnecessary during the AC/DC conversion stage. The DC characteristics also reduce the losses because it does not show issues like skin effects, current harmonics, or reactive power. Moreover, when a voltage sag a blackout takes place, the DC bus voltage does not change because the capacitor stores power and the AC/DC converter keeps on

working. Besides, there is no need to change wires, which support the voltage levels. Using DC has its own issues like it needs expensive and complex distribution systems protections. Another issue with DC MGs its requirement of AC power supply to connect the AC loads directly to the DC bus; so, it needs a DC-AC converter. In addition, when AC is used for the purpose of distribution, a DC microgrid connects to the AC grid at the same time; therefore, DC microgrids should be equipped with AC buses as regular components of a mixed AC/DC microgrid that is coupled with the AC grid at point PCC [36].

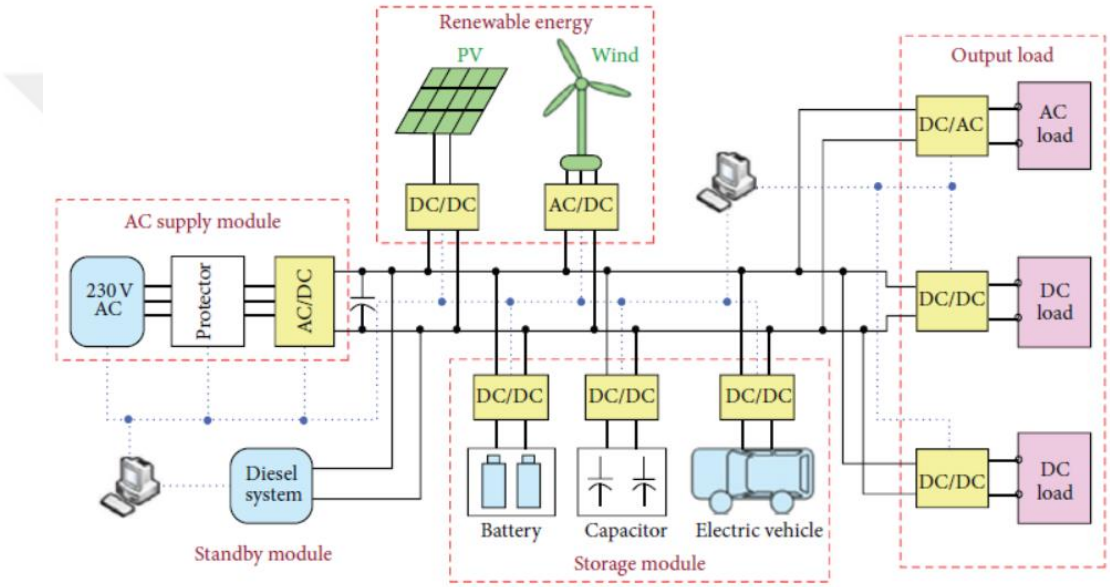

Figure 2.6. DC Microgrid system [37].

Table 2.1. Advantages and drawbacks of DC MGs versus AC MGs.

Advantages	Disadvantages
Lower losses	Complex protection system
No harmonics	Absence of zero-crossing points
No reactive power	Higher levels of voltage
No synchronization of distributed generation	Inappropriate for HVDC transmission
No power factor correction circuit	Unavailability of Low-distance power transmission
No DC bus voltage changes when a voltage sag/blackout happens	There is not telecommunication/wireless network interference
Efficiency of DC–DC switching regulators for certain loads.	
Do not require changing wires under certain situations	

2.3.2. AC Microgrid

Generally, AC type of MGs are commonly used because they directly implement the distributed generation power sources. Figure 2.7 illustrates an example of AC MG configuration system. AC MGs have high DG unit penetration, while the storage devices possess higher control flexibilities and capacities for connecting to traditional AC power systems both in islanding and grid-tied conditions but some new energy sources of a microgrid like batteries, solar generation, and fuel cells have substantial DC sources, which need inverters for connecting to the grid. Moreover, end users are increasingly adapting DC loads like computers and LED lighting, which need power factor correctors (PFCs) for AC- DC conversion. Establishing a DC power supply for connecting DC loads and sources using efficient DC/DC converters can decrease the control complexity and reduce the power conversion circuit. When this is performed, a DC grid shows its characteristics and have low power conversion cost and exhibit high efficiency [38]. In Table 2.2, the advantages and drawback of AC MGs have been shown.

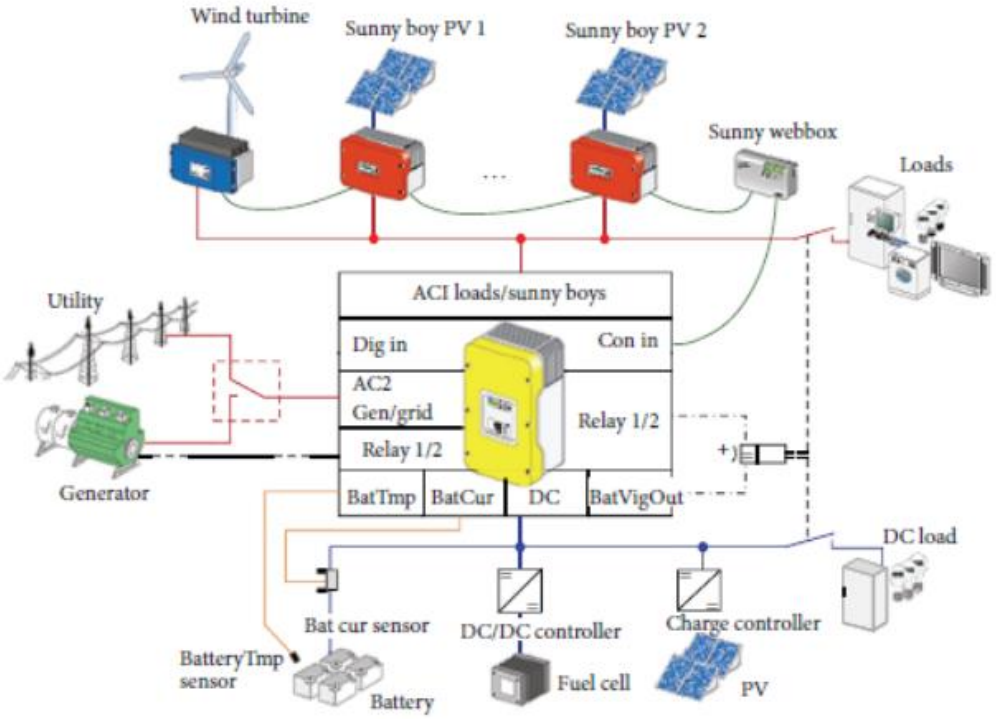

Figure 2.7. DC Microgrid system [37].

Table 2.2. Advantages and drawbacks of AC MGs [36].

Advantages	**Disadvantages**
1	2
Directly connect to distribution network via AC bus	The distributed utility and generation grid coupling need a synchronized AC bus
No inverters require for power supply AC loads	It substantially affects the power quality; for instance, induction machines and transformers produce
Easy and economic maintenance	Generally, peak voltage is 1.4 times more than usual
The transmission of AC power is possible over long distances	Anxiety of three-phase unbalances in PVs emerge (single phase loads and generators).
Providing quick start generation by each DG to power supply, and the loads are generally in the islanded mode that automatically return to the grid-connected mode.	The reactive power should be monitored continuously

Table 2.2. Advantages and drawbacks of AC MGs **(**continued)

1	**2**
Protection of the system is low-tech, cheaper and modified	The AC system analysis work with complex number; therefore, it is complicated.

2.3.2.1. Line-Frequency AC Microgrid

In the common MGs, there are line-frequency AC (LFAC) microgrids. Generally, DERs are interconnected with MV/LV buses in the MGs. The DERs' DC current is forwarded to AC with 50 Hz using DC-AC inverter and then transformed to loads. Various LFAC MG operational scenarios and concepts are given in the literature [33,36,39]. The typical structure of LFAC MG is illustrated in Figure 2.8. The three-phase LFAC MGs have more stages of power processing that reduce the system's overall efficiency. This microgrid class requires different DC-DC, AC-DC, and DC-AC converters. For providing galvanic isolation or increasing the transmission line voltage, an LFAC microgrid needs heavy three-phase low-frequency transformers [40].

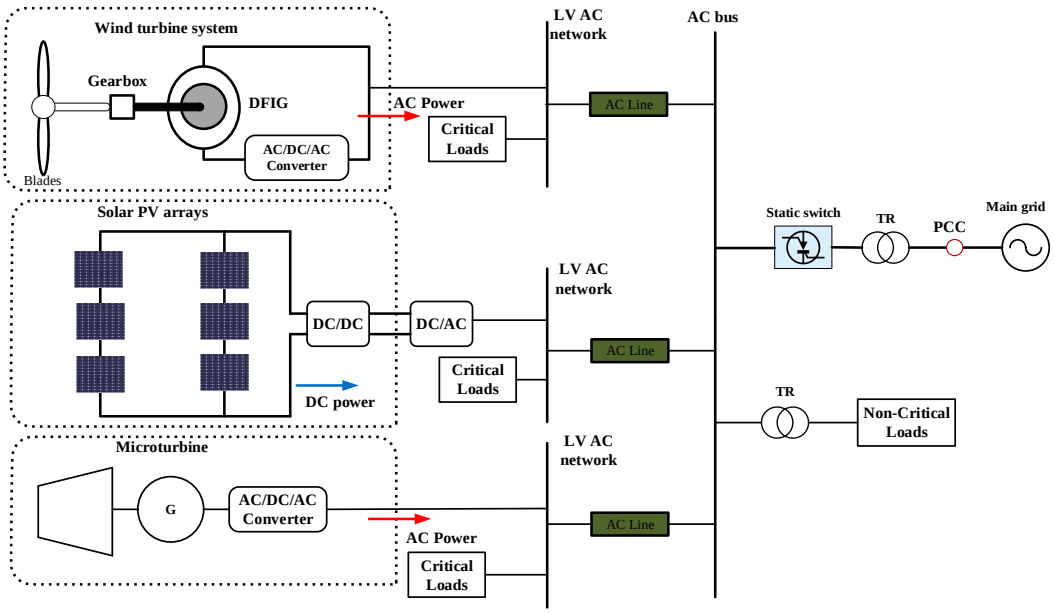

Figure 2.8. Typical structure of LFAC MG.

2.3.2.2. High-Frequency AC Microgrid

High-Frequency AC (HFAC) MGs are only locally used because their losses dramatically increase with distance; so, it is suitable for small areas [41]. Applying HFAC for transmitting power through MGs is a novel concept but it is in its early stages. The conventional HFAC MG schematic chart has been shown in Figure 2.9. DERs are linked with a common bus. The DERs' power generation is transformed into 500 Hz AC through power electronics devices that is transmitted to the load side where it is converted into AC 50 Hz through an AC/AC converter.

The distribution network is linked to the load side that guarantees effective interaction between the distribution network and the microgrid. On-the-line HFAC causes substantial reactance, causes more electricity losses and drop in voltage as compared to the 50 Hz AC power. Since microgrids are small-scale with short transmission distance; in that case, there is insignificant power loss and voltage drop.

HFAC MGs are equipped with electronic units, including a Universal Active Power Line Conditioner (UPLC), and a Unified Power Quality Conditioner (UPQC), A UPQC is compensates for the voltage distortions and the current harmonics through non-linear loads. It links the utility grid with the HFAC for performing functions such as controlling active/reactive powers and compensating for current harmonics, which might happen between the main grid and the microgrid.

Some researches [42,43] have highlighted the benefits and issues of HFAC MGs. Their advantages are given below:

- When the frequencies are higher, the higher order harmonics can be conveniently handled.
- The direct lighting equipment-HFAC microgrid connection effectively improves the power efficiency and the lighting brightness.
- It is possible to directly connect the HFAC line to the high-frequency AC motors or other high-frequency AC equipment that no longer requires transition devices.

- The size of passive circuit components and high-frequency transformers has become smaller and they are more compact.
- It is easy to connect the high-frequency resources to the storage units of a flywheel.

Besides such promising advantages, HFAC MGs have the following certain disadvantages:

- The HFAC technology enhances power losses and line reactance, which reduces the distance of power transmission.
- Along the line, HFAC results in substantial voltage drop.
- The HFAC MG control device is comparatively complex as compared to the traditional control devices.

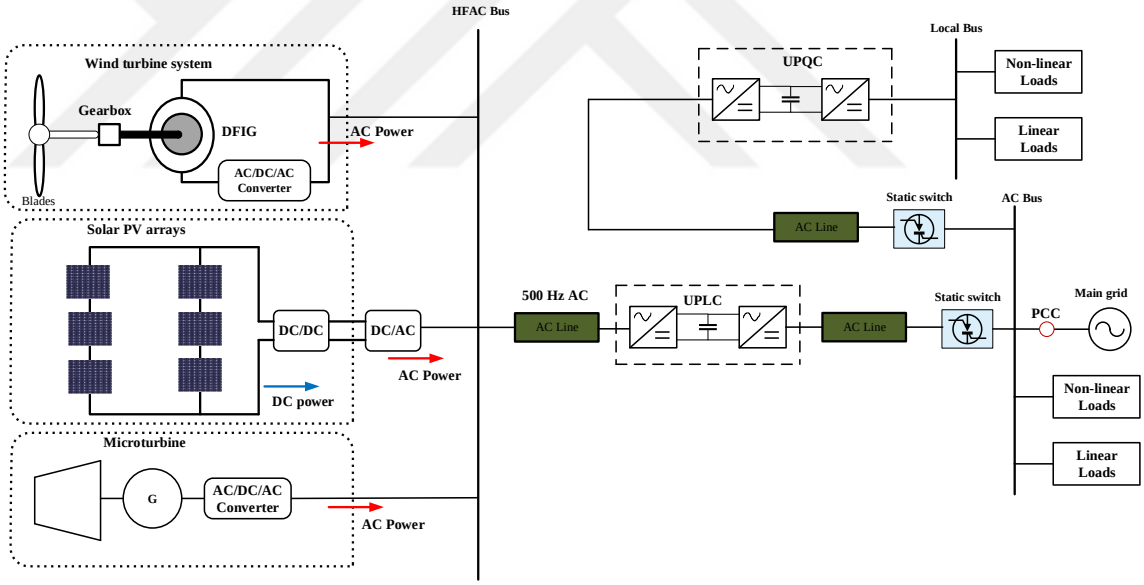

Figure 2.9. Typical schematic chart of HFAC MG.

2.3.3. Hybrid Microgrid

Hybrid microgrids are clusters of bi-directional converters, AC and DC microgrids, energy management system, and control equipment. Hybrid MG has been illustrated in Figure 2.10. It effectively integrates different DERs in a given distribution system. Hybrid AC- and DC-coupled microgrids bring the DC part in use to connect the

distributed energy storage systems, which are part of the bi-directional AC-DC converters, and PV systems, which are connected by means of small turbines and DC-DC Boost converters through rectifiers. The decoupled AC and DC control is possible by using power converters [44]. Despite the fact that the hybrid MGs are flexible approach for integration between the DER structures, units, operations, and issues such as protection and stability, but it needs further investigation.

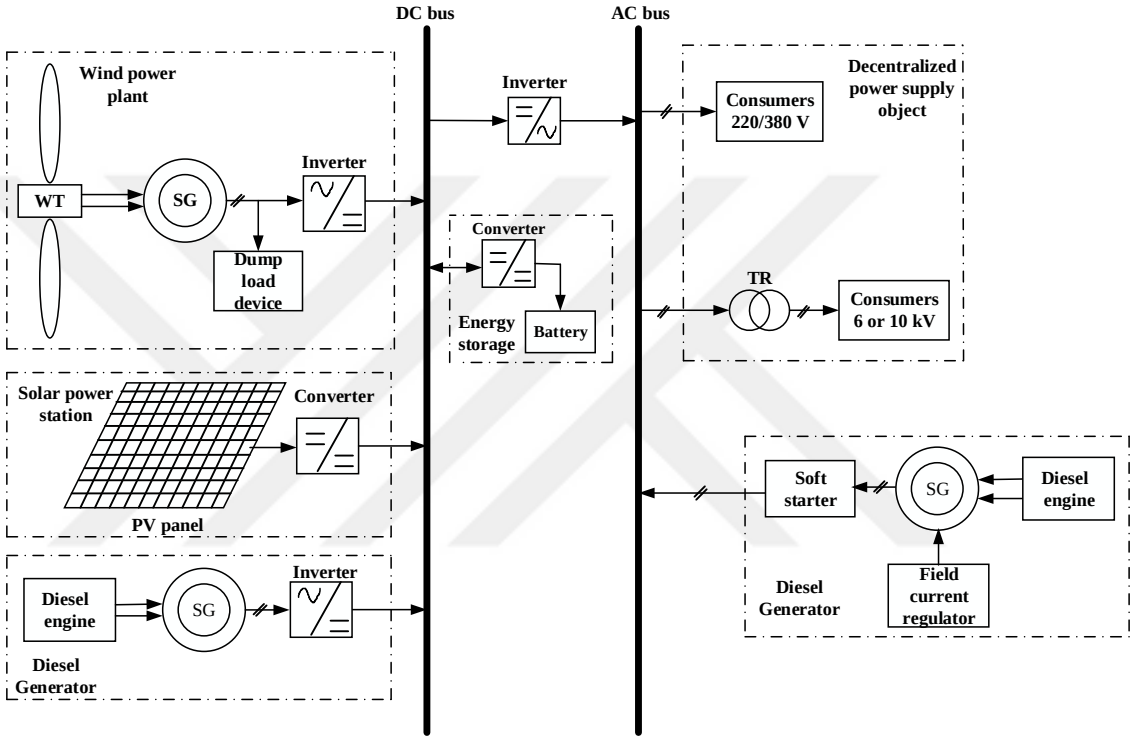

Figure 2.10. Topology of Hybrid MG.

2.4. STANDARDS FOR MICROGRIDS

Conventionally, the electric power systems (EPS) were unable to handle the active storage or generation process on the level of distribution. Such operational concepts and technologies integrate DERs in the already installed EPS, and they further develop so as to realize the operational advantages and reduce the issues pertaining to system safety and reliability. It is important to finalize a single document of consensus on the technical requirements for the interconnection of DERs rather than following several local guidelines and practices.

Some institutions, for example, the International Electro-technical Commission (IEC) and Institute of Electrical and Electronics Engineers (IEEE) have finalized some interoperability and interconnection standards for DERs with EPS. Different standards have been developed so as to address the critical needs through establishing a list of requirements and uniform criteria for the interconnection operation, performance, safety, testing, and maintenance. Table 2.3 shows some common MG-related standards, which were developed by IEC and IEEE.

Table 2.3. MG related standards developed by IEC and IEEE.

IEC		
IEC/TS 62898-1	Microgrids. Part 1. Guidelines for microgrid projects planning and specifications	Published
IEC/TS 62898-2	Microgrids. Part 2. Guidelines for operations	Published
IEC 62898-3-1	Microgrids. Technical Requirements. Protection requirements in microgrids.	In development
IEC 62898-3-2	Microgrids. Technical Requirements. Self-regulation of dispatchable loads	In development
IEC 62898-3-3	Microgrids. Technical Requirements. Energy management systems	In development
IEC 61850	Communication networks and systems in substations.	
IEEE		
IEEE 1547	Interoperability and interconnection between the DERs with Associated Electric Power System Interfaces	
IEEE 2030	Smart Grid Interoperability Guide for Energy Technology and IT Operations with the EPS, End-use Applications, and Loads	
IEEE 2030.7	Specification of Microgrid Controllers	

Figure 2.11 shows a general MG configuration containing DERs, static switches (SS), and loads at the common coupling point between utility grid and MGs. This figure indicates all common standards that can be used for MG energy management, monitoring, control, and protection systems. In this chapter we will consider the following main standards used for MGs architecture:

- IEEE 1547 Series of Standard
- IEC 61850 Standard

- Ul 1741 Standard

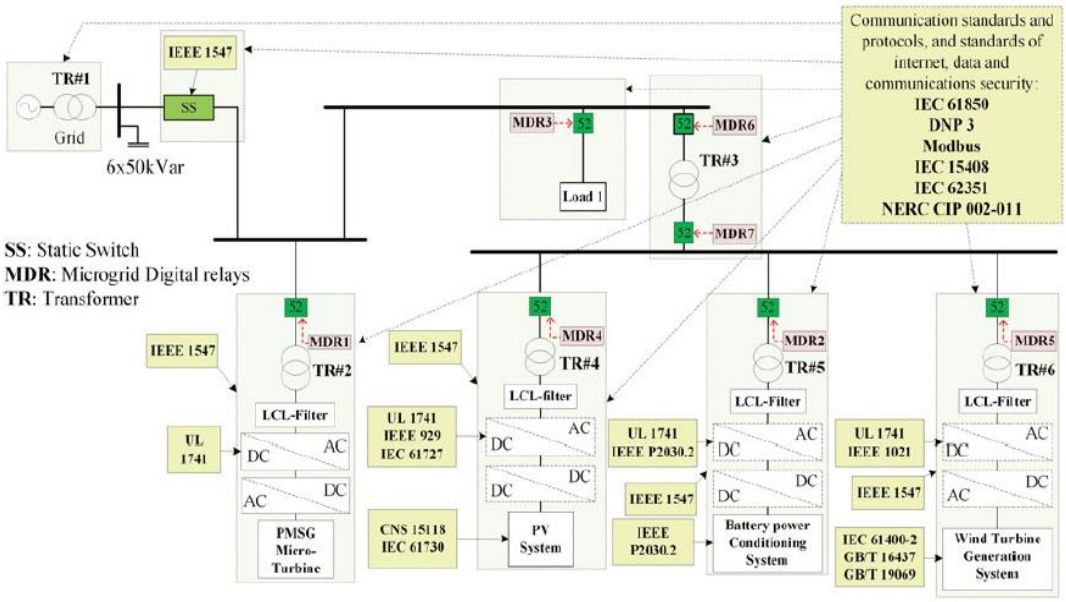

Figure 2.11. Common standards used for a general MG architecture [45].

2.4.1. 1547 Series of Standards

Arguably they are the most important standards for MGs. This series was developed by the IEEE Standards Coordinating Committee 21 (SCC21) on PVs, Fuel Cells, Energy Storage and Dispersed Generation in 2003 by the name as IEEE Std 1547-2003 (IEEE Standards for Interconnecting DERs with EPS). In 2014 IEEE 1547 was amended to IEEE Std 1547a™-2014 due to the changes in sub-clauses pertaining to the voltage and frequency responses to area of EPS under abnormal conditions, and voltage regulation.

IEEE 1547 has helped to modernize the traditional EPS infrastructure through laying the foundation to integrate the clean renewable energy generation with other ESS and distributed generation technologies. It provides compulsory technical and functional guidelines and provides choices and flexibility in terms of operations and equipment. IEEE 1547 also provides certain requirements for specific performances, operations, testing procedures, interconnection maintenance, and safety initiatives. It provides information about the response to abnormal conditions, general requirements, islanding, power quality, and requirements and specifications for design tests, production, commissioning, periodic tests, and installation evaluation. The mentioned requirements are required for DER interconnection for induction machines, synchronous machines, or power converters/inverters. They are sufficient in most cases.

The requirements and criteria apply to all the DER technologies, which have the approximate capacity 10 MVA or lower at the common coupling point, when the EPS is connected at typical primary/secondary distribution voltage. DER installation on radial primary/secondary distribution systems is an objective of the current document, for which, we considered the primary and secondary network distribution systems.

IEEE1547 recognizes that the distributed energy resources need to be integrated into the EPS Area in coordination with the operator. The functions specified in this standard may need to be supplemented in coordination with the Area EPS operator for specific situations.

2.4.2. IEC 61850 Standard

It is an international standard that deals with communication systems and networks in the sub-stations. This standard covers electric power, communications and software engineering areas. It assures integration, control, protection, monitoring functions, and measurement, which also provides sources for high-speed protection applications for substations. This series has been established to provide inter-devices communication in the substations through flexible communication architecture and object-oriented modelling technology. It has a standard system language, service protocols, semantics, and architecture, which assure extendibility and interoperability for several applications [46]. The relation between IEC 61850 parts is illustrated in Figure 2.12.

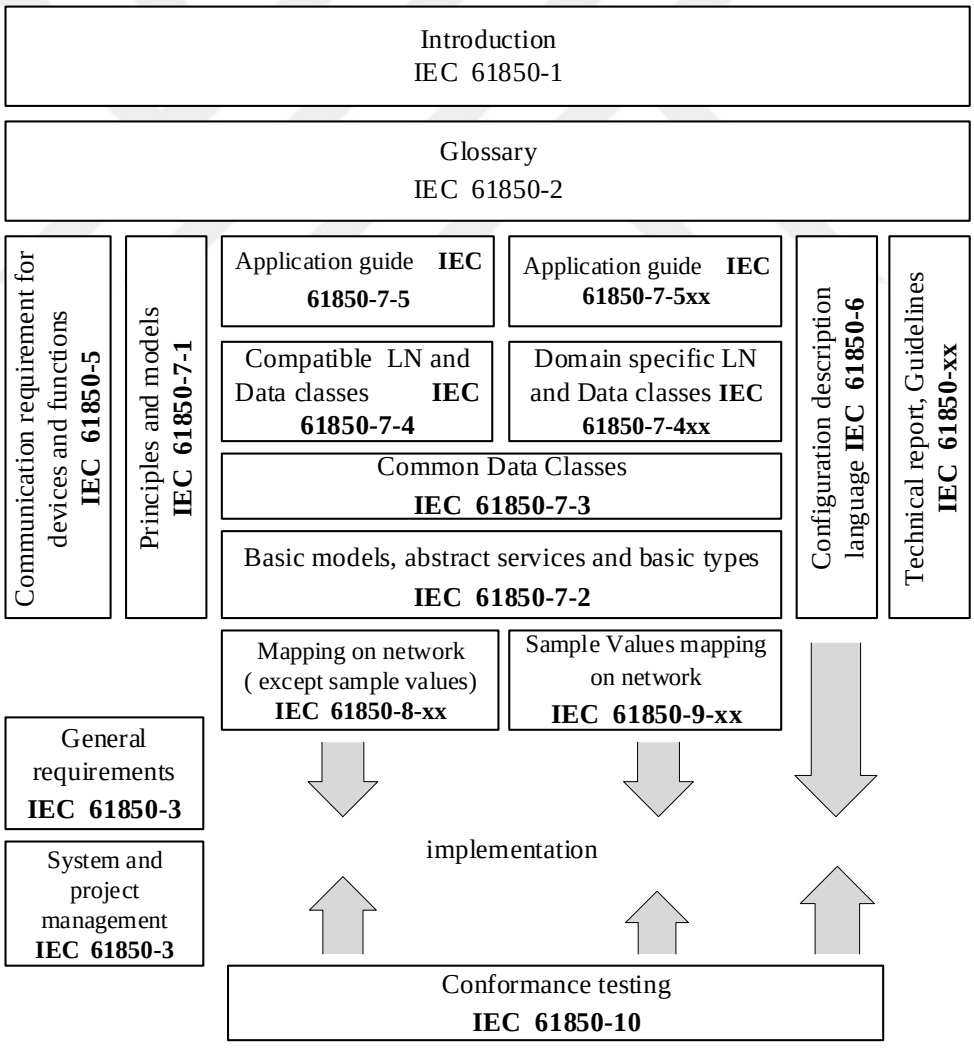

Figure 2.12. IEC 61850 Standard Structure.

Part 1 of the standard describes introduction, principles and concepts. In Part 2, we have included the glossary. Part 3 gives general requirements for the standard. It deals with the design, construction, and environmental situations for the intelligent electronic devices (IEDs) to perform. Sub-station automation systems (SAS), utility automation systems (UAS), and their project management have been presented in Part 4, which describes the engineers' responsibilities towards the project requirements, system architecture, equipment shipment, describing the different UAS components' interoperability, IEDs' parametrization, process environment, and commissioning.

The fifth part is mainly focused on the SAS [47]. It stresses on the inter-IED communication and its requirements. As an SAS component, the ability of IEDs to perform one or more functions should be assured. These functions include control, protection, and measurement. Different standardized functions can be divided into independent pieces that perform particular tasks and besides, they can be applied in two or more functions. Such pieces are termed as Logical Nodes (LN), which have pieces of information to communicate (PICOM) between the IDEs and the different functions.
Part 6 describes the object-oriented XML-based language called as System Configuration Language (SCL) [48]. They depict primary electrical circuit and its communication, functions, LN, and physical devices.

Basic commination structure is explained in Part 7. This part of the standard consists of four parts:

In parts 8 and 9, the abstract data classes and the communication protocols have been focused and they also describe serial unidirectional communication specifications and the samples values for transmission [49]. The client-server communication, its conformance testing and its engineering tools are mentioned in Part 10 [IEC 61850-10:2006. Communication networks and systems in substations – Part 10: Conformance testing].

For micro-grid "plug and play" function and information modelling, IEC 61850 has become an effective solution that has lower complexity and the system integration

cost. Moreover, it has publish/subscribe mechanism and real-time data transmission, which helps IEC 61850 support the fast control for operational mode conversion in MGs. The researches pertaining to IEC 61850 applications in MGs provide the relavant information and methods to implement the “plug and play” functions, modelling and information mapping conventional devices like fuel cells, PVs, electric vehicles, WPs, and the intelligent electronic device (IED) design. [50].

2.4.3. UL 1741 Standard

Underwriters Laboratories 1741 is a standard for converters, safety inverters, interconnection system equipment, and controllers for usage with DERs, supplementing interactive inverters, grid support utility and controllers (UL 1741 Supplement SA). It acts as a standard to defines the certification and testing needs of distributed generation systems, which meet the requirements of IEEE 1547 [51].

The UL 1741/IEEE 1547 is a combination that has its requirements, which evaluate the grid-tied distributed generation products for both utility interconnection and electrical safety. UL 1741 supplement A (SA) mentioned some testing methods required for building the basis for distributed generation devices, and make them adapt their output stabilize the grid during abnormal operations rather than disconnecting, and stay online [52]. It was created as a standard to handle several grid interactive requirements, which were not mentioned in IEEE 1547-2003. The source requirement documents (SRDs), like California CPUC Rule 21 have been applied according to UL 1741 that mentioned the particular converter configuration parameters, which are used with UL 1741 SA.

Besides, UL1741 is special in terms of UL regulations because it integrates the performance needs for grid interactions, which is not the case with majority of other UL standards, which are only concerned with electrical safety but not with performance. UL 1741 is used as a standard for converters, inverters, interconnection system equipment, and controllers, when the mentioned devices are integrated with DERs. It also deals with DGs, FCs, PVs, wind and hydro turbines, micro-turbines, and engine generators interconnections. The IEEE 1547 and Standards UL 1741

combination has been proposed for the evaluation of grid-connected DGs (evaluation of synchronization, surge withstanding, flicker, immunity protection, and temperature stability) [45].

PART 3

CONTROL STRATEGIES OF MICROGRID

The MG system management and control are multi-objective systems because they include the power flow regulation, control over power electronic devices, energy resource management, and power quality. A main characteristic feature that separates MGs from traditional grids is their state-of-the-art control strategy that manages devices, which are linked to the network. It is an essential strategy for optimal power generation and management because of the microgrids' distributed nature [53]. The DG units show intermittent behavior that needs to be optimally controlled using ESS units, which assures a stable as well as consistent power flow. Besides, MGs should be properly controlled while operating an autonomous mode, which assures seamless transition between the operational modes, which provide stable frequency and voltage; so, MG control strategies are challenging because they require wide research to explore the most viable solution that depends on the needs. Normally, main control objectives in the MG environment are the following [13,54,55]:

- **Protection**: It involves energy flow monitoring and critical devices' checkup, and managing faults of the grid.
- **Stability**: It means regulating voltage and frequency while using the MGs in different modes. It also assures a reliable and stable power networks in AC as well as DC MGs.
- **Power balance**: It includes DG supply coordination and optimal load-sharing.
- **Power transmission**: It implies power exchange between the grid and the MGs.
- **Transition**: It is a stage that seamlessly happen between the microgrids' operational modes like grid-connected-to-islanding mode or islanding-to-grid-connected.

- **Optimization**: It depends on the situation of the utility grid and the MG (like power demand, market situation, energy forecast, or power supply), cost reduction, and improved energy efficiency.
- **Synchronization**: This process links the MGs with a power network in order to assure optimal power transmission.

Such kind of features result in creating complex control architecture unlike traditional distribution networks. A conventional power grid does not control or manage power generation or storage units. Control strategies aren't easy-to-identify or classify because they are dependent on the MGs characteristics but most researchers investigated the control strategies because it is significant to describe their features, which depend on their hierarchical structures [55-60]. In this approach, there are the following control levels of MG that are identified in the literature:

- Primary control
- Secondary
- Tertiary.

Every level differently controls the MG functions; so, we have mentioned their main functions in Figure 3.1.

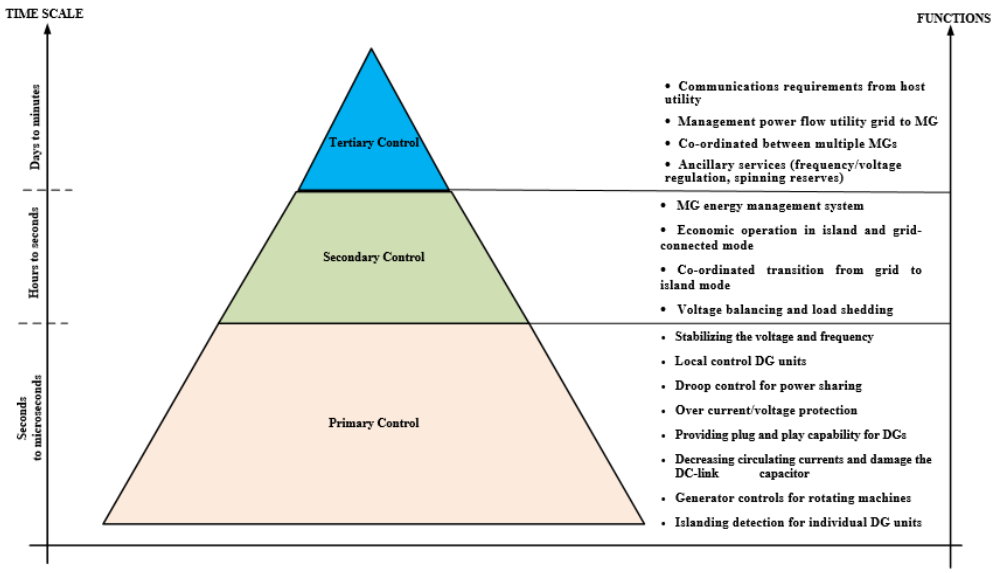

Figure 3.1. Control strategies of MG and their main functions.

The most applicable control strategies on the hierarchical level have been mentioned in the research work [55,60-62]. They are illustrated in Figure 3.2. Their classification has been done based on the available research studies while their properties are given along with their links as follows:

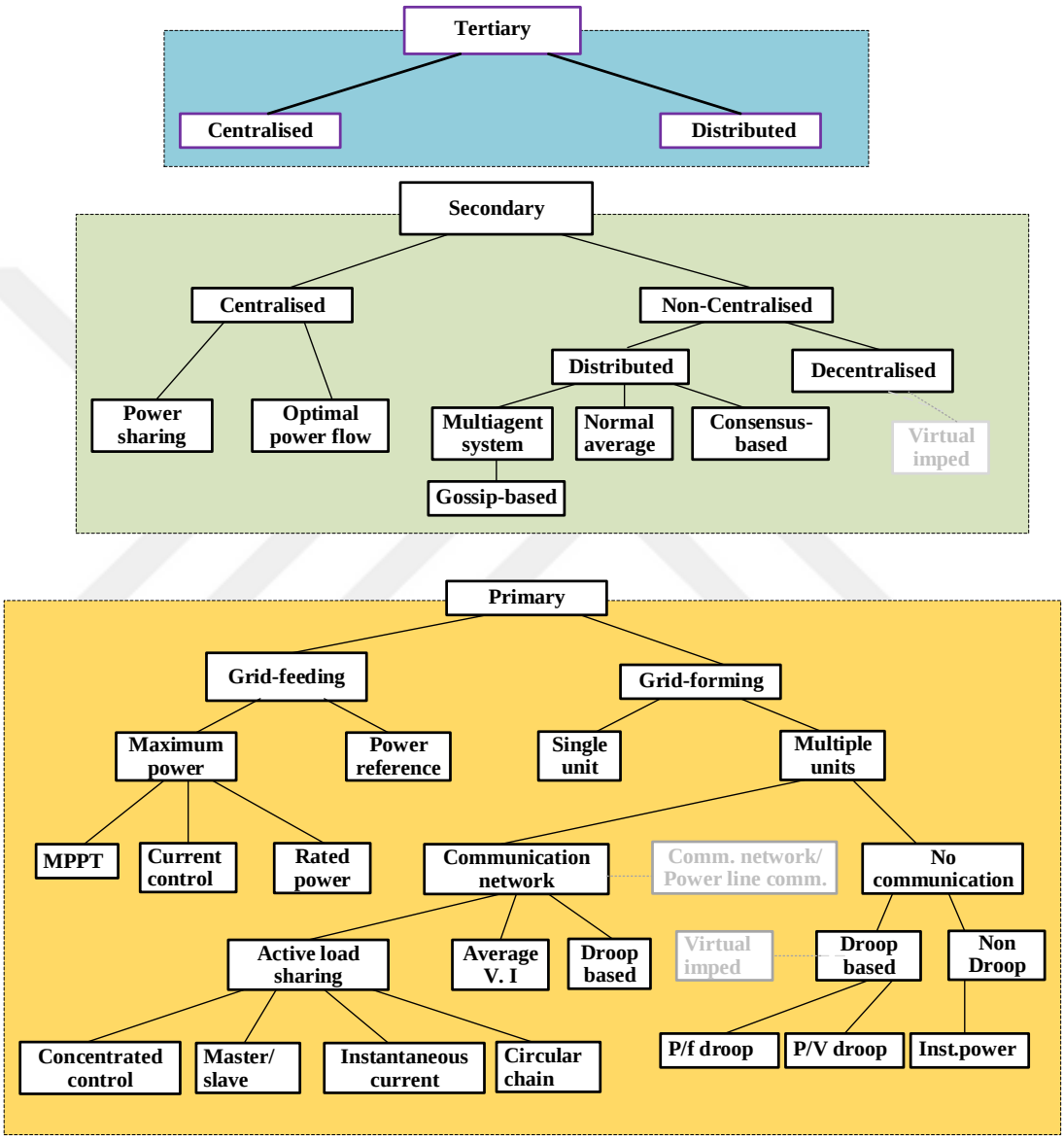

Figure 3.2. Classification of MG control strategies.

3.1. PRIMARY CONTROL

The primary control level is the first level in the control hierarchy and implemented at every DG. Main difference of this level from another levels that It requires no

communication. According to the literature, the main function of the primary control can be expressed as follows [21,63]:

- Stabilizing the voltage and frequency: after switching to the island mode, there may be unstable frequency and voltage in MG because of a mismatch between power generation and consumption.
- Locally-controlled DG units
- Droop control for power-sharing
- Over current/voltage protection
- Providing the capability of plug and play to DGs
- Decreasing the circulating current and damages to the DC-link capacitor
- Generator controls for rotating machines
- Islanding detection for individual DG units.

Usually, two levels of primary control have been recognized in the literature, depending on their function [61]:

- Grid-feeding controls
- Grid-forming controls.

3.1.1. Grid-feeding Controls

While operating the MG in grid-connected mode, the frequency and voltage of the MGs form on the utility grid; therefore, the local RES system controllers normally operate in a current-control mode for extracting maximum power from energy resources like the maximum power point tracking (MPPT) mode in a photovoltaic system or wind turbine, in which, rated power operate in biomass or diesel generators. [59]. Besides, these controls have the capability of working on a non-optimal point in the maximum power range. Commonly, this approach is used with a purpose of optimizing power-sharing network strategies, which are equally used in AC and DC units while AC-based synchronization is a main difference [64]. In a research paper [65], some relevant grid-feeding DG system control strategies are used for synchronizing the most suitable network for DGs operating in an AC network. The

strategies include grid voltage filtering, zero crossing, and phase locked loop (PLL). A study has been conducted to review some primary control strategies [61]. In this study, the authors identified common techniques used in the grid-feeding method, which include stationary reference frame ($\alpha\beta$), synchronous reference frame (dq), and natural frame (abc).

3.1.2. Grid-forming Control

The strategies of grid-forming control are implemented through voltage control when the MG is in the islanded mode, and in this mode, at least a single converter should operate, which provides the voltage reference [66]. The DG units require the network voltage control when MG is in a grid-forming mode. In this context, two configurations have been identified [25]:

Single grid-forming: In this type of grid formation, an interface converter, which is connected to the DG units, operates in the grid-forming mode while it is connected to supply a specific frequency and voltage. The remaining devices, which are linked to this network, absorb the maximum power through energy resources in the grid-following mode [25].

Multiple grid-forming: It is used as a strategy when multiple converters are controlled in the grid-forming mode, which requires synchronization process to ensure the stability of frequency and voltage for AC as well as DC MGs that results in a balanced process of power-sharing. Research shows that this kind of approaches are distinguishable, which depends on the interconnection between the interface converters [67-69]. An example has been filed in a research paper [68]. The classification was observed during a wide-ranging review of the grid-forming control strategies that has multiple DG converters. Figure 3.2 shows that the multiple units' primary control in grid- forming situation can operate:

- With communication link;
- Without any communication link.

3.1.2.1. Control Methods with Communication Link

This method is usually based on active load sharing, i.e. using parallel configuration of converters. The active load sharing process requires higher bandwidth control and communication links but that offers high power quality with limited current sharing [70]. The reference point of the current or active/reactive power can be determined by means of approaches like concentrated, master-slave, circular chain control, and average load sharing methods; so, active load sharing has the following options [61,71,72]:

- *Concentrated control,*
- *Master/slave,*
- *Instantaneous current sharing*
- *Circular chain* approaches.

In the *concentrated control* method, both reactive as well as active powers are controlled through a centralized controller. Such strategies require a communication link between the units and the central control. So far, the concentrated method is introduced in two versions, including the *central limit control* [73,74] and the *power deviation* [75].

The *central limit control* is equipped with a voltage controller, which provides reference voltage while a controller defines the reference value of current for other units. This value depends on load variations and the total units. This method assures high power quality; so even during transients, the power is controllable. This method has a shortcoming that it requires a link that allows high-bandwidth communications [25,61].

The *master-slave* control strategy makes a master converter operate as VSC to regulate the voltage output, for which, the slave converters work like individual current-source converters, which follow the master converter's current pattern. A master unit can be either central or decentralized. This method has a grid-connected operational mode,

and in case only a central controller is functioning, the grid becomes master; therefore, the island mode and special control should not be detected [76-78].

The *instantaneous current sharing* process implies average current-sharing without needing any master unit. The voltage and current reference are individually determined in each module with the help of voltage-reference synchronization and a common current-sharing bus, but not the load current.

The *circular chain* control works using the principle of current-sharing, and in this process, the current and voltage values (reference values) are determined by calculating the peak-value of phase angle and voltage amplitude; thus, this method is termed as "peak-value current-sharing technique." In fact, when the island-mode operation is in progress, a voltage-based control converter obtains the reference value while the other converters just use a current-control loop [79,80].

3.1.2.2. Control Methods without Communication Link

A primary control strategy that has no communication link works on the basis of droop control. These controls are reliable and have low cost as compared to other communication processes [55]. The mentioned droop-based control is a common and popular method, because there is not communication between the devices [81-84]. In the last ten years, many researches were conducted on this topic because it has certain advantages as compared to other alternatives like power sharing, plug and play, and besides, it results in few faults because it is simple and there is no communication network.

The droop control principle for the MV and HV networks works because of synchronous generator control. An important difference between MGs, which are equipped with converters, and the one equipped with synchronous generators is inertia. When inertia is low in MGs, it implies that active and reactive power strategies have online features [60,68,85].

The droop control changes the voltage frequencies and amplitudes depending on reactive and active demand for inter-device power-sharing. It is a widely-used strategy to share power of the synchronous generators operating in a traditional utility grid. Generally, in MGs, the ESS units often have a capability to perform optimal current-sharing that operates in grid-connected or islanded modes. In addition, it has limited integration in the DG systems, which is generally limited to the islanded mode because it performs at an optimal power-sharing point.

Conventional droop methods operate with a principle that has an equivalent circuit of an AC bus connected to a VSC as Figure 3.3 shows. In case high frequency harmonics and switching ripples are neglected, a VSC is modeled as the AC source, while the voltage can be expressed by $E\angle\delta$. Moreover, it is assumed that normal AC bus voltage is $V_{com}\angle 0$ while the impedance of the converter output and the line join as a single effective line impedance, which is $Z\angle\theta$. The common AC bus receives complex power, which is calculated as:

$$S = V_{com}I^* = \frac{V_{com}E\angle\theta - \delta}{Z} - \frac{V_{com}^2\angle\theta}{Z}, \tag{3.1}$$

where, real and reactive powers are:

$$\begin{cases} P = \frac{V_{com}E}{Z}\cos(\theta - \delta) - \frac{V_{com}^2}{Z}\cos(\theta), \\ Q = \frac{V_{com}E}{Z}\sin(\theta - \delta) - \frac{V_{com}^2}{Z}\sin(\theta). \end{cases} \tag{3.2}$$

If the line impedance is effective, $Z\angle\theta$ is purely inductive, $\theta = 90^o$, so Equation 3.2 can be mentioned as:

$$\begin{cases} P = \frac{V_{com}E}{Z}\sin\delta, \\ Q = \frac{V_{com}E\cos\delta - V_{com}^2}{Z}. \end{cases} \tag{3.3}$$

In case of small δ, which is the phase difference between the common AC bus voltage and the converter output voltage $\sin\delta \approx \delta$ and $\cos\delta = 1$; so, it is possible to apply

the voltage droop and frequency characteristics, which fine-tune the VSC voltage reference, as Figure 3.4 shows

$$\begin{cases} \omega = \omega^* - D_p P, \\ E = E^* - D_Q Q, \end{cases} \tag{3.4}$$

where: E^* – DG output voltage and the RMS value when there is no-load;

ω^* – angular frequency;

D_P and D_Q – the droop coefficients.

It is possible to adjust the droop coefficients heuristically or tuning algorithms (such as the particle swarm optimization method). The former approach shows that D_P and D_Q have been determined through the power rating of the converter and maximum allowable frequency and voltage deviations [86]. In an MG that has *n*-numbers of DGs, with D_P and D_Q as they satisfy the given constraints [87].

$$\begin{cases} D_{P1}P_{n1} = D_{P2}P_{n2} = \dots D_{PN}P_{nN} = \Delta\omega_{max}, \\ D_{Q1}Q_{n1} = D_{Q2}Q_{n2} = \dots D_{QN}Q_{nN} = \Delta E_{max}, \end{cases} \tag{3.5}$$

where: $\Delta\omega_{max}$ and ΔE_{max} represent the highest possible angular frequency and voltage deviations;

Moreover, P_{ni} and Q_{ni} represent the nominal active and reactive powers in the *i*-th DG. When the MG is in a grid-connected operational mode, angular frequency and the DG voltage ω E, are grid-enforced. The active and reactive power references of the DG output, P_{ref} and Q_{ref} are respectively adjusted through E^* and ω^* [88] as

$$\begin{cases} P^{ref} = \frac{\omega^* - \omega}{D_P}, \\ Q^{ref} = \frac{E^* - E}{D_Q}, \end{cases} \tag{3.6}$$

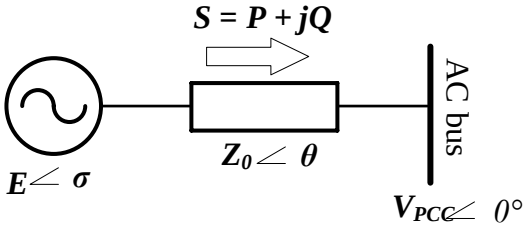

Figure 3.3. Equivalent circuit of connection between VSC and AC bus.

According to the equivalent circuit of the system (Figure 3.3), active power in Equation 3.3 and frequency in Equation 3.4 for the conventional droop control's dynamic response are linearized as:

$$\begin{cases} \Delta P = G\Delta\delta \\ \Delta\omega = \Delta\omega^* - D_P\Delta P. \end{cases}, \tag{3.7}$$

Here at the operating point of V_{com0}, E_0, and δ_0

$$G = \frac{V_{com0}E_0}{Z} \tag{3.8}$$

and

$$\Delta\delta = \int \Delta\omega dt. \tag{3.9}$$

Thus, through Equation 3.4, we can get:

$$\Delta P(s) = \frac{G}{s+D_PG}\Delta\omega^*(s). \tag{3.10}$$

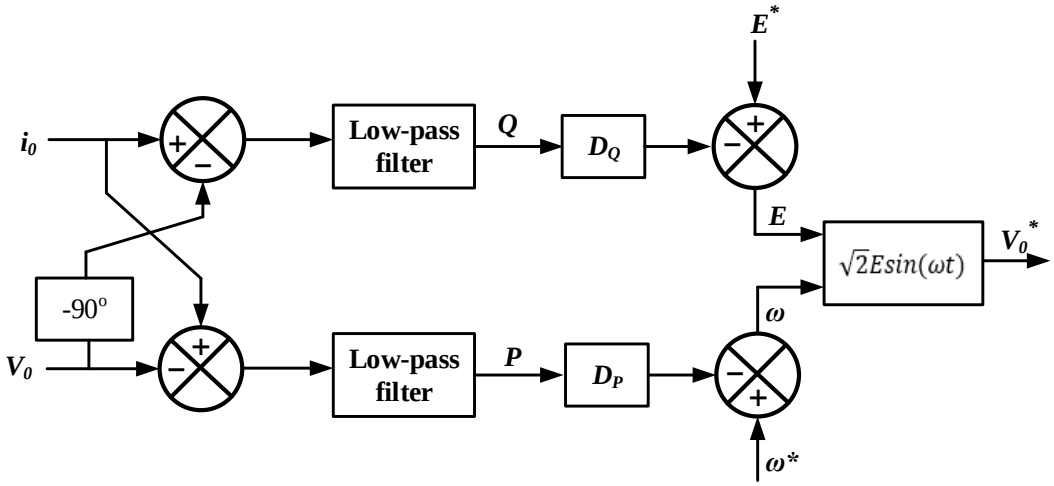

Figure 3.4. Conventional droop method.

Another procedure is adopted for extracting the reactive power control and its small-signal model. The small-signal model can be expressed in a block diagram (Equation 3.4), which is illustrated in Figure 3.5. Equation 3.10 shows the closed-loop control's time constant that is adjusted when D_p is tuned. According to Equation 3.4, D_p affects the DG frequency; therefore, there is a basic trade-off, which exists between the frequency regulation and the time constant of the control system.

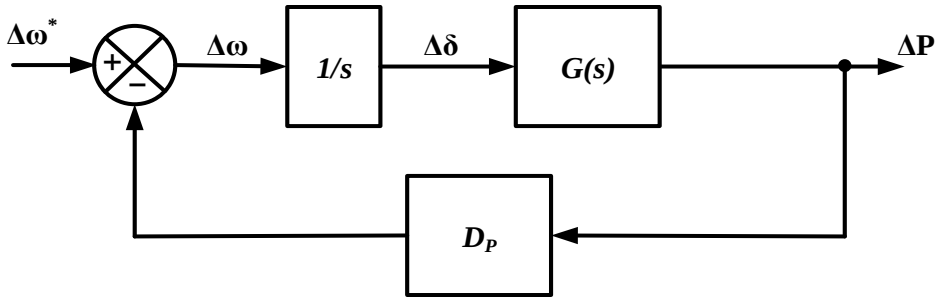

Figure 3.5. Small-signal model (conventional active power control) [56].

Contrary to the active load-sharing method, the droop method is implemented without a communication link, so, it is considered as reliable. The conventional droop method has the following drawbacks [89-92]:

- Although for each droop characteristic, there is just a single control variable. Satisfying more than a single control objective is impossible. For instance,

a design trade-off should be considered between the voltage and frequency regulation and the time constant of the control system.

- The traditional droop methodology has been developed considering highly-inductive impedance between the AC bus and the voltage-controlled voltage source inverter (VCVSI). Still, in MG applications, this assumption is challenged because the low-voltage transmission lines show resistance; therefore, Equation 3.3 is invalid for the MGs.
- Contrary to the frequency, voltage is not considered as a global quantity for MGs; so, the reactive power control has been expressed in Equation 3.4 that can negatively affect the critical loads of the voltage regulation.
- When there are non-linear loads, the traditional droop methodology cannot distinguish the current harmonics of the load from its circulating current. In addition, the DG output voltage is distorted as a result of the current harmonics. It is possible to modify the conventional droop method for reducing the output issue, termed as total harmonic distortion (THD).

The conventional droop methods have potential advantages and disadvantages for AC MGs, that has been published in a research paper [55]. There are some conclusions about this method:

- It is needed to identify the system to find out some techniques' line parameters like virtual frame transformation methods and adaptive voltage droop.
- The droop techniques in the modified form, other than the LV MGs, decouple the control of active and reactive powers.
- The only techniques, which offer voltage regulation, include adaptive voltage droop and adjustable load sharing methods.
- The complicated control techniques like virtual impedance should be used to accommodate the nonlinear loads. Other methods like the signal injection, or non-linear load sharing mitigate harmonics in the MGs.

3.2. SECONDARY CONTROL

This control level has a main purpose to compensate the deviations in frequency and voltage in the networks, which form the MGs (DC side of MGs). When any change takes place in the load/MG generation, the difference is regulated by a secondary control. The mentioned difference exists between the established frequency/voltage reference and measured values [93]. The secondary control is a main hierarchical control when it operates in the islanded mode; so other features like resynchronization or black-start management are needed on this level when there is transition from the islanded to grid-tied operational mode. Figure 3.6 shows the principles of the microgrids' secondary control level. Practically, the secondary control shows slow dynamic response to variations when compared to the level of primary control [55].

The strategies of secondary control are either centralized or decentralized [14,94,95]. The control levels adopt different responsibility levels, depending on the state and the architecture of the MG.

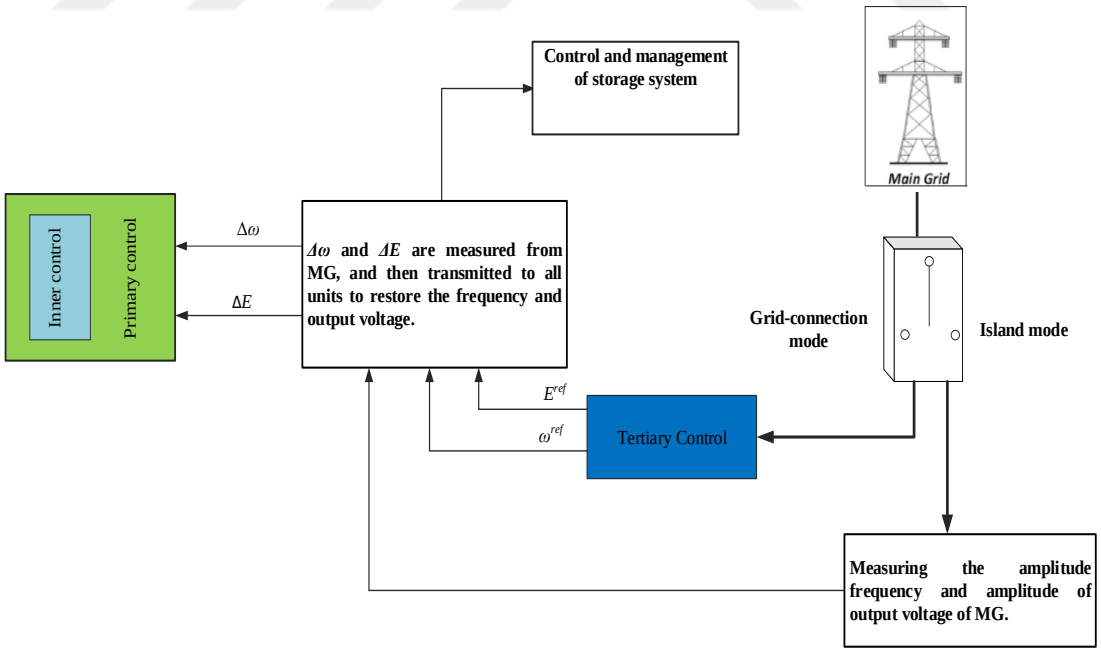

Figure 3.6. The principle behind the secondary control strategy in MGs [61].

3.2.1. Centralized Control

This technique of MG control is generally implemented through a central controller, which exists at the global control level, which is normally termed as MG central controller (MGCC). This kind of strategies are very difficult to implement in cases when several devices are interconnected in different locations while their owners' interests are not the same. Such control form is suitable to manage small MGs with a single or a few DG and ESS owners, providing with high-end plug-and-play options [95]. In fact, the distinction between centralized or decentralized control depends on the MGCC and its position. Figure 3.7 shows the control structure of centralized secondary MG control.

In this kind of control, the measurement of frequency/voltage amplitude of DERs is done, and it is compared to the reference values, which are obtained using the main network (when MG is grid-connection). Equation 3.4 uses Park's transformation that is substituted as given below:

$$\begin{cases} \omega = \omega^{ref} - T_{P(S)}[(P - P^{ref})sin\theta - (Q - Q^{ref})cos\theta], \\ E = E^{ref} - T_{Q(S)}[(P - P^{ref})cos\theta - (Q - Q^{ref})sin\theta], \end{cases} \tag{3.11}$$

where:

$$T_{P(s)} = \frac{\overbrace{f^{ref} - f^{min}}^{\Delta f}}{\underbrace{P^{ref} - P^{max}}_{\Delta P}} < 0, \quad T_{Q(s)} = \frac{\overbrace{E^{ref} - E^{min}}^{\Delta E}}{\underbrace{Q^{ref} - Q^{max}}_{\Delta Q}} < 0$$

In this case, the measurement error is sent to primary control, which restores the frequency and voltage; so, the restoration compensator will be as follows:

$$\begin{cases} \Delta\omega = G_{pf}\left(\omega_{mg}^{ref} - \omega_{mg}\right) + G_{if}\int\left(\omega_{mg}^{ref} - \omega_{mg}\right)dt + \delta f_s \\ \Delta E = G_{pv}\left(V_{mg}^{ref} - V_{mg}\right) + G_{iv}\int\left(V_{mg}^{ref} - V_{mg}\right)dt \end{cases} \tag{3.12}$$

For connecting an MG to a grid, first the measurement of the frequency and voltage is done because they serve as reference values for the secondary control. Synchronization control loop synchronizes the phase angle between the grid and MG that disables when the grid ($\delta f_s = 0$) is absent but in grid-connected mode, a phase-locked loop (PLL) module performs the synchronization that helps measuring the voltage angle that is required for the inverter control [21,96].

Based on the discussion above, the centralized control strategy is more suitable at the secondary control level for the following MGs [95,97,98]:

- Small MGs that involve low communication and computation costs for centralized decision-making and information collection.
- All the microgrid properties are based on a common goal to help the EMS/MGSC, which operate the MG as a unity;
- Some military/defense-related MGs that require high privacy;
- When there is almost a fixed system configuration that doesn't needs high expandability/flexibility.

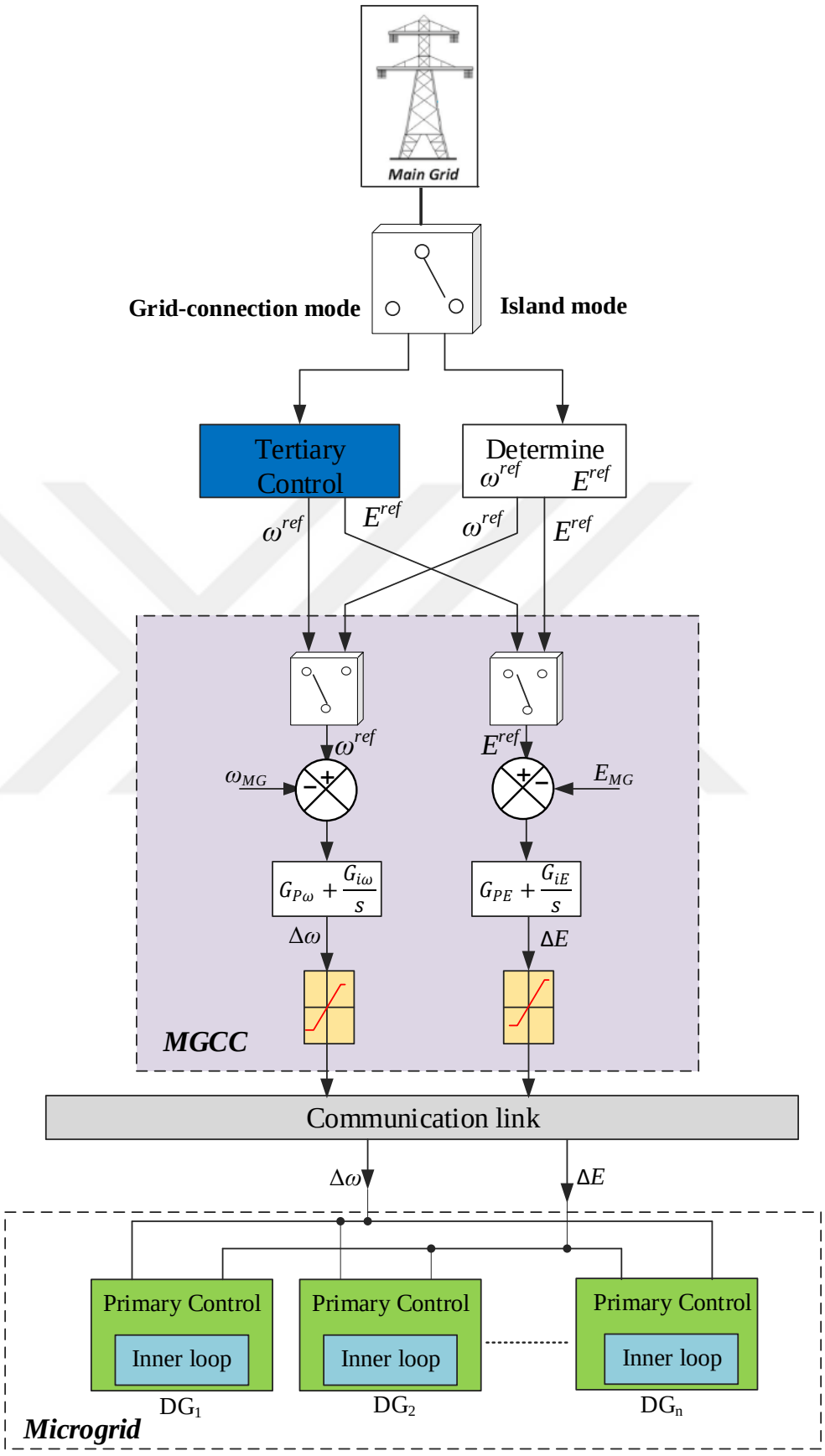

Figure 3.7. Centralized secondary control structure [21].

3.2.2. Decentralized Control

The decentralized control mainly performs the duty to specify the maximum power that a controller generates while considering the MG's capabilities, which support the consumers and improve the addition of power to the grid. Figure 3.7 shows the secondary controls and their location keeping in view the primary controls and the communication link. This method distributes the secondary control outcomes (the error) to the primary controllers but Shafiee et al. [99] suggested another distributed secondary control process that has a secondary control with every primary control and before the communications link. It means that this process shifts the MGCC role to control and support the primary controls. Figure 3.8 shows the control structure of a decentralized secondary control that measures the frequency and voltage amplitude over the communication link. Later, the measured values' average is shifted to the primary control with the measurement errors to restore voltage and frequency.
Normally, there are two methods of decentralized control [57]:

- Distributed control
- Decentralized control.

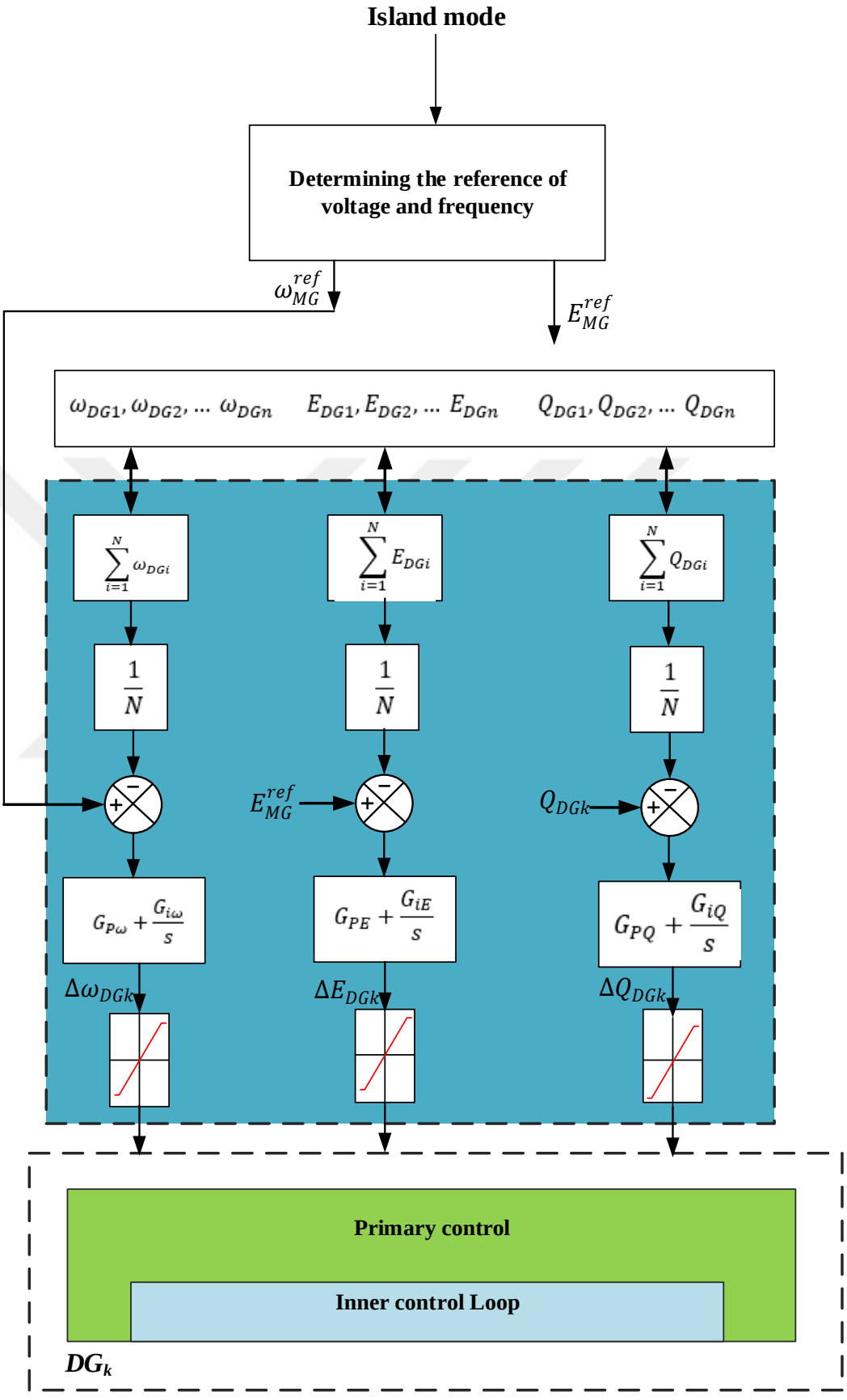

Figure 3.8. Decentralized secondary control structure.

3.2.2.1. Distributed Secondary Control

It is a frequently-studied secondary technique that shows good performance and needs comparatively simpler communication network (Figure 3.9). In a research paper [58], the researchers performed some suitable solutions, including agent-based processes, which show higher performance as compared to both decentralized and centralized methods because of interaction between the MG units. The multi-agent systems (MAS) offer solution to the MGs' distributed management. According to this approach, every local controller performs like an agent to control the DG or ESS unit parameters. In this case, the communication takes place just between neighboring devices because it is a distributed strategy.

The communication between various devices within MG system through a wireless connection is accomplished through a MAS-based control algorithm. It has been discussed in a research paper [100]. According to the authors, even when the MG convergence is slower because of interferences in the vicinity, the strategy increases the performances of MAS-based algorithms through decreasing the multi-agent coordination errors.

Despite MAS-based methods, the literature includes other distributed strategies, for example, Shafiee et al. suggested several secondary control strategies for controlling frequency and voltage, which assure reactive power sharing [99,101]. The strategies, which have been mentioned in the literature, are divided into three groups: gossip-based (a MAS technique), normal averaging, and consensus-based strategies. The normal averaging control strategy was validated and experimentally compared to the centralized control structure. The researchers concluded that the strategy performs well and considerably simplifies the communication network [99].

Another approach has been proposed in the literature [102], when the technique called distributed averages was applied to the secondary frequency and voltage control. According to the authors, each device has a control strategy that just needs the neighboring devices' information to share power and control frequency. Some researchers [103] used the average voltage sharing strategy to compensate the voltage

deviations, which are consequences of the primary droop-based control. Another study was performed by several researchers [104], which integrated the voltage sharing and the average current sharing techniques for regulating the bus voltage and promoting accurate current sharing.

It is possible to restore voltages and frequencies through consensus-based secondary control strategy, and the power-sharing is assured among the connected devices [105].

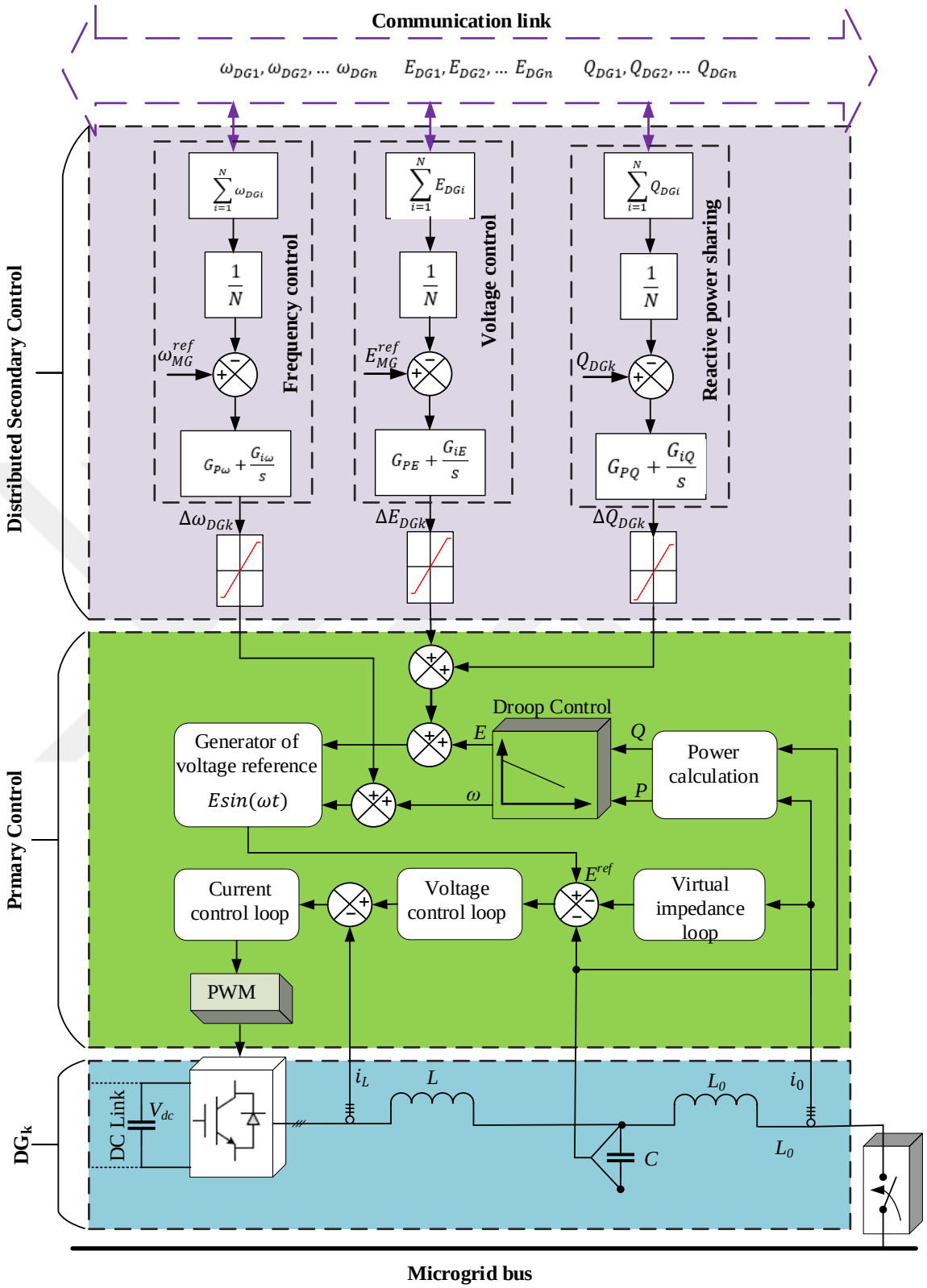

Figure 3.9. Distributed secondary control of MG [99].

3.2.2.2. Decentralized Secondary Control

For MG systems, decentralized control strategies are suitable because they do not require communication; so, it is possible to assure plug and play connections, and it is possible to correctly perform the power sharing despite variations in loads [106]. In this strategy, control strategies depend on locally-measured parameters. Local variables are used in decentralized control strategies to perform the ESS unit control that fuzzy inference-based. Adequately balancing the charge in the ESS is possible when there is low-voltage deviation [107]. In the same way, for restoring the frequency deviation of the droop primary control, a decentralized secondary control strategy is used [108].

Moreover, distributed and decentralized secondary control strategies were compared that indicates that the distributed control strategies show better reliability and performance as compared to decentralized controls in the secondary level, and require no communication [53,109].

It is obvious in the table that for MGs, the centralized approach is effective in case of a single owner or in case when multiple owners have the same interests; so, it is used for small MGs, which have few but integrated control-able devices, and some expected future integrations but still, MGs, which are managed through non-centralized controls, have the largest MG applications, because they allow high flexibility through adding some plug-and play devices. MGs, which are administered through decentralized controls, have several applications, which offer high flexibility when plug-and play devices are connected.

3.3. TERTIARY CONTROL

In the grid-connected situation, tertiary controls manage active and reactive power flows between the main grid and the MG through frequency and voltage regulators. When the P/Q ratio is evaluated through the PCC, both active/reactive powers are compared to the reference values, which is the slowest and final control level. The tertiary control scheme has been illustrated by Figure 3.10. It provides economically-

optimal operations using the gossiping algorithm or grid-following power converters [55,64]. In the technical sense, when there is any non-plane islanding fault, the tertiary control absorbs P from the grid. In case, the grid is unavailable, it will decrease the frequency. In case when the expected value is attained, the MG disconnects from the grid for the purpose of safety, and it disables the tertiary control [60]. Just like the secondary control, this level can be implemented in one of the two ways: First, it is a centralized strategy, in which, the tertiary control exists at the MGCC (SCADA system), or it can function as a distributed methodology, in which, the entire control lies at the local levels.

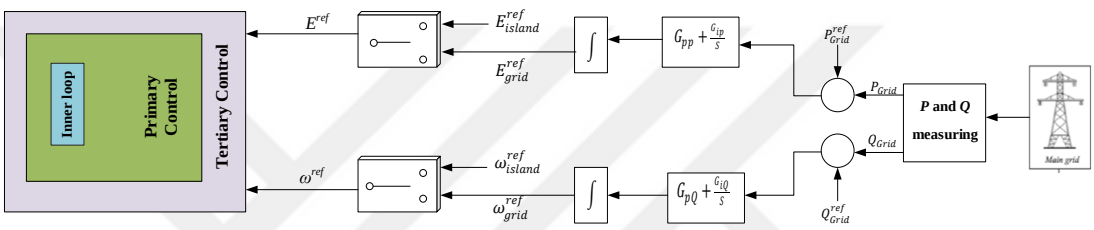

Figure 3.10. Structure of tertiary control in MGs.

3.3.1. Centralized Tertiary Control

This technique requires measurement of power values at the PCC, which are compared to the required outcomes. The reference values of P/Q have been obtained keeping in view the microgrid power needs and the situation of the market factors (power generation, energy cost, storage, and load forecasting). Thus, it is possible to optimize different variables including economic benefit, efficiency, power quality, and simplicity of control.

This type of control level has been explained in a research paper on microgrids [21], whereas MGs' centralized controls have three levels. This solution shows how active and reactive powers are calculated in the PCC. They are compared with desired values for generating the reference frequency and voltage values on the secondary level. Simulation was conducted to test the algorithm, which showed that the overall control strategy showed good overall performance in islanded, grid-connected, and

transitioning cases. Furthermore, the researchers mentioned that the multiple microgrid management is feasible through the proposed control technique.

3.3.2. Distributed Tertiary Control

Generally, tertiary controls are not in the MGs, but they are placed in the main grid's MGCC (at SCADA). Still, some approaches exist, which place the tertiary control in the MGs in a distributed way [110]. This research paper is based on an algorithm, which is a tertiary gossip-based control algorithm, which is located where the local controllers are located. Furthermore, these devices are interlinked through internet that increases both the efficiency and reliability of the overall system.

Despite the fact that the mentioned strategies substantially increase the MGs' flexibility, employing centralized tertiary control strategies is the most common trend in the literature. A main reason behind this trend is the inter-device coordination between the devices linked to the MG. Such factors include factors like demand and generation profiles, forecasting, MGs' energy flow, and energy marketing.

PART 4

MICROGRID MODELING AND DYNAMICS

It is significant to understand that applying the right modeling technique is essential for significant microgrid (MG) control issues and analyzing its stability. Despite the fact that MGs are mostly small-scale, they still have several complexities, which large traditional power systems also have; so, they need dynamic analysis to assure stability in the MG operations keeping the frequency and voltage under control. Specifically, all the transitions from grid-connected to islanded mode might create some issues. The MG dynamics are likely to change depending on the type, configuration, and components,, and besides, different modeling methodologies are needed for different applications. Many researches show that dynamic stabiltiy analysis and modeling MGs is tougher as compared to the same procedures in the traditional power systems, and sometimes, they can be very challenging [14,111-115]. These difficulties exist because of certain reasons, which are given below:

- Closer proximity to electricity, dynamics' speed, and short-duration DG/RES response time;
- Intrinsic imbalance in the MGs' nature;
- Lack of inertia and low capacity to store energy storage capacity;
- Existence of several and diverse power electronic converters, power microsources, and influencing devices or circuits;
- High parametric or topological uncertainty.

Dynamic modeling is generally conducted to analyze the stability (small-signal stability) of MGs. Traditional power grids are generally stable because they have well-established stability analysis since they use standard, tried and tested models of governors, synchronous machines, and excitation systems that have different orders, which can capture significant modes to deal with specific problems. In MGs, they

still do not exist, which can be hard-to-achieve because in this case, it is possible to deploy a wide range of power technologies [116].

4.1. STUDIED SYSTEM CHARACTERISTICS

Karabuk University campus has over 53,000 people including students, staff, and academic personnel; so, its power consumption is significant. There are some issues such as increasing utility bills, indirect carbon emissions, and cost of maintaining a complex distribution infrastructure that provides electricity to the large university community. The management of Karabuk university has intended to reduce energy consumption and power managing costs by integrating solar photovoltaic (PV) panels to the utility grid of the university campus. Nowadays, PV panels have been installed in five of eight main educational buildings of Karabuk University (KBU) campus; therefore, MG planning, modeling and design are performed in this work on the example of Engineering faculty at KBU.

Demir Celik Campus is the central campus of Karabuk University with building area 3.5 million m^2. Karabuk University latitude is 41º12'22"N and longitude is 32°39'35"E. Demir Celik Campus of KBU is shown in Figure 4.1. Engineering faculty building of KBU is chosen as a case study for microgrid.

Figure 4.1. Engineering faculty in Demir Celik Campus of Karabuk University.

The electric power of Karabuk University (KBU) campus is supplied by power supply substation of BAŞKENT EDAS A.Ş. Electric power supply structure of KBU is illustrated in Figure 4.2. Engineering faculty building of KBU is chosen as a case study for microgrid. Power supply of the building is provided by substation TR 6 (red dashed lines in Figure 4.2). The proposed KBU engineering faculty MG is a 50 Hz MG with 0.4 kV LV network, which consists of a diesel generator, a few PV panels, a battery storage system, and two load types: critical (controllable) and non-critical loads (non-controllable).

Technical specifications of KBU substation and distribution center transformers are given in the *Appendix A*. Technical characteristics of PV panel, battery storage unit and inverter are given in *Appendix B*, also distribution panel of Engineering faculty that is used to specify loads is given in *Appendix C*.

Critical loads – when power supply of loads must provide by energy source independent of normal main grid distribution networks and has to be maintained under any circumstances Power supply to these loads should not ever be interrupted during 24 hours in day.

Non-critical loads are versus to critical loads will not be served during failures or outages in main grid, they just have disconnected from main power source.

Therefore, we have identified data center, heating and booster pumps, fire alarm system as critical loads that ought to be power supplied continuously at 24 hours day. Critical loads list of the Engineering faculty is given in *Appendix D*.

One of the main requirements in MG is to provide the balance between generation and demand of electricity in either island or grid-connected modes. MG in island mode should meet the balance between local supply and demand by reducing generation or load shedding. In grid-connected mode MG exchanges electricity with main grid to the balance. Therefore, the loads profile of research object is specified according to the distribution panel specification due to the smart electric meter has not installed in Engineering faculty building.

Distributed generation units are located near area of electrical consumption to prevent the possible electrical losses. Critical-load power supply is generally provided by a diesel generator and a solar PV system.

According to the research analysis [117,118] we identified that potential of wind energy in Karabuk region is low with 2.4 m/s annual average wind speed and 21.3 W/m^2 annual average wind density. Therefore, modeling of MG with wind turbine for Karabuk university is not proper.

Contrary to the traditional power systems, in the MG modeling, we generally ignore too slow/fast dynamics. In MGs, DGs act as current source inverters (CSIs), or voltage source inverters (VSIs) [119].

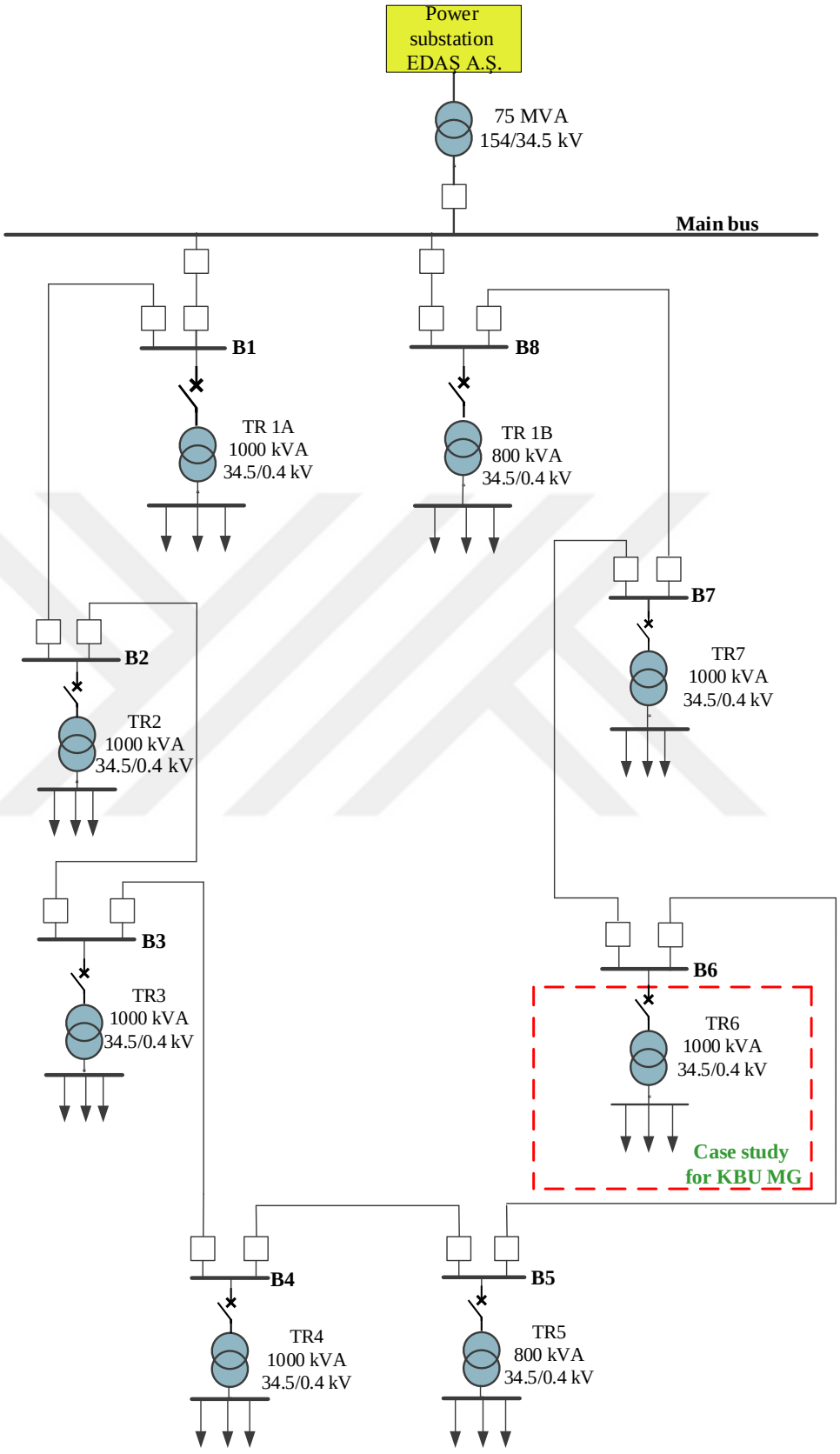

Figure 4.2. Electric power supply diagram of Karabuk University.

Single line diagram of Engineering faculty microgrid is illustrated in Figure 4.3. From this single line diagram of Engineering faculty MG, we can see that the main components of the KBU MG are in LV network and connected to main distribution network via static switch. While faults or outages occur in main grid MG will disconnect from main distribution network and critical loads can be supplied from DERs, i.e. from PV-system and diesel generator in our case.

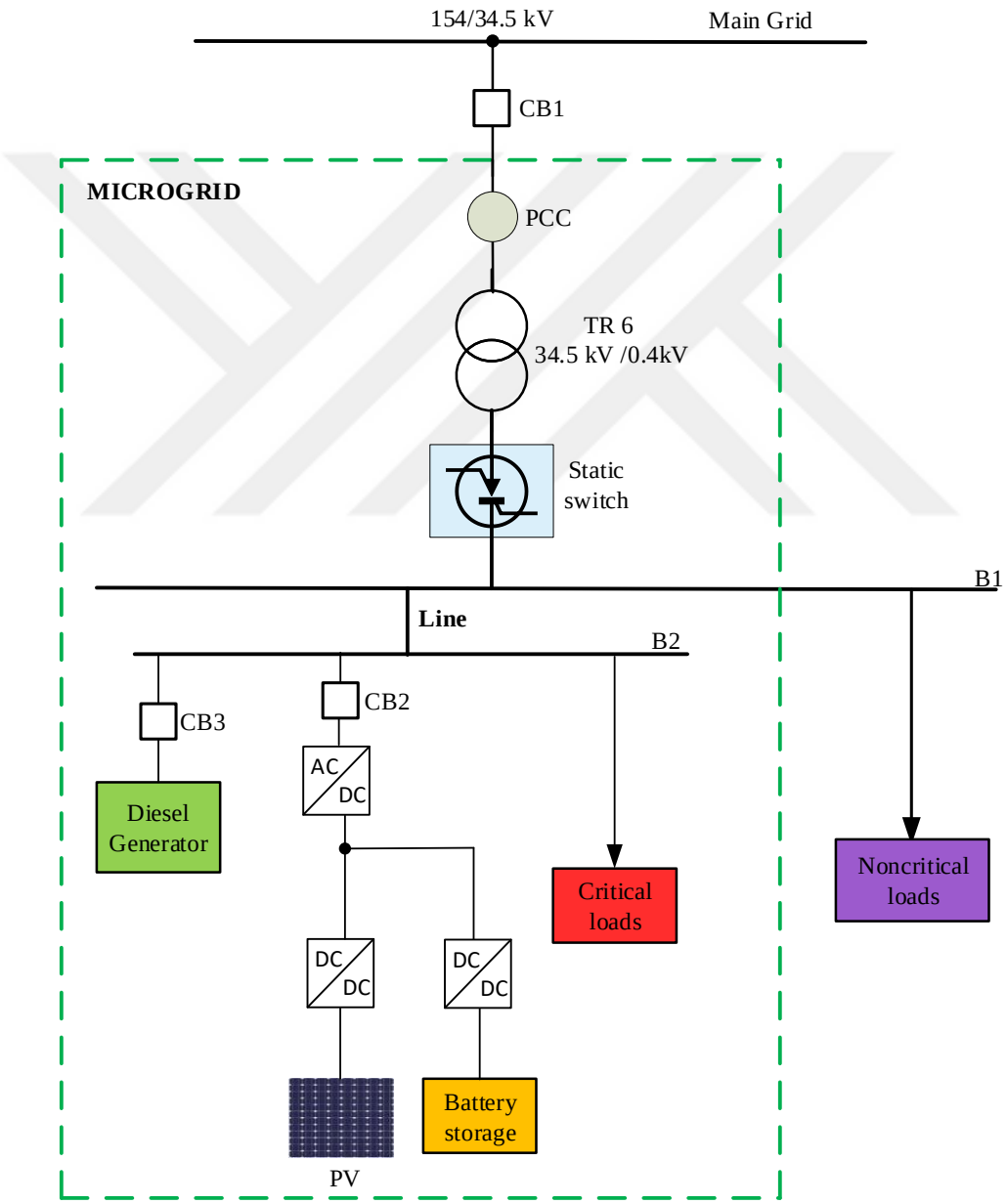

Figure 4.3. Microgrid single line diagram of KBU Engineering faculty.

Figure 4.4 illustrates the overall structure of the KBU MG in a grid-connected mode. In this overall structure are illustrated all main components of MG, a step-down transformer which is between MV network and LV network, simplified MV line equivalent circuit, grid bus and main grid. While the main components of this MG have been presented; therefore, the following MG components are considered as the parts of the model:

- MV transmission line
- Three-phase transformer
- Passive loads
- Bus (grid bus, MV bus, LV bus)
- Diesel generator
- PV-system
- Battery storage
- Voltage source inverter.

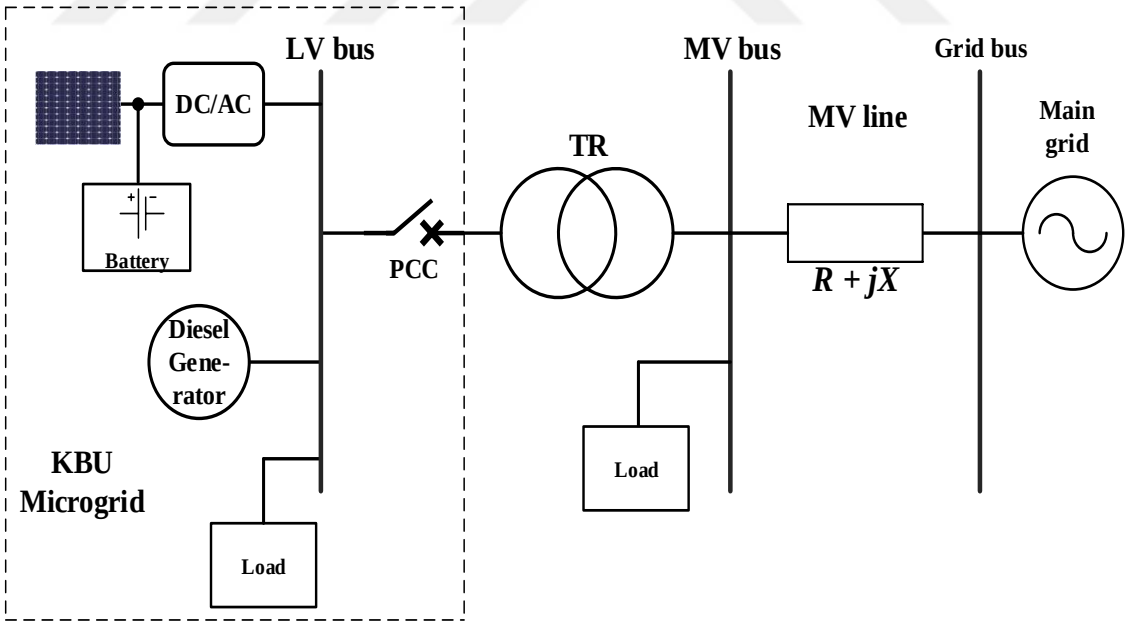

Figure 4.4. Overall structure of KBU MG in grid-connected mode.

4.2. CONNECTION MODELING BETWEEN THE MAIN GRID AND THE KBU MICROGRID

4.2.1. Modeling of the Medium Voltage Transmission Lines

The medium voltage (MV) transmission lines are modelled using the π model that has a reactance, a resistor, and a couple of capacitors in every line. In the transmission line, small resistors are used, which show the power losses. In this case, we have neglected the capacitor because of its minimum value and besides, its influence on the MG is very poor [120]. Thus, just like the three-phase filter modeling, the MV transmission line modeling can be mathematically expressed as given below:

$$\frac{di_{-lmv}}{dt} = \frac{1}{L_{mv}} v_{-lmv\_l} \tag{4.1}$$

$$v_{-lmv\_l} = v_{-lmv\_rl} - v_{-lmv_r} \tag{4.2}$$

$$v_{-lmv\_l} = C_{ucs} \cdot \left(u_{-gdb} - u_{-mvb}\right) \tag{4.3}$$

$$v_{-lmv\_rl} = R_{mv} i_{-lmv} \tag{4.4}$$

where:

$i_{-lmv} = [i_{lmv1}, i_{lmv2}]^T$ – the MV transmission line currents' vector,
L_{mv} and R_{mv} – the resistor and inductor of the model of the MV transmission line,
$v_{-lmv\_l} = [v_{lmv\_l1}, v_{lmv\_l2}]^T$ – the vector of modeled inductor terminal voltages,
$v_{-lmv\_r} = [v_{lmv\_r1}, v_{lmv\_r2}]^T$ – the modeled resistor terminal voltage vector,
$v_{-lmv\_rl} = [v_{lmv\_rl1}, v_{lmv\_rl2}]^T$ – the modeled element terminal voltage vector,
u_{gdb} = $[u_{gdb12}, u_{gdb23}]^T$ – the phase-to-phase voltage vector for the diesel group bus
$u_{mvb} = [u_{mvb12}, u_{mvb23}]^T$ – the phase-to-phase voltage vector for the MV bus,
C_{ucs} – the matrix that represents the passage from phase-to-phase voltages to the single-phase voltages.

The single-phase model of the MV transmission line has been illustrated in Figure 4.5.

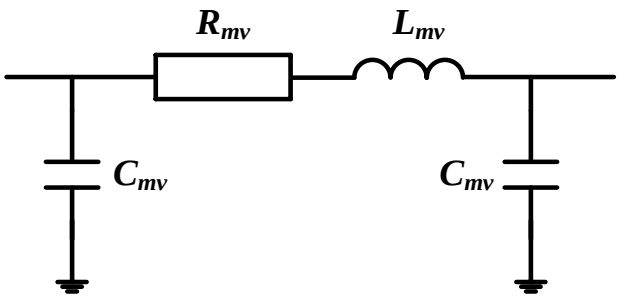

Figure 4.5. One phase model of MV transmission line.

The block diagram of MV transmission line is represented in Figure 4.6 and its single block representation is shown in Figure 4.7.

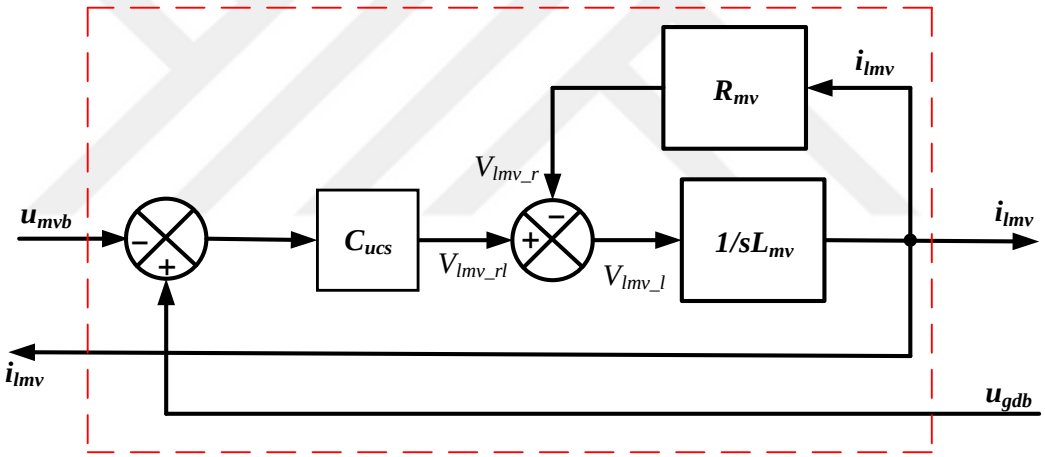

Figure 4.6. Block diagram of the MV transmission line.

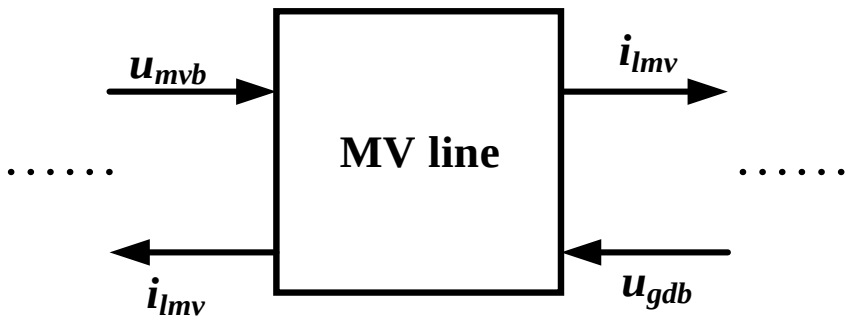

Figure 4.7. Single block representation of MV transmission line.

4.2.2. Modeling of Medium Voltage Transmission Lines

A simplified ideal three-phase transformer model can be presented as follows [119]:

$$u_{-tr} = k_{tr} u_{-mgb} \tag{4.5}$$

$$i_{tr} = k_{tr} i_{-mvb} \tag{4.6}$$

where: $u_{-tr} = [u_{tr13}, u_{tr23}]^T$ – the phase-to-phase voltage vector;
$u_{-mgb} = [u_{mgb13}, u_{mgb23}]^T$ – the input phase-to-phase voltage vector;
$i_{-tr} = [i_{tr1}, i_{tr2}]^T$ – the vector of transformer currents;
$i = [i_{mvb1}, i_{mvb2}]^T$ – the vector of input currents.

The block diagram of three-phase transformer is depicted in Figure 4.8 and its single block is illustrated in Figure 4.9.

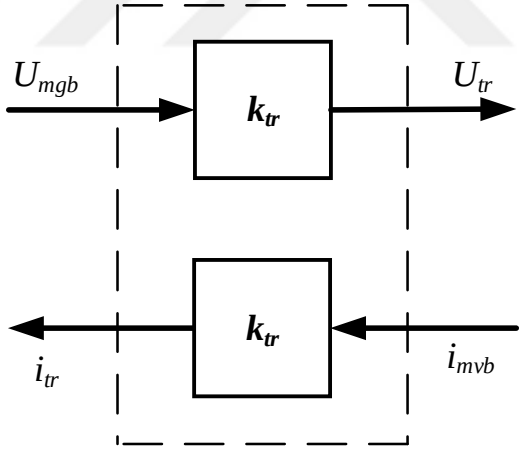

Figure 4.8. Block diagram of three-phase transformer.

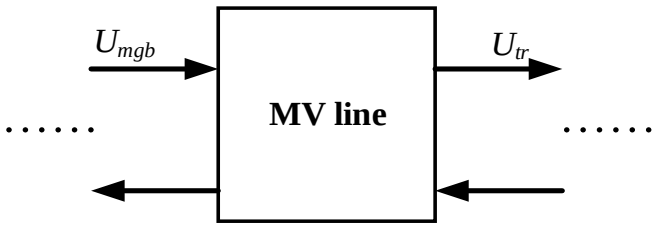

Figure 4.9. Single block of transformer.

4.2.3. Passive Load Modeling

The modeling of passive loads can be executed through two types of receptors: voltage and current receptors.

The current is the output of the voltage receptor, which can be written as:

$$i_{-cp} = \frac{1}{R_{exl}} C_{ucs} \cdot u_{-mvb} \tag{4.7}$$

where:

$u_{-mvb} = [u_{tr13}, u_{tr23}]^T$ – the phase-to-phase voltage vector;
$i_{-cp} = [i_{cp1}, i_{cp2}]^T$ – the vector of load currents;
R_{exl} – the resistor that corresponds to the actual load power (P_{exl}).

The voltage receptor load model is given in Figure 4.10.

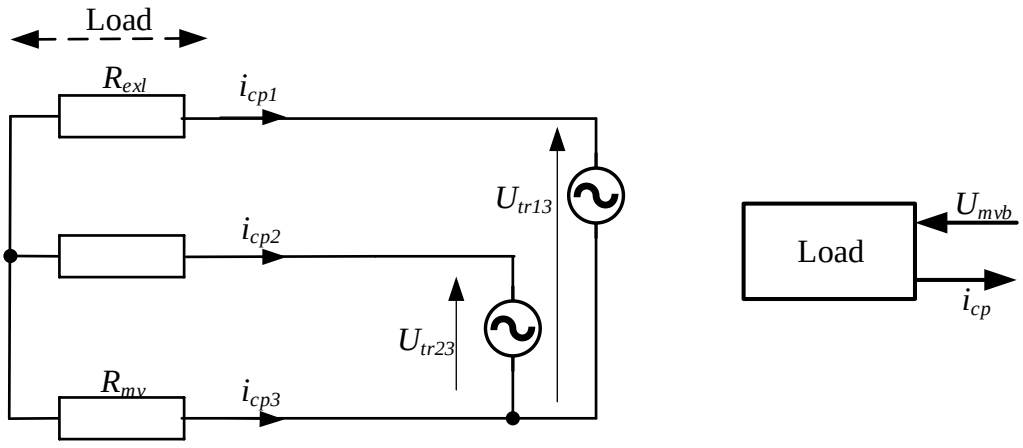

Figure 4.10. Model of voltage receptor load.

$$R_{exl} = \frac{U_{nmvb}^2}{P_{exl}} \tag{4.8}$$

where:

U_{mnvb} – shows the load voltages' nominal value.

The load on current receptor is a "phase-to-phase" or "voltage-type" source load, because it has voltage output:

$$u_{-mvb} = C_{ucs} \cdot \left(R_{exl} i_{-cp}\right) \tag{4.9}$$

where:

R_{exl} – resistor that corresponds to real load power (P_{exl})

C_{ucs} – the matrix calculated from single-phase to phase-to-phase voltages.

$$R_{exl} = \frac{P_{exl}}{I_{nmvb}^2} \tag{4.10}$$

I_{nmvb} is the load currents' nominal value.

The model of the current receptor load has been given in Figure 4.11.

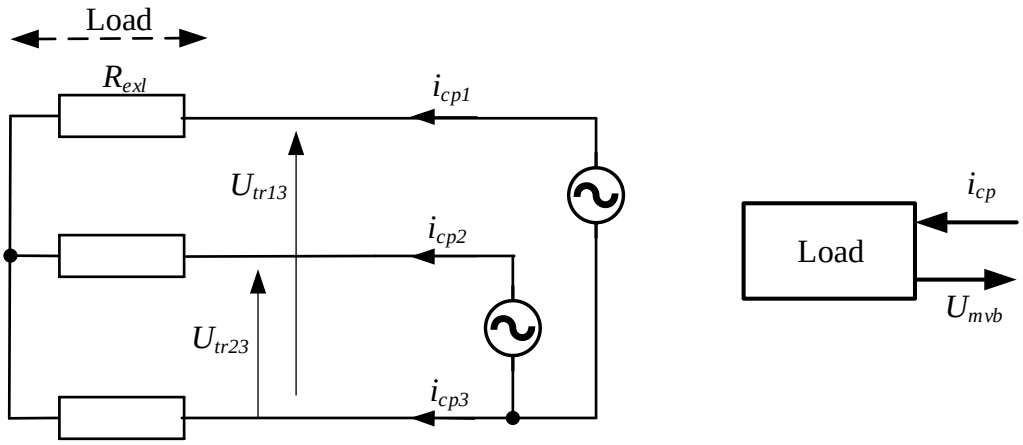

Figure 4.11. Model of current receptor load.

4.2.4. Modeling of Relevant Buses

This modeling method in a grid architecture depends on characterization process of the coupling bus. Considering that "*the bus voltage should be adjusted according to a*

unique type of voltage" because it makes the modeling of connected buses simpler between the maingrid and the MG. Consequently, various units (bus-connected) should include a single voltage-type source unit while others act as "current-type" sources. In this way, two buses including the grid bus and the MV bus exist between the main grid (Figure 4.4). Now we'll look at modeling of these buses.

4.2.5. Grid Bus

The grid bus connects just two units: the MV lines and the main grid (see Figure 4.4). Since the diesel group controls its terminal voltages, it is a voltage-type source; so, the MV lines can be modeled like a current-type source:

$$i_{-lmv} = i_{-gdb} \tag{4.11}$$

$$u_{-gdb} = u_{-gd} \tag{4.12}$$

The grid bus in single-line diagram is shown in Figure 4.12 and block diagram of grid bus is shown in Figure 4.13.

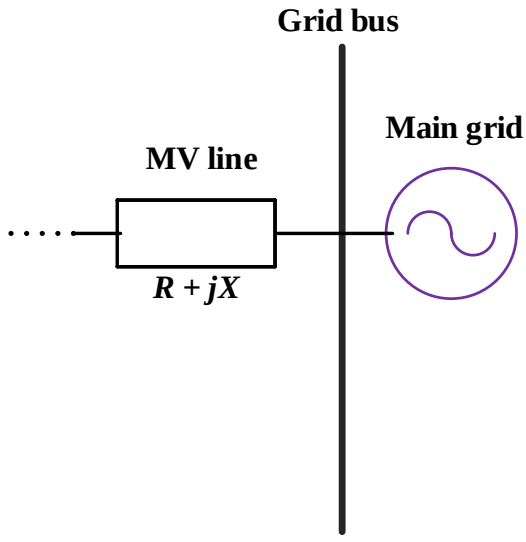

Figure 4.12. Single-line diagram of grid bus.

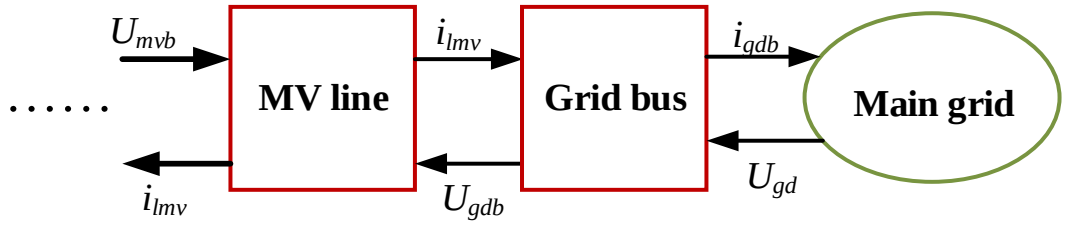

Figure 4.13. Block diagram of grid bus.

4.2.6. MV Bus

An MV bus connects three units: Equivalent MV loads, MV lines, and the transformer. In this case, the MV lines act as current-type sources that is obvious from the previous analysis; so, the transformer or the MV loads are modeled like voltage-type sources. Choosing a transformer as a voltage-type source is interesting because it always remains connected to the whole network; so, modeling of the transformer is possible like a voltage-type source while the MV loads are modeled as a current-type source. The single line diagram of MV bus model and its block diagram have been shown in Figure 4.14 and Figure 4.15, respectively.

$$u_{-mvb} = u_{-tr} \tag{4.13}$$

$$i_{-mvb} = -i_{lmv} - i_{-cp} \tag{4.14}$$

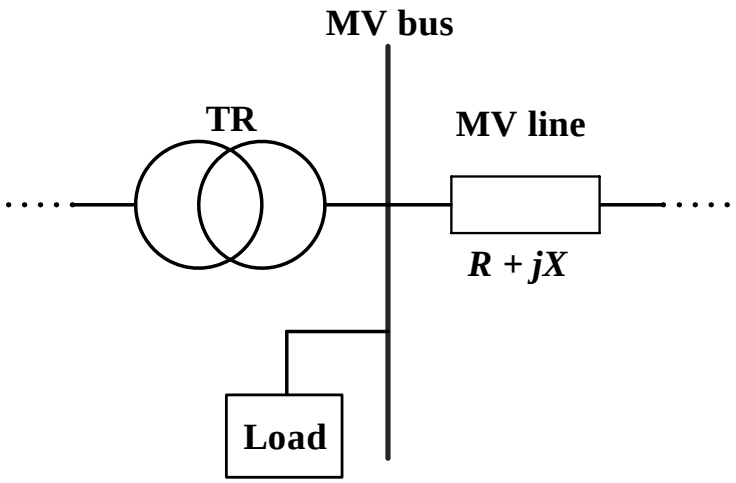

Figure 4.14. The single line diagram of MV bus.

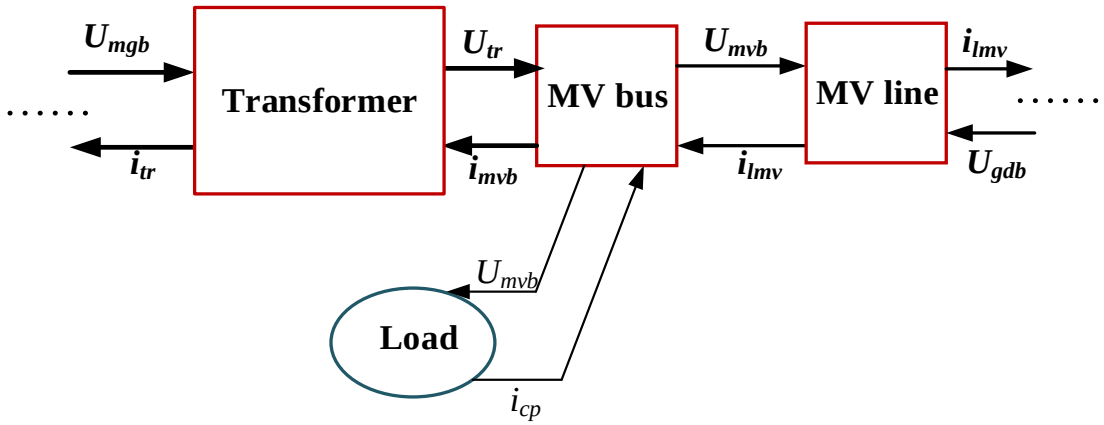

Figure 4.15. The block diagram of MV bus.

4.3. GRID-CONNECTED KBU MICROGRID

4.3.1. Microgrid Bus

Generally, distributed energy resources (microturbines, PV-systems, fuel-cells. etc.), energy storage system units, local loads, and transformer are linked with the LV MG bus. It has been already mentioned that a transformer can be modeled and handled like a voltage-type source on the side of the MV line; so, it is a current-type source that applies to an MG bus. The MG bus connects all the DG units using three-phase filters, which always behave like current-type sources. Consequently, it is appropriate to model the local loads at the MG bus as a voltage-type source.

$$u_{-mvb} = u_{-cp} \tag{4.15}$$

$$i_{-cp} = -i_{-tr} - i_{DG1} - i_{DG2} - \ldots - - i_{DGn} \tag{4.16}$$

The MG bus model description and their connected units are shown in Figure 4.16.

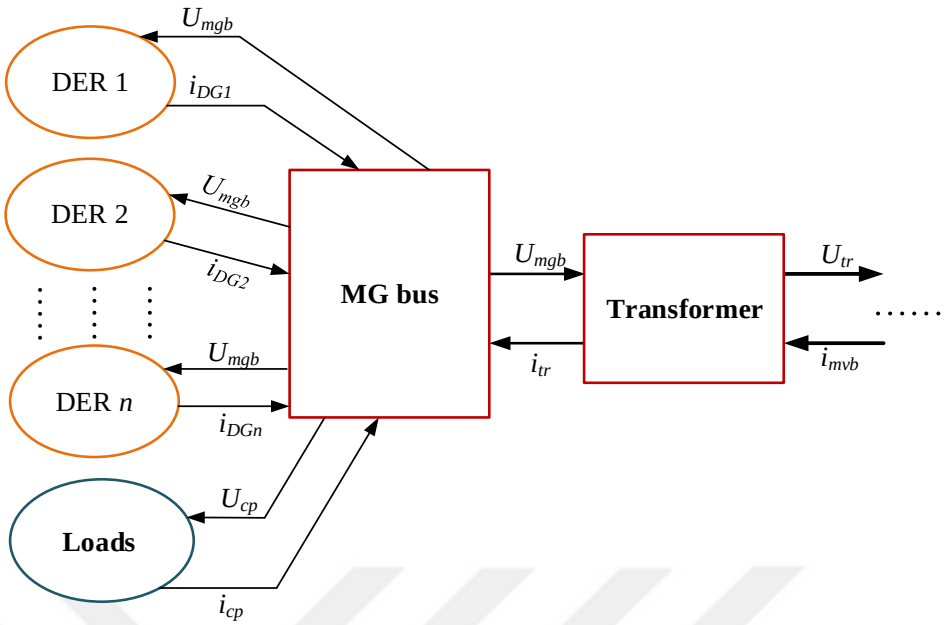

Figure 4.16. Coupling MV bus.

4.3.2. Overall Microgrid Architecture

As mentioned above, in Figure 4.2. has been presented electric power supply structure of KBU and we have chosen one substation as studied object for MG. Finally, we have summurized block diagrams of the gird bus, MV bus, MV line and transformer, and presented as one the overall architecture of a grid-connected MG. The global MG architecture is presented in Figure 4.17. Using this, evaluation and study of the dynamic behaviors of the distribution network, and the interconnected MG were accomplished.

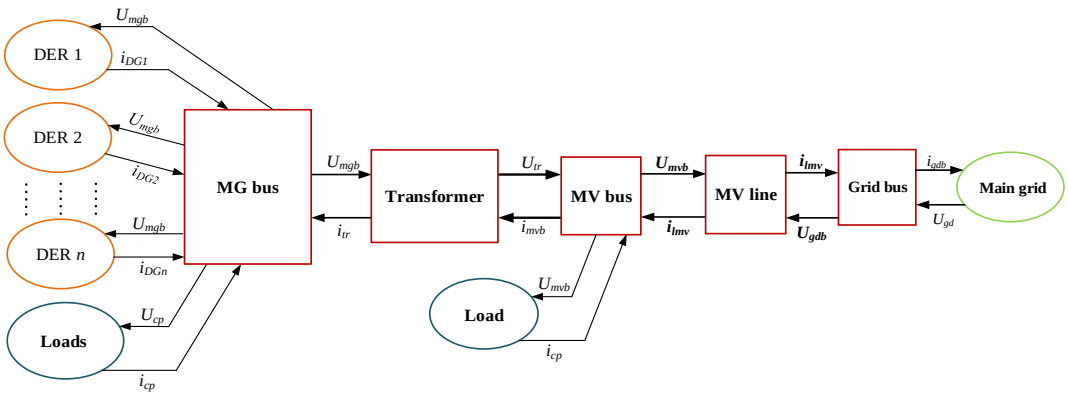

Figure 4.17. Overall Microgrid architecture.

4.4. KBU MICROGRID ARCHITECTURE IN ISLANDED MODE

For the modeling process of KBU MG in the islanded mode, we should only consider distributed generation (PV-system, diesel generator), battery storage system, and loads in the LV (MG) bus.

The architecture modeling principle is similar to what we have presented in the previous analysis. DG and energy storage units, which are linked to the MG with the help of three-phase filters, perform like current-type sources when the MG bus is modeled. In the nutshell, the local loads need to be modeled like voltage-type sources while performing the modeling of the MG bus. The model of KBU MG in islanded operational mode is shown in Figure 4.18.

At the LV (MG) bus, all the DG units were linked in parallel; so, the load terminal voltage U_{cp} results in the MG voltage U_{mgb} (4.17). All DG currents have been computed applying Kirchhoff's law (4.18).

$$u_{mgb-PV} = u_{mgb-gen} = u_{mgb-bat} = u_{cp} \tag{4.17}$$

$$i_{cp} = -i_{PV} - i_{gen} - i_{bat} \tag{4.18}$$

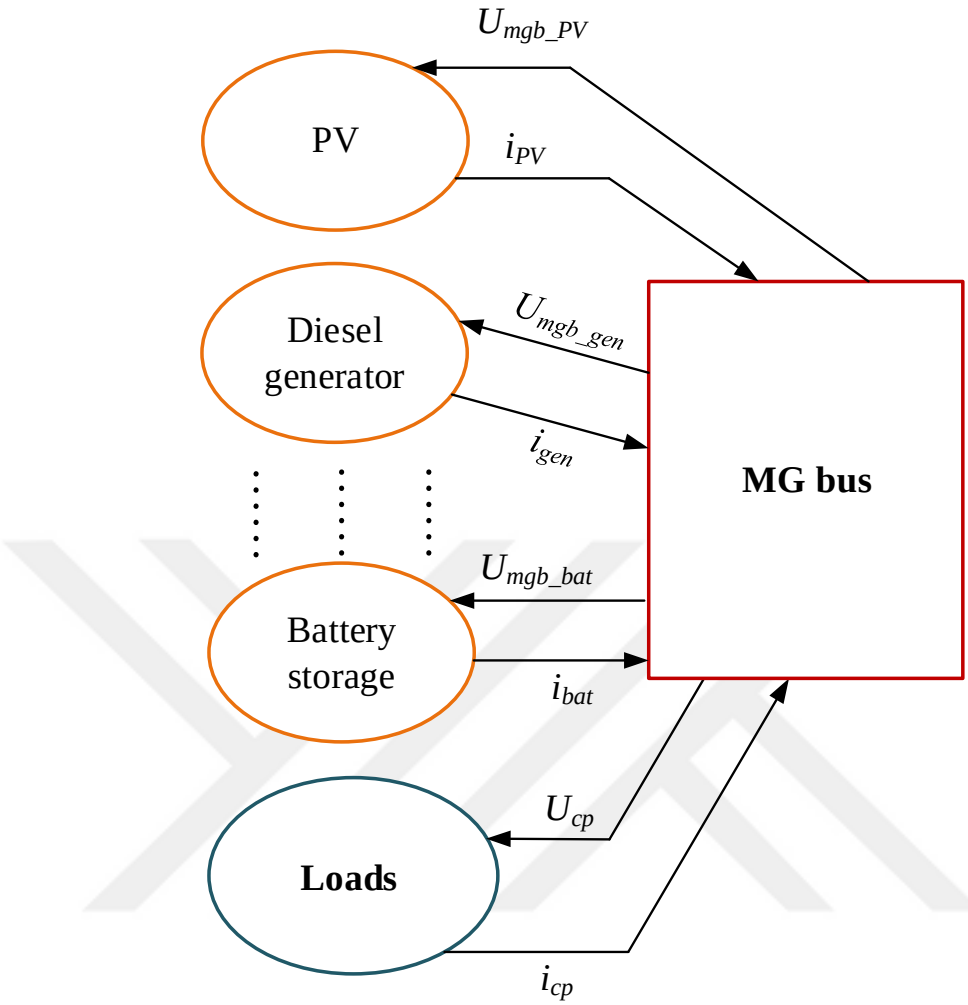

Figure 4.18. The overall model of KBU MG in islanded mode.

4.5. MODELING OF KBU MICROGRID COMPONENTS

KBU MG has the followig main components:

- Diesel generator
- PV panels
- Power converters
- Energy storage system (battery storage unit)
- Voltage source inverter
- Static transfer switch.

The modeling of components is helpful to understand the MGs' dynamic behaviors This makes it easier to perform the closed-loop dynamic analysis and the control synthesis. In this section, each component of the mentioned KBU MG has been modeled.

4.5.1. Modeling a Diesel Generator

Some internal combustion engines are linked with diesel and electric generators for generating electric energy. The diesel generator engine usually uses the diesel fuel; however, some types of generators use other liquid or gaseous fuels. Although micro-turbines cannot be linked to the utility grid, but these generators can be connected needing no interface. When the operation is initiated, there is a low spinning speed, and the output power frequency can be adjusted at 50 Hz. The schematic model of the diesel engine-synchronous generator is shown in Figure 4.19 [121].

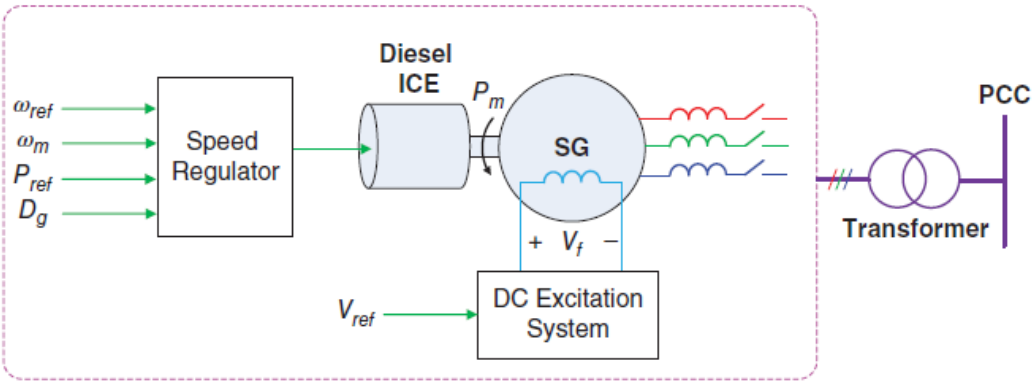

Figure 4.19. The model of a conventional diesel engine synchronous generator system.

Through a transformer, a synchronous machine is linked to the grid. *Pm* represents the mechanical power that is sent according to the speed reference ω_{ref} and power reference *Pref*. A synchronous generator also has a DC excitation system, which controls/manages the generator V_f and its field voltage according to set points and a reactive power mode as well. According to a research [122], the transformation of the three-phase *abc* coordinate to the *0dq* rotating reference frame can be written as:

$$Qx_{abcn} = x_{0dq} \tag{4.19}$$

where:

Q – 3x3 Park's transformation matrix

x – 3x1 vector of electrical states.

If we rewrite Equation 4.19 in the matrix form, we have

$$Q = \frac{2}{3}\begin{bmatrix} 1/2 & 1/2 & 1/2 \\ \cos(\omega t) & cos(\omega t - 2\pi/3) & cos(\omega t + 2\pi/3) \\ -sin(\omega t) & -sin(\omega t - 2\pi/3) & -sin(\omega t + 2\pi/3) \end{bmatrix} \tag{4.20}$$

Figure 4.20 illustrates the association of synchronous machine that has an *abc* stationary reference frame and the *0dq* rotating frame. In this figure, *a*, *b* and *c* apply to the windings of the stator phase, D applies to the *d* axis damper winding, F is concerned with the field winding, and Q to the damper winding along the *q*-axis. Field flux is directed along the *d* axis, with voltage induction along the *q* axis. The angle δ represents the power angle and it should have a steady-state value greater than zero in the generating conditions. Taking into account the reference, which is *a* phase magnetic field axis, and the projections of *abc* quantities onto the *d* and *q* axes, we got the following diagram:

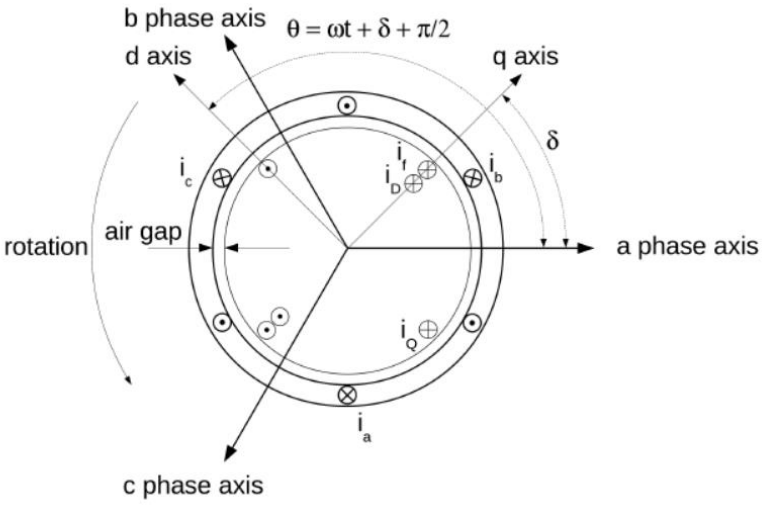

Figure 4.20. Synchronous machine *abc* stationary frame and *0dq* rotating frame association.

$$x_d = \frac{2}{3\left[x_a \cos\ (\theta) + x_b \cos\left(\theta - \frac{2\pi}{3}\right) + x_c \cos\left(\theta + \frac{2\pi}{3}\right)\right]}$$

$$x_q = \frac{2}{3\left[x_a \sin\ (\theta) + x_b \sin\left(\theta - \frac{2\pi}{3}\right) + x_c \sin\left(\theta + \frac{2\pi}{3}\right)\right]} \tag{4.21}$$

The Park transform can be expressed as [121]:

$$P = \sqrt{2/3}\begin{bmatrix} 1/\sqrt{2} & 1/\sqrt{2} & 1/\sqrt{2} \\ \cos\ (\omega t) & \cos\ (\omega t - 2\pi/3) & \cos\ (\omega t + 2\pi/3) \\ \sin\ (\omega t) & \sin\ (\omega t - 2\pi/3) & \sin\ (\omega t + 2\pi/3) \end{bmatrix} \tag{4.22}$$

An electrical system model of generator in *abc* frame is illustrated in Figure 4.21. In this figure, all mutual inductances are not included, for instance, L_{Fc} which is the mutual inductance between *c* phase winding and the field winding is given; however, L_{Fa} and L_{Fb} between the field winding and *a* and *b* phase windings is not. Similarly, the mutual inductance L_{Da} (L_{Qa}) between the phase winding and the *d* axis (*q* axis) damper winding is given, but L_{Db} (L_{Qb}) and L_{Dc} (L_{Qc}) are not. The mutual inductance is excluded between the two windings on the *d* axis and the *q* axis damper winding, which happens due to the quadrature relationship: there is no mutual coupling between these windings.

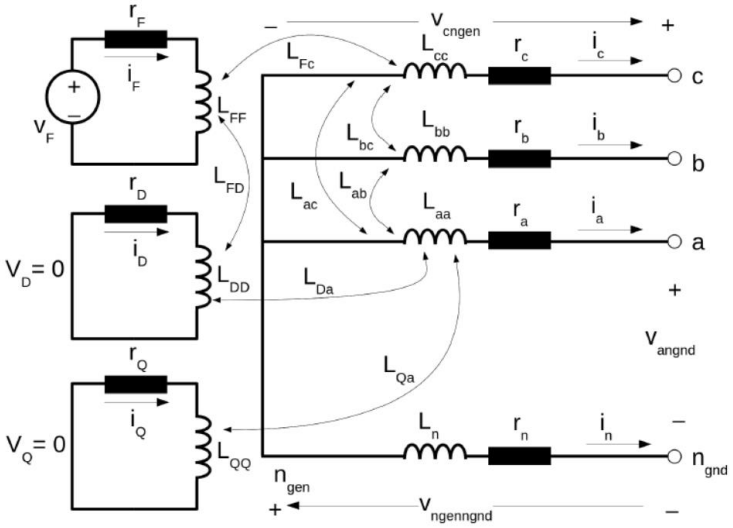

Figure 4.21. Electrical model of a generator in the *abc* frame.

We suppose that: $L_{Da} = L_{aD}$, $L_{FD} = L_{DF}$, $L_{Fa} = L_{aF}$, and so on. These symmetrical properties will be used to simplify the electrical system model of a generator. A study [123] indicates that inductances with two subscripts are time-varying, and those with single subscripts are constant. The single upper case letters were used to represent the rotor parameters:

- D – (*d* axis) damper winding
- F – field winding
- Q – (*q* axis) damper winding.

The generator voltage equations for *0dq* frame will be:

$$\begin{bmatrix} v_0 \\ v_d \\ v_q \\ -v_F \\ v_D \\ v_Q \end{bmatrix} = -\begin{bmatrix} r+3r_n & 0 & 0 & 0 & 0 & 0 \\ 0 & r & \omega L_q & 0 & 0 & \omega k M_Q \\ 0 & -\omega L_d & r & -\omega k M_F & -\omega k M_D & 0 \\ 0 & 0 & 0 & r_F & 0 & 0 \\ 0 & 0 & 0 & 0 & r_D & 0 \\ 0 & 0 & 0 & 0 & 0 & r_Q \end{bmatrix} \begin{bmatrix} i_0 \\ i_d \\ i_q \\ i_F \\ i_D \\ i_Q \end{bmatrix}$$
$$-\begin{bmatrix} L_0+3L_n & 0 & 0 & 0 & 0 & 0 \\ 0 & L_d & 0 & kM_F & kM_D & 0 \\ 0 & 0 & L_q & 0 & 0 & kM_Q \\ 0 & kM_F & 0 & L_F & M_R & 0 \\ 0 & kM_D & 0 & M_R & L_D & 0 \\ 0 & 0 & kM_Q & 0 & 0 & L_Q \end{bmatrix} \begin{bmatrix} \dot{i_0} \\ \dot{i_d} \\ \dot{i_q} \\ \dot{i_F} \\ \dot{i_D} \\ \dot{i_Q} \end{bmatrix} \quad (4.23)$$

Referring to all values to the stator:

v_{0dq} – The voltages of generator stator in *0*, *d* and *q* axis;

v_{FDQ} – The voltages of rotor field, and in damper windings in *q and d*-axis

i_{0dq} – The currents of generator stator in *0*, *d* and *q* axis;

i_{FDQ} – The currents of generator rotor field, and in damper windings in *q and d*-axis;

r – The stator armature resistance; r_F – the resistance of rotor field;

r_n – The resistance inserted in the neutral connection between the generator and the system neutral;

r_D and r_Q – damper resistances in *d* and *q* axis;

L_n – The inductance between the generator and system neutral;

ω – Electrical frequency;

L_{0dq} – The synchronous inductances of stator in *0*, *d* and *q* axis;

L_{FDQ} – The synchronous inductances of rotor field (*a* and *d*-axis damper);

kM_F – The mutual stator *d*-axis inductance to rotor field;

kM_D – The mutual stator *d*-axis inductance to the rotor *d*-axis damper;

kM_Q – The stator *d* axis' mutual inductance to the rotor *d*-axis damper.

$L_{AD} = kM_F = kM_D = M_R$ and $L_{AQ} = kM_Q$ – the stator has mutual inductance in *q* axis to the *q* rotor axis damper

In matrix form, it will be as follows:

$$r = \begin{bmatrix} r + 3r_n & 0 & 0 & 0 & 0 & 0 \\ 0 & r & \omega L_q & 0 & 0 & \omega k M_Q \\ 0 & -\omega L_d & r & -\omega k M_F & -\omega k M_D & 0 \\ 0 & 0 & 0 & r_F & 0 & 0 \\ 0 & 0 & 0 & 0 & r_D & 0 \\ 0 & 0 & 0 & 0 & 0 & r_Q \end{bmatrix} \tag{4.24}$$

and

$$L = \begin{bmatrix} L_0 + 3L_n & 0 & 0 & 0 & 0 & 0 \\ 0 & L_d & 0 & kM_F & kM_D & 0 \\ 0 & 0 & L_q & 0 & 0 & kM_Q \\ 0 & kM_F & 0 & L_F & M_R & 0 \\ 0 & kM_D & 0 & M_R & L_D & 0 \\ 0 & 0 & kM_Q & 0 & 0 & L_Q \end{bmatrix} \tag{4.25}$$

Rearranging into first order differential equation form, recognizing $v_d = v_q = 0$, and treating v_F as an input, we get:

$$\begin{bmatrix} \dot{\imath_0} \\ \dot{\imath_d} \\ \dot{\imath_q} \\ \dot{\imath_F} \\ \dot{\imath_D} \\ \dot{\imath_Q} \end{bmatrix} = -L^{-1} r \begin{bmatrix} i_0 \\ i_d \\ i_q \\ i_F \\ i_D \\ i_Q \end{bmatrix} - L^{-1} \begin{bmatrix} v_0 \\ v_d \\ v_q \\ 0 \\ 0 \\ 0 \end{bmatrix} + L^{-1} \begin{bmatrix} 0 \\ 0 \\ 0 \\ v_F \\ 0 \\ 0 \end{bmatrix} \tag{4.26}$$

Therefore, Equation 4.26 can be written as:

$$\begin{bmatrix} \dot{\imath}_0 \\ \dot{\imath}_d \\ \dot{\imath}_q \\ \dot{\imath}_F \\ \dot{\imath}_D \\ \dot{\imath}_Q \end{bmatrix} = -L^{-1}r \begin{bmatrix} i_0 \\ i_d \\ i_q \\ i_F \\ i_D \\ i_Q \end{bmatrix} - L^{-1} \begin{bmatrix} P \begin{bmatrix} v_a \\ v_b \\ v_c \end{bmatrix} \\ 0 \\ 0 \\ 0 \end{bmatrix} + L^{-1} \begin{bmatrix} 0 \\ 0 \\ 0 \\ v_F \\ 0 \\ 0 \end{bmatrix} \tag{4.27}$$

The model of electrical generator in the *0dq* reference frame is shown in Figure 4.22.

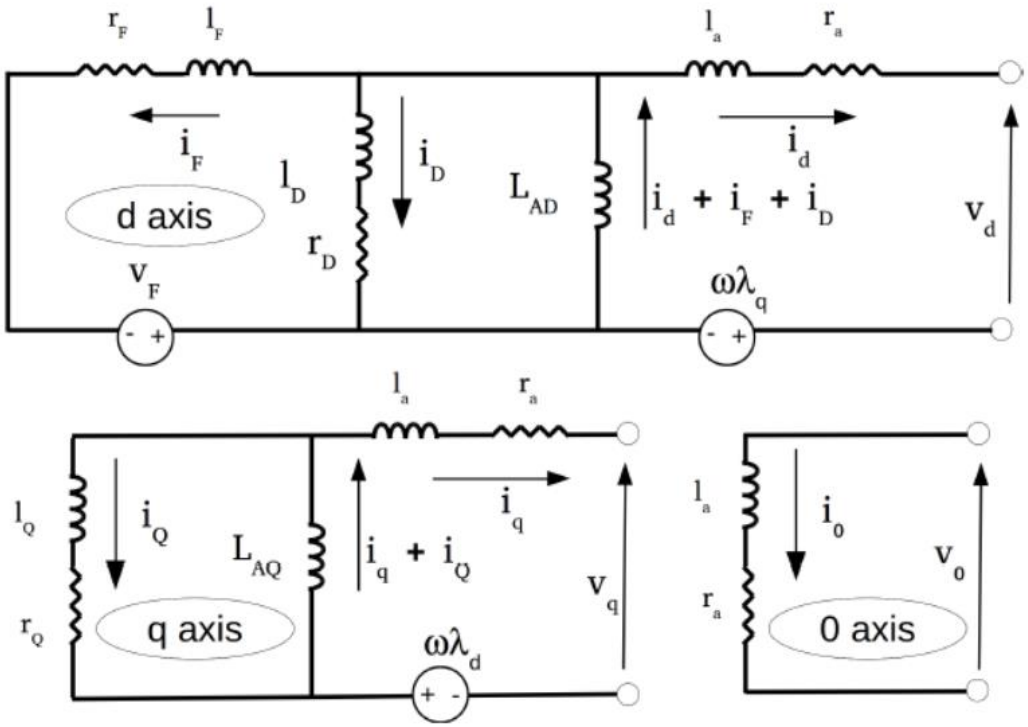

Figure 4.22. The model of electrical generator in the *0dq* reference frame.

4.5.2. PV Panels

For analysis of the PVs' dynamic behaviors, we considered an equivalent electrical model. The ideal PV cell can be termed as a current source, which is parallel to a diode. Practically, it is not ideal to use a PV cell; therefore, series and shunt resistances are included in the model [123,124]. Figure 4.23 shows the resulting equivalent circuit.

The PV cell is a source of current in an equivalent circuit because that has photovoltaic effect. We can express the output as:

$$I(t) = I_L(t) - I_D(t) - I_{SH}(t) \tag{4.28}$$

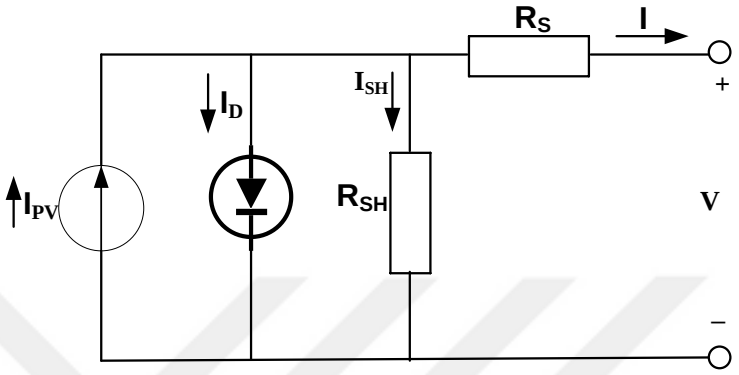

Figure 4.23. Equivalent electric circuit of a PV cell.

Here, I_L is photo generated current, I is output current, I_{SH} is shunt current, and I_D is diode current while the voltage governs the current through the mentioned elements:

$$V_j(t) = V(t) + I(t)\, R_s \tag{4.29}$$

Here V_j represents voltage in the shunt resistor R_{SH} and the diode, while V represents the output terminals' voltage, and R_S represents the series resistor. Applying the Shockley diode equation, which expresses the current through the diode as:

$$I_D(t) = I_o \left\{ exp\left[\frac{qV_{j(t)}}{nKT}\right] - 1 \right\} \tag{4.30}$$

In this equation, n is the diode's ideality factor (for an ideal diode), I_0 represents the reverse saturation current, k represents Boltzmann's constant (1.3806 × 10–23 J/K), q shows the elementary charge (1.6022 × 10–19 C), and T represents the absolute temperature while at 25 ℃ with Ohm's law, $kT/q \approx 0.0259$V. The shunt resistor current is expressed as:

$$I_{SH}(t) = \frac{V_J(t)}{R_{SH}} \tag{4.31}$$

After substituting Equation 4.28 – 4.30 in Equation 4.27, we get a PV cell's characteristic equation that relates the parameters of a PV cell parameters with the output voltage and current:

$$I(t) = I_L(t) - I_0 \left\{ exp\left[\frac{q(V(t)+I(t)R_s}{nKT}\right] - 1 \right\} - \frac{V(t)+I(t)R_s}{R_{SH}} \tag{4.32}$$

When a specific voltage $V(t)$ is given, we'll solve the equation to compute the output current $I(t)$, since it has the current as a variable of a transcendental function. Still, the equation offers no generalizable analytical solution but it can be solved using some numerical processes. Some parameters like R_S, I_o, n, and R_{SH} cannot be directly measured, so we used a characteristic equation that has non-linear regression, which extracts these parameters' values based on their overall impact on the behavior of a PV cell.

In case the cell undergoes a short circuit, $V = 0$ and the current $I(t)$ will become equal to the short-circuit current ($I_{SC}(t)$). In case of a quality PV cell (low R_S and I_0 value, and high R_{SH} value), we can express the short-circuit current I_{SC} as:

$$I_{SC}(t) \approx I_L(t) \tag{4.33}$$

Considering the temperature and the irradiance, we can express the current I_{SC} as:

$$I_{SC}(t) = I_{SC}\frac{G(t)}{Gs}[1+\Delta I_{SC}(T(t) - T_S)] = I_L(t) \tag{4.34}$$

Here, T is the cell temperature (K), G represents irradiance (W/m^2), G_S means standard illumination (1000 W/m^2), I_{SCS} represents the short circuit current in standardized test conditions (STCs), ΔI_{SC} is temperature coefficient, and T_S is standard temperature (298.15 K) of the short circuit current. In case, a cell operates in an open circuit when $I = 0$, the output terminals' voltage will be open-circuit voltage (V_{oc}). If we assume

that a shunt resistor (R_{SH}) is significant enough that the characteristic equation's final term can be neglected (4.31), so we can express the open-circuit voltage as:

$$V_{OC}(t) \approx \frac{kT}{q} ln\left(\frac{I_L(t)}{I_0} + 1\right) \tag{4.35}$$

In case of open-circuit, $I = 0$ and $V = V_{OC}$, Equation 4.27 can also be expressed as:

$$I_L(t) = I_D(t) + I_{SH}(t) = I_{sat}\left[exp\frac{V_{OC}(t)}{V_t} - 1\right] + \frac{V_{OC}(t)}{R_{SH}} \tag{4.36}$$

Here $V_t = AkT/q$ while A stands of the diode's ideal factor, so we can define the saturation current as:

$$I_{sat} = \frac{I_L(t) - \frac{V_{OC}(t)}{R_{SH}}}{exp\left(\frac{V_{OC}(t)}{V_t}\right) - 1} \tag{4.37}$$

We can express the open-circuit voltage as:

$$V_{oc} = V_{ocs} + \Delta V_{oc}(T - T_s) \tag{4.38}$$

In STC, V_{ocs}stands for open-circuit voltage while for the open circuit voltage, ΔV_{oc} stands for the temperature coefficient. It should be noticed that the ideal factor and the resistors are temperature-affected [125]. For simplifying this model, we placed these values in STC.

4.5.3. Modeling MPPT with Boost Converter

A PV cell is able to perform over wide range of currents (I) and voltages (V). When the irradiated cell voltage increases from zero to a certain maximum, we can determine the maximum-power point (MPP). When the cell releases the maximum power for a certain irradiation level, the required point is achieved. To calculate the MPP, we use the following equation [126]:

$$P_{PV}(t) = V_{PV}(t) \cdot I_{PV}(t) \tag{4.39}$$

When Equation 4.38 is differentiated with respect to voltage V_{PV}:

$$\frac{dP_{PV}}{dV_{PV}} = I_{PV}(t) + V_{PV}(t) \cdot \frac{dI_{PV}}{dV_{PV}} \tag{4.40}$$

while the MPP is:

$$\frac{dP_{PV}}{dV_{PV}} = 0 \tag{4.41}$$

$$\frac{dI_{PV}}{dV_{PV}} = -\frac{I_{PV}}{V_{PV}} \tag{4.42}$$

In this case, the algorithm tries to reach a point where conductance increment $\left(\frac{dP_{PV}}{dV_{PV}}\right)$ equals conductance $\left(\frac{dI_{PV}}{dV_{PV}}\right)$. Figure 4.24 shows the I (f , V) characteristic that has four values: open-circuit voltage (V_{SC}), short-circuit current (I_{SC}), voltage at the MPP (V_{mp}), and current at the MPP (I_{mp}).

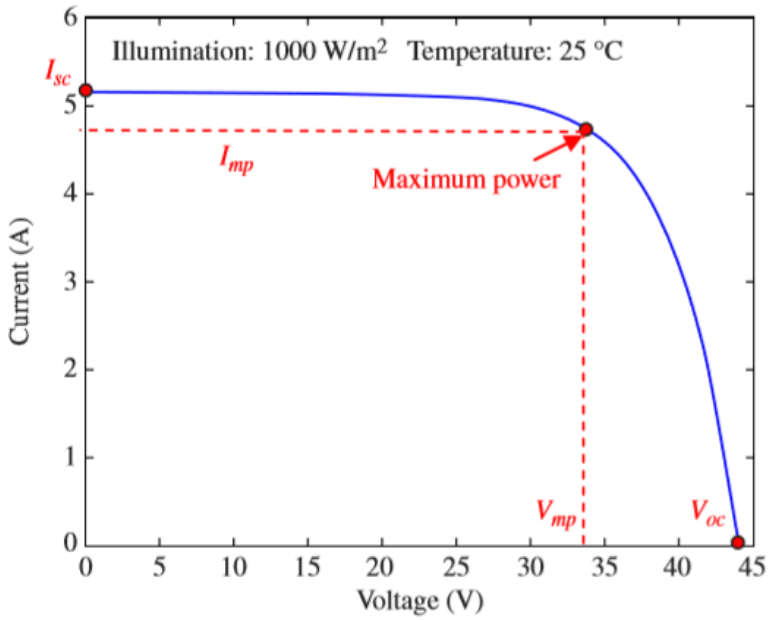

Figure 4.24. I (V) characteristic of a PV panel.

The equations required for generating a cell's *I–V* characteristic curve are as follows [127]:

$$I(t) = I_{SC}\left[1 - C_1\left(exp\left(\frac{V(t)}{C_2 V_{OC}}\right) - 1\right)\right] \tag{4.43}$$

$$C_1 = \left(1 - \frac{I_{mp}}{I_{SC}}\right) exp\left(\frac{V_{mp}}{C_2 V_{OC}}\right) \tag{4.44}$$

$$C_2 = \frac{\frac{V_{mp}}{V_{OC}} - 1}{In\left(1 - \frac{I_{mp}}{I_{SC}}\right)} \tag{4.45}$$

Here, the current, when there is maximum power, can be given as:

$$I_{mp} = I_{mps}\frac{G}{G_S}\left[1 + \Delta I_{mp}(T - T_S\right] \tag{4.46}$$

In this case, I_{mps} represents current at the MPP that is calculated in STCs, while at MPP, ΔI_{mps} represents the temperature coefficient. We can calculate the voltage corresponding to the maximum power [128]:

$$V_{mp} = V_{mps}\left[1 + \Delta V_{mp}(T - T_S)\right] + K_1 V_t ln\left(\frac{G}{G_S}\right) + K_2\left[V_t ln\left(\frac{G}{G_S}\right)\right]^2 \tag{4.47}$$

In this equation, V_{mps} means voltage in STC where the the point of maximum power lies, K_1 and K_2 are constants, and at MPP, ΔV_{mp} is the temperature coefficient for voltage. In the normal PV system operations, it is the MPP that MPPT inverter always searches. It simplifies this model because only voltage and current exist in the MPP (I_{mp} and V_{mp}).

The boost converter provides maximum efficiency operations to a PV system by extracting maximum achievable power from a PV system. The P&O method creates perturbation when it either decreases/increases a boost converter's duty cycle, and later, it observes the direction of change in the output of a PV. The P&O methodology

has been explained with the help of a flow chart (Figure 4.25). For implementing a P&O algorithm, the PV current and voltage should be measured in the beginning. Later, the changes in the voltage (ΔV) and power (ΔP) need to be computed. A constant value perturbs the PV voltage. In case the voltage perturbation increases the power, it is essential to keep the next perturbation in the same direction to prevent it from getting reversed [127, 128].

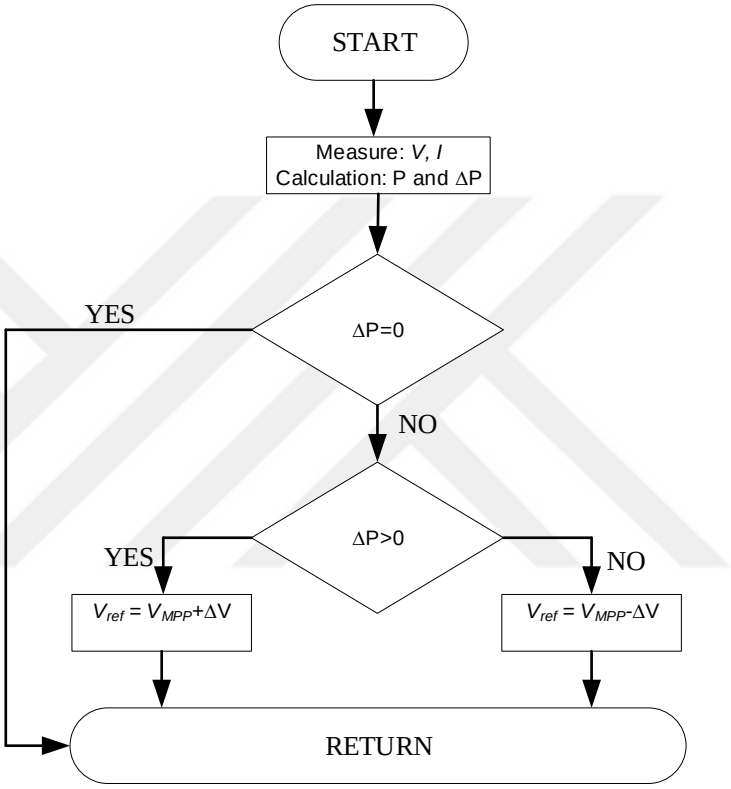

Figure 4.25. Flow chart of P&O method.

4.5.4. Modeling of Battery Storage System

Nowadays, the battery storage systems have different applications, and battery models are available with different complexities and modularity. A common battery model has constant resistance, which is linked to the ideal voltage supply in series. SoC is unnecessary in this model, and besides, it is suitable just for LV applications. Thevenin battery model is commonly used because it has internal resistance, which is linked in series to the combination of resistance and capacitance. It is possible to keep all these elements constant in this model, but the battery characteristics can vary that

depends on SOC and the discharge rate [129]. For avoiding complexity of the battery, researchers have proposed a generic dynamic battery model. Currently BESS is considered as the most efficient electrochemical energy storage technology, which is easily available. This thesis includes a storage bank with lead acid batteries. This type of battery bank delivers the stored energy when PV array fails to generate the needed voltage [130]. Mathematical model of the battery is shown in Figure 4.26 that uses a conventional battery circuit [131].

$$V_{bat} = E_g - i_{bat}R_{bat} \tag{4.48}$$

$$E_g = E_{go} - K\frac{Q}{Q - \int i_{bat}dt} + Aexp(B\int i_{bat}dt) \tag{4.49}$$

where E_g is the open circuit voltage found between the battery terminals and the stored energy.

State of charge (SOC) for a battery is as follows:

$$SOC(t_i) = \frac{1}{Q(t_i)}\int_{\infty}^{t_i}\eta_c(t)\, I_{bat}dt \tag{4.50}$$

$$Q(t_i) = \frac{C_{nom}C_{tcost}}{1+A_{cap}\left(\frac{|I_{bat}(t)|}{I_{nom}}\right)^{B_{cap}}}(1 + \alpha_c\Delta T(t) + \beta_c\Delta T^2(t)) \tag{4.51}$$

$$I_{nom} = \frac{C_{nom}}{n} \tag{4.52}$$

where: η_c – the charging efficiency; *C (t)* – the battery capacity;

$I_{bat}(t)$ – The current flowing through battery;

C_{tcost}, A_{cap} and B_{cap} – parameters of the model,

ΔT – the variation at reference temperature (25°C);

C_{nom} – the rated battery capacity (*n* hours);

I_{nom} – the discharge current that corresponds to C_{nom} rated capacity;

α_c and β_c –temperature parameters; *n* – number of hours.

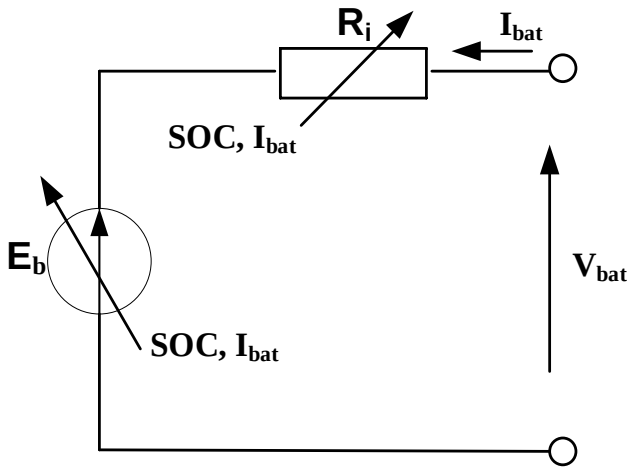

Figure 4.26. Circuit model of a typical battery.

4.5.5. Modeling Voltage Source Inverter

Inverters operate mainly as voltage source (also current source is known) and control the voltage magnitude of each phase. The sinusoidal voltage form can be obtained by using reference waveform and modulator, also controled through use of low-frequency signals. The drawback of voltage-source inverters (VSIs) is there are high frequency distortions that become by switching action of the inverters. Three-phase VSIs are used in MGs for connecting the DC bus with the AC grid [132,133]. The purpose of the inverter is inverting DC into AC. The three-phase inverter model is shown in Figure 4.27. The circuit consists of voltage source *vr* in series and output impedance $Z_0\angle\theta$, where δ is power angle – difference between v_r and v_0, while E is the amplitude of the voltage source and δ.

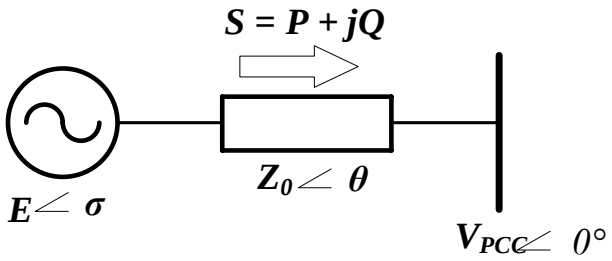

Figure 4.27. The equivalent model of three-phase inverter [133].

In some research papers [86,132,133], the block diagram of VSI control loop has been developed in detail for MG systems. One of the block diagrams of VSI control loop is illustrated in Figure 4.28 [86].

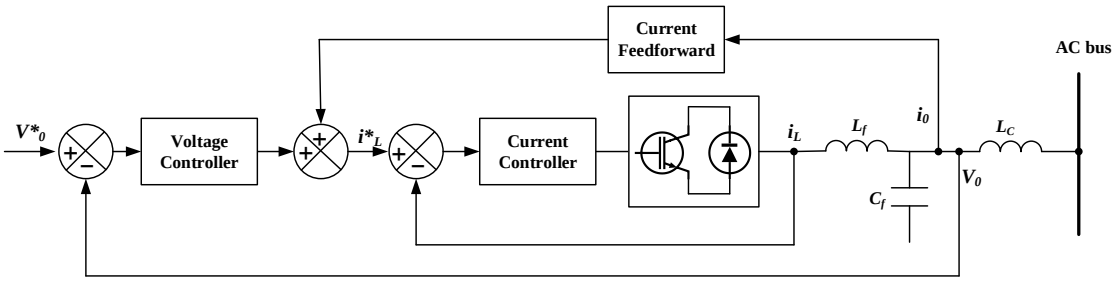

Figure 4.28. Block diagram of VSI control loops.

4.5.6. Static Transfer Switch

The static transfer switch or shortly static switch connects the main grid with the microgrid. There are two types of static switch utilized in the microgrid the first one is IGBT- based switch and the second one is SCR- based switch. IGBT- based switch uses fully- controlled instruments which make fast turn-on and turn-off and offer accurate control through the drive circuit. But at the same time its cost high and the overload capacity is limited. SCR- based switch treatments the previous disadvantages where it is low cost and stable with strong overload. The disadvantage in this switch its complex control [134]. Single-phase scheme of static switch is illustrated in Figure 4.29 [135]. The static transfer switch contains of two three-phase static switches, two three-phase mechanical bypass switches and isolating switches. The static switch is used for synchronization of main grid with MG, fault detection and reverse power detection.

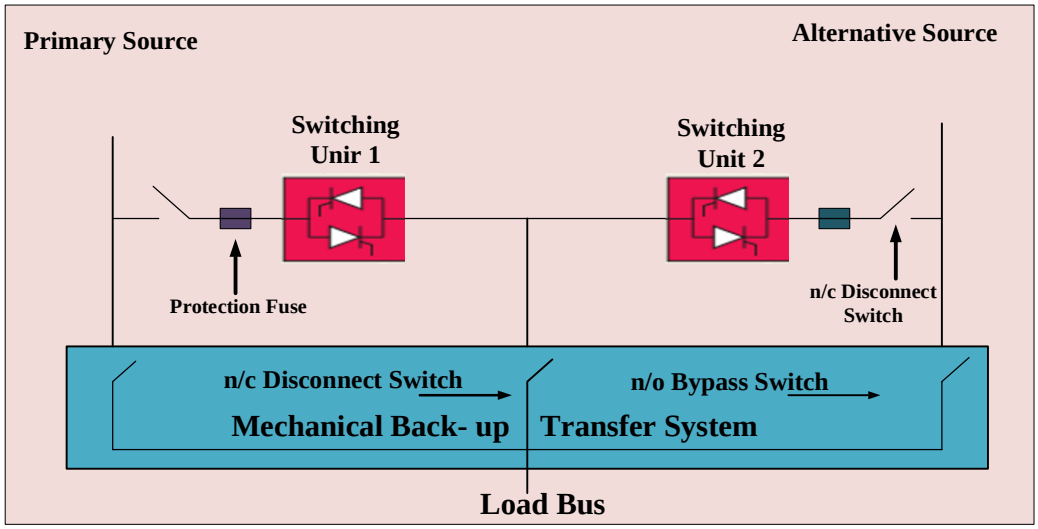

Figure 4.29. Configuration of static switch.

In Figure 4.30 is depicted MG connection with main grid via static switch. Protection of microgrid by isolating it from the main grid during emergency or maintenance cases is one of the important issues in MG applications. If there are failures in main grid or maintenance required, the static switch can disconnection MG from utility grid or connect to utility grid after main grid synchronization.

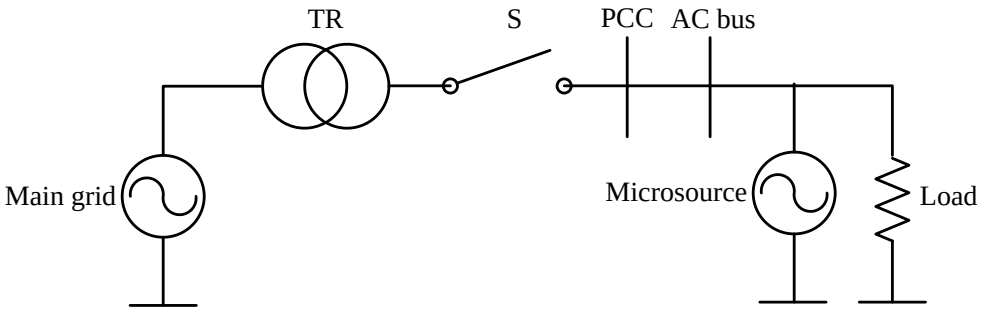

Figure 4.30. Main grid and MG connection via static switch.

PART 5

LOAD SHARING AND FAULT CONTROL OF MICROGRID SYSTEM

5.1. INTRODUCTION

The need of power supply demand for isolated area is increases rapidly in last two decades. The constant electrical energy should be available due to increases in number consumers such as hospitals, multi-storage buildings, information centers, etc. in recent years. In these situations, distributed energy with distributed energy storage system are necessary to provide constant power to the consumers without interruption [136-140].

In general, the electricity generation from renewable energy sources is most suited method than convention energy generations. But it has some disadvantages such it is not stable due to climate change, inefficient and initial cost for installation is high. In other hand, diesel power generator used during emergency situation and peak hours and normally used for standby power to supply the peak loads and it used only isolated area. Even though it has some advantages such as reliable, flexible, low cost, high efficiency. Advantages of both renewable energy and diesel generations are included in microgrid [141-146].

In general, microgrid defines as planning and controlling of distributed energy sources of micro generators and it is controlled by single window system to supply the energy to group of loads in the isolated area. The structure of microgrid has the following advantages:

- The distance between power generation and consumer loads are short

- Power generation level is low with standard distribution voltage level.

The main goal of microgrid system is to provide continues power to consumer load without any interruption. Moreover, the combination of renewable energy with distributed storage system and diesel power generator in micro grid is most promising solutions to assurance for continuity of power generation with moderate expenditures on equipment. Apart from these advantages of microgrid, so many challenges and issues are there in the system. First one is planning, designing, and available technology at low cost to install the system in microgrid. The precise measuring and controlling is required to maintain stable operation due to use of power electronic devices in the microgrid [147-151].

This part of the thesis proposes a microgrid system with power flow control in all distributed energy system along with fault control. The proposed microgrid consists of solar PV array with battery storage with local load and diesel generator with local load. The prime objective of this part is to design and develop the autonomous control system in microgrid to ensure the power balance between distributed energy sources and load along with continues energy supply during fault conditions.

5.2. MODELING AND SIMULATION OF KBU MICROGRID

As mentioned above, MG is cluster of integrated DERs and systems energy storage (ESS) that create a network by suppling loads in a LV network. There are two operation modes of MG, first of them – connected to the LV/MV distribution network, and another one – autonomous [152,153]. Other infrastructures required by the MG are the following:

- Renewable energy sources / diesel generators
- Energy conversion systems
- Distribution lines
- Monitoring devices and instruments
- Controller suitable for under different modes of operation.

The MG must be protected against circuit failures such as short circuit currents, high or low voltage due to abnormal conditions For adequate protection, it protection relays must be installed to detect conditions abnormal and circuit breakers must be started to isolate the part where the fault occurred [154-156].

Most energy source technologies do not can connect directly to the MG due to various features. The investor plays an important role in the network connection. Electronic power converters they must continue to function when the main network does not provide the voltage and frequency of the MG, and must be controlled with DER. The quality of the power must also keep. MGs are designed to improve the self-sustainability of future networks. MG works in mode connected to the network, or independent mode that extracts / supplies power from / to the network. Therefore, it implements an appropriate control method for an enhanced operation of the MG in an intelligent way. Stability problems should be considered for the correct operation of the MG in stable state and transitory conditions. Steady state stability refers to the calculation of the maximum limit, and fluctuations.

Microgrids also face demand-supply difficulties due to the lack of adequate sources of energy generation. The erratic existence of the loads and renewable energy sources creates this challenge. This contributes to the need for an energy management program to address this problem. EMS for a microgrid represents relatively new and popular topics which have recently attracted a lot of attention. An EMS seeks to determine the optimal use of DGs for feeding the electrical charges. The EMS can be handled in two ways, in other words centralized and decentralized. The central controller, in unified mode, aims to optimize the shared microgrid power based on security constraints. DGs and controllable loads have greater degree of freedom in decentralized mode. As a result, the microgrid components are considered intelligent, and by interacting with each other, they try to maximize the microgrid revenue. In both centralized and decentralized mode, the initial duty of EMS is to ensure that the microgrid provides balance for load generation.

The flow chart to implement load sharing and fault control of KBU MG system is shown in Figure 5.1.

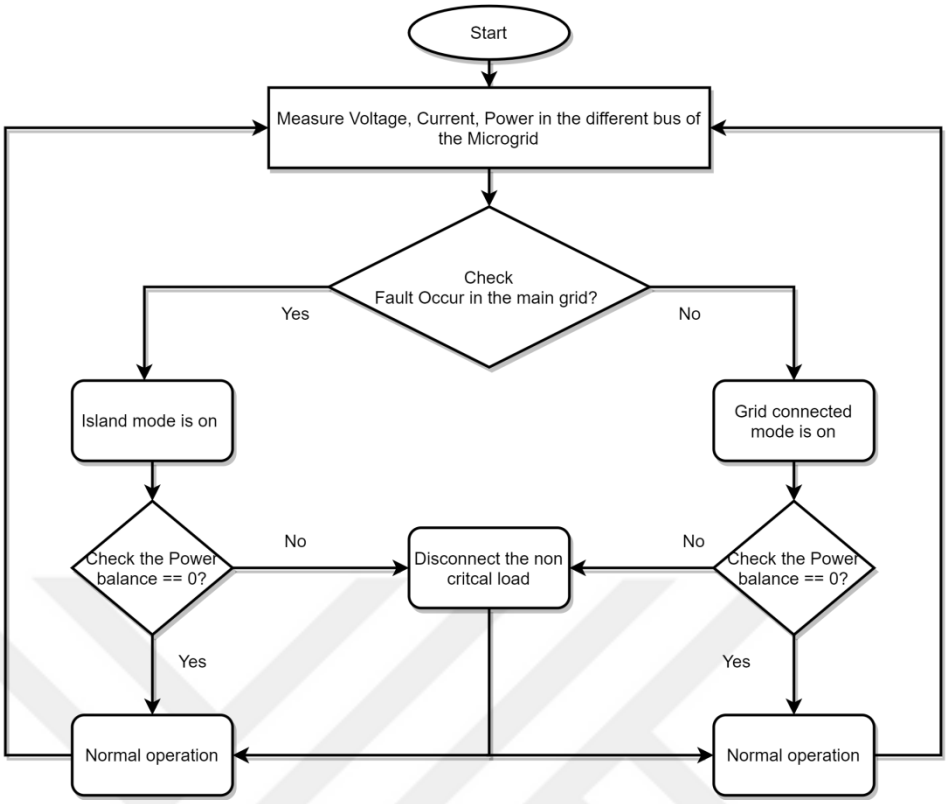

Figure 5.1. Flow chart of load sharing and fault control of KBU MG system.

Events or Faults during Grid Connected and Islanded Mode: For a microgrid failure, the line or feeder protection solution must be to isolate the faulty section from the rest of the system as quickly as possible and how it is achieved depends on the characteristics and nature of the microgrid and security technique being used. Fault control done by differential protection and over current protection and optimal power flow control done by master slave concept i.e., centralized control with local control; centralized control used during grid connected mode and local used during island mode.

5.3. MATLAB SIMULATIONS OF KBU MICROGRID

A microgrid is illustrated as a small power system with three primary components (some MW or less in scale): distributed energy sources with suitable energy storage component, independent load hub, and network capacity to work interconnected or isolated from a superior electrical utility grid. Different microgrids cover multiple

buildings or facilities, with loads usually varying from 2 MW to 5 MW, for example campuses (metropolitan, medical, university, etc.), Military bases, industrial and commercial parks, and housing development [142]. Figure 5.2 shows the representation of simple microgrid to conduct simulation results.

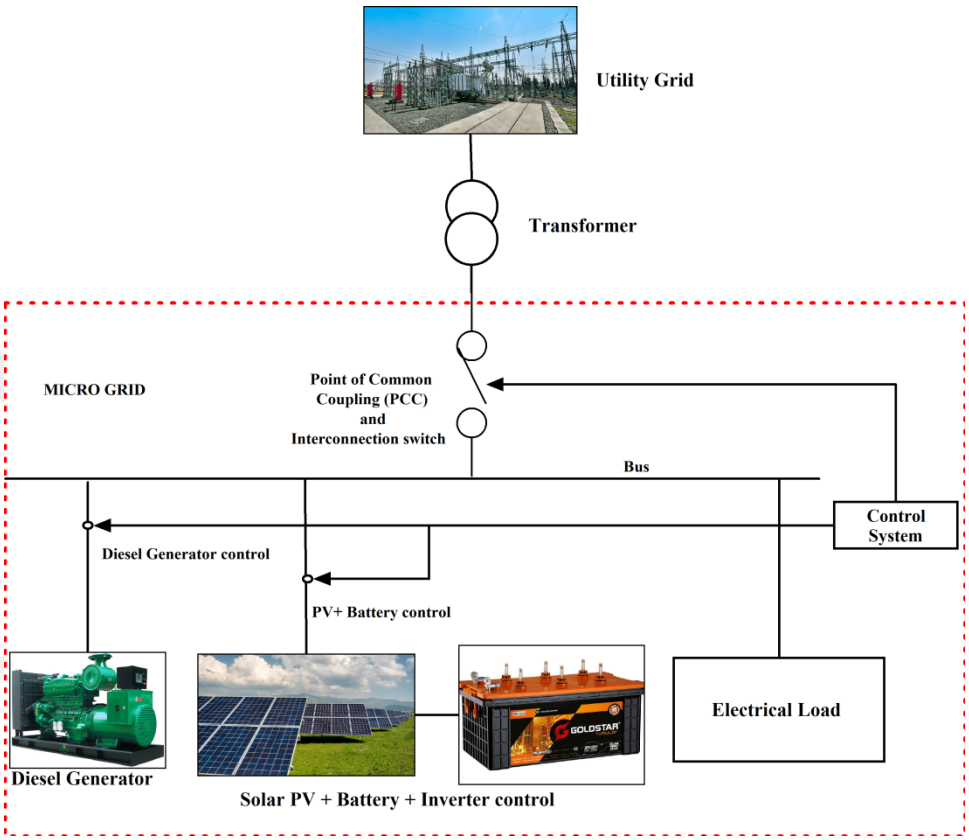

Figure 5.2. Simple Microgrid system.

A microgrid may be a grid with a DC or an AC. An AC microgrid may be either a single phase system or a three phase network. It can be connected to power distribution networks with low voltage or medium voltage. This part of the work only concerns an AC microgrid linked to utility grid. A microgrid generally includes four basic operating technologies: distributed generation units, distributed energy storage systems, point of common coupling with a control system.

In this study we used the Engineering faculty of KBU as Microgrid system. This system is shown in Figure 5.3.

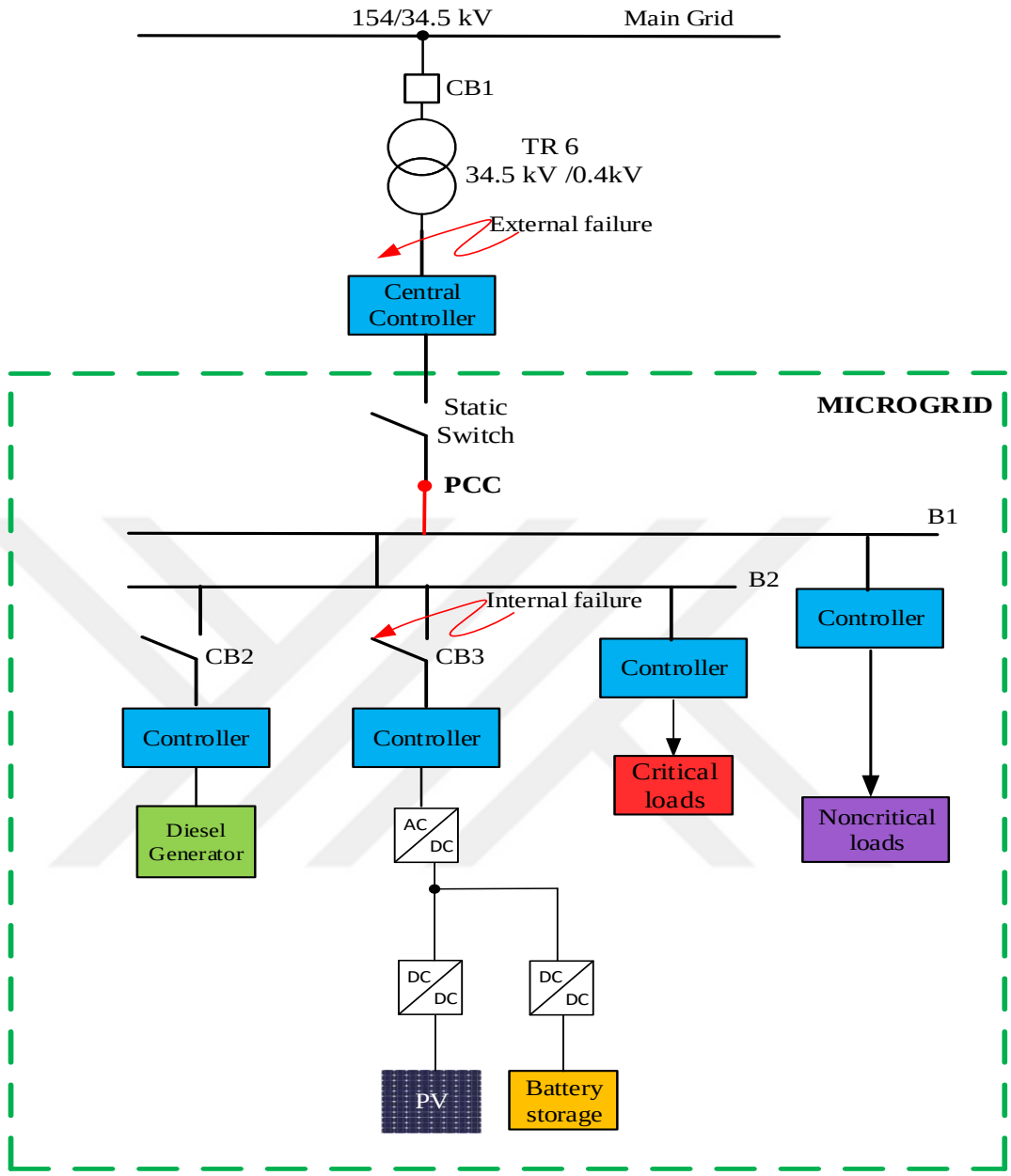

Figure 5.3. Single line diagram of Karabuk university microgrid.

The technical parameters of KBU MG components for modeling of grid-connected microgrid on MATLAB/Simulink are given in Table 5.1.

Small energy sources of generating units are situated near to point of supplying loads. These energy sources categorized into two classes; first one is DC energy sources i.e., fuel cell, PV etc. and second one is AC sources i.e., diesel generator, micro turbine

and wind generator. In this work, microgrid has the following energy sources such as diesel power generator and solar PV [143].

Table 5.1. Specification of KBU Microgrid.

	Utility grid	Solar PV	Battery	Diesel generator	Transformer	Load
Power	154 MW	50 kW	40 kW	430 kW	154 MVA	Critical load – 400 kW at diesel generator
Voltage	34.5/0.4 kV	400 V	480 V	400 V	34.5kV/0.4kV	Critical load – 80 kW at PV-battery-inverter
Frequency	50 Hz	50 Hz (Inverter frequency)	50 Hz (Inverter frequency)	50 Hz	50 Hz	Non-critical load – 500 kW at grid bus
Type					Y-Y type	
Capacity			500Ah			

Normally, the power balance between power generating unit and load could not be exactly equal. In order to balance the power between source and load, distributed storage device should be present in the microgrid such battery, super capacitor and flywheels etc. these energy storage systems provide constant and stable output power independent varying loading conditions, dynamic variations of primary power sources.

The microgrid and main grid is connected in common point or point of common coupling via interconnected switches. Normally this switch consists of following component relay, power switch, and communication element and signal processor. The interconnect switches are designed to meet the requirements of interconnecting grids [144].

A microgrid may either operate connected to or disconnected from the main grid. Therefore, there are two steady, grid-connected and island operating states. In addition,

the microgrid has two transient modes of operation: from grid-connected mode to isolated mode and vice versa. A microgrid control system is designed to operate the system securely in both of these modes. This microgrid system is control by central unit or each distribution system has autonomous control unit [145,146].

5.4. SIMULATION RESULTS AND DISCUSSION

The KBU microgrid system has been created on MATLAB/Simulink environment. The simulation is executed in the Windows 10 64 bit OS, a dual-core 1.7 GHz Intel Core i3 processor. The Simulink model of the overall microgrid is shown in the Figure 5.4.

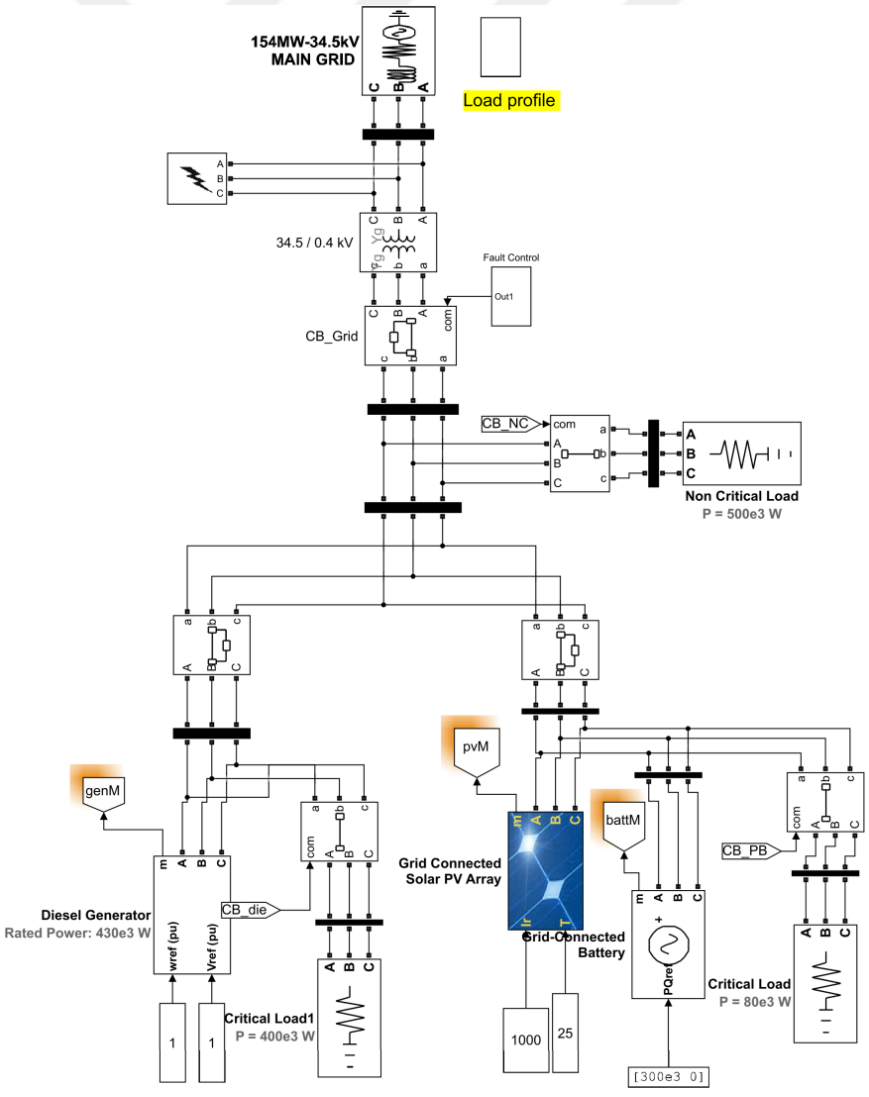

Figure 5.4. Simulink model of fault and power flow control of MG system.

Simulink model of the voltage-source control inverter is illustrated in Figure 5.5. The grid inverter is controlled by inverter control system and it consists of maximum power point control (MPPT), voltage regulator, current regulator and pulse generation circuit for the inverter.

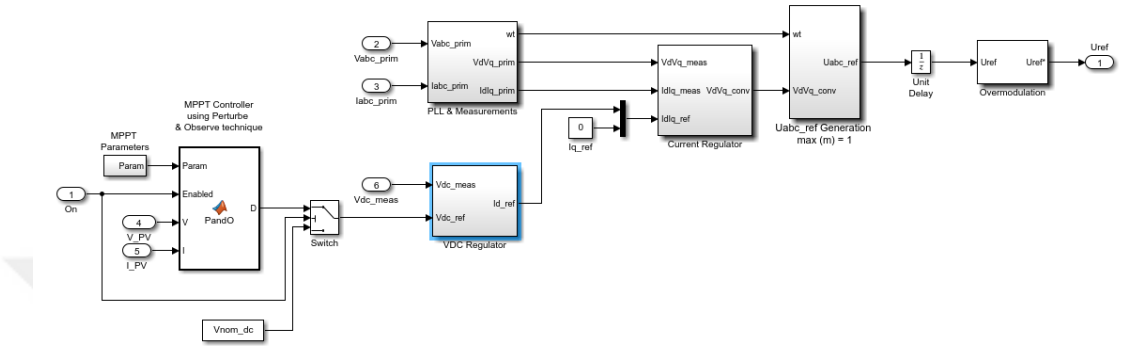

Figure 5.5. Simulink model of the inverter control.

Simulink model of the Solar PV with grid integration circuit is given in Figure 5.6. In this Simulink model, the output of the solar PV is fed to grid inverter via DC link capacitor. The output of the inverter is connected to the gird line.

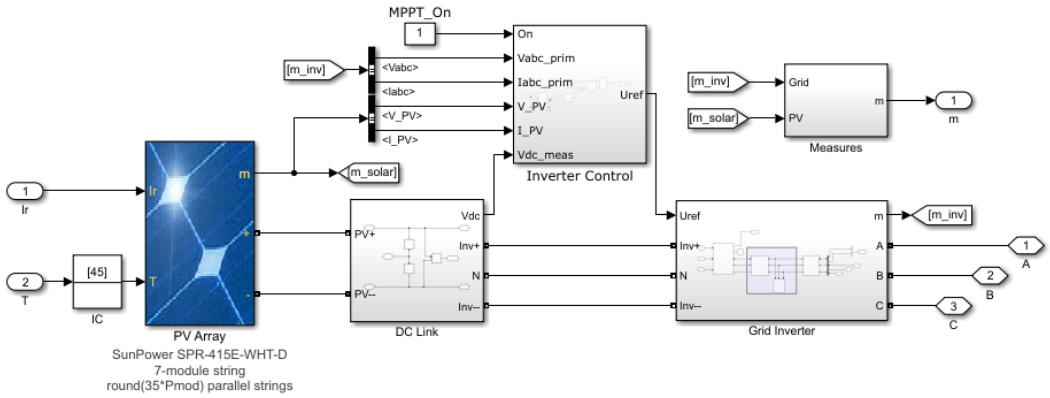

Figure 5.6. Simulink model of the solar PV with grid connected inverter.

Simulink model of the Battery is fed to grid integration circuit is shown in Figure 5.7. In this Simulink model, the output of the battery is fed to grid inverter via DC link capacitor. The grid inverter is controlled by inverter control system and it consists of

voltage regulator, current regulator and pulse generation circuit for the inverter. The battery controller is used to control the charging and discharging function of the battery. The output of the inverter is connected to the gird line.

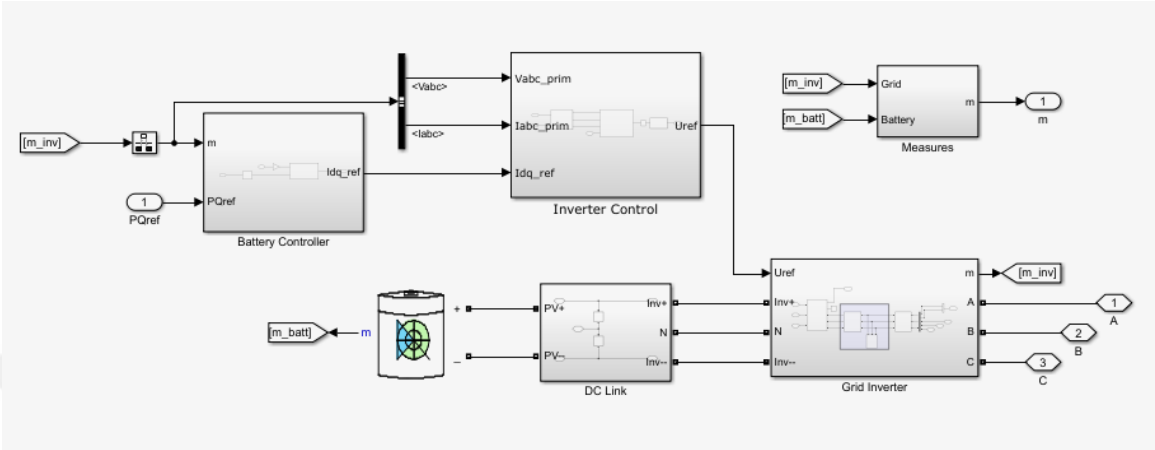

Figure 5.7. Simulink model of the battery.

Simulink model of the diesel generator is shown in Figure 5.8. The output of the diesel generator is fed to grid via distribution lines. The output power of the diesel generator is controlled using diesel engine governor, and terminal voltage of the diesel generator is controlled by voltage regulator.

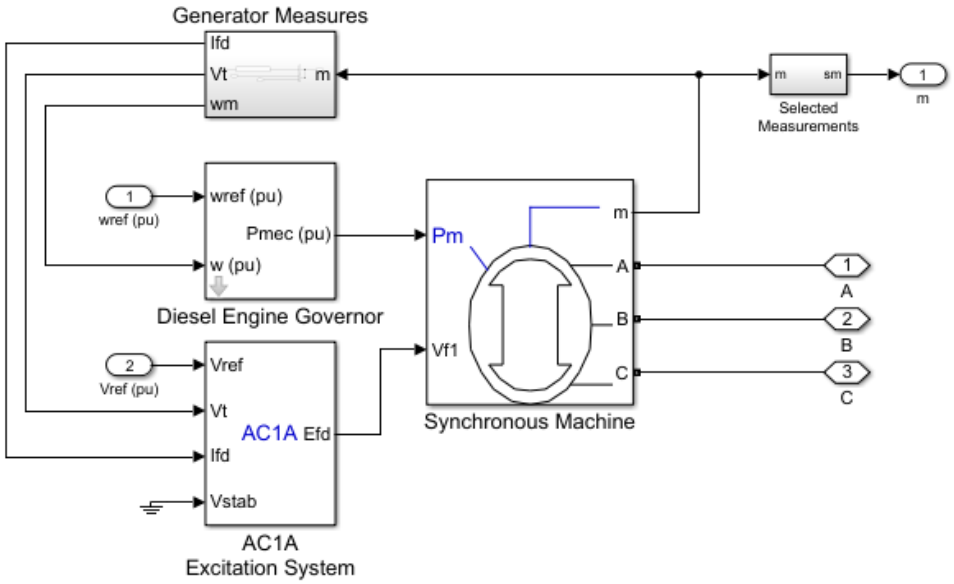

Figure 5.8. Simulink model of the diesel generator

Simulink model of the three-phase two windings transformer is demonstrated in Figure 5.9.

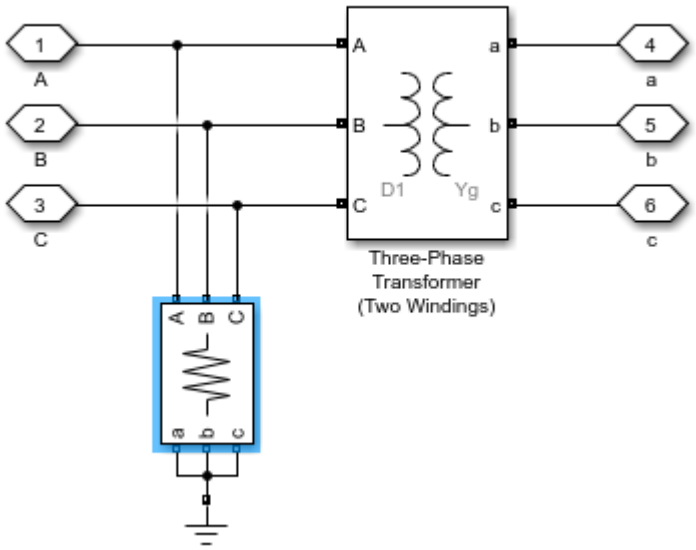

Figure 5.9. Simulink model of the three-phase transformer.

The Simulink model of the load profile settings is shown in Figure 5.10. In this system, repeating sequence used to generate the load profile and it is compared with predefined load values. Based upon the conditions, circuit breaker of critical and non-critical loads has been operated. 400 kW load is present in the diesel generator bus, 80 kW load is present in the bus of PV-Battery system and 500 kW load is present in the grid bus. These predefined values are compared with load profile command settings i.e., if load profile is equal to 400 kW than circuit breaker in the diesel load bus is closed, if load profile is equal to 80 kW than circuit breaker in the PV-Battery load bus is closed, if profile is equal to 500 than circuit breaker of the grid load bus is closed and if load profile is equal to 980 kW than circuit breakers of the all load buses are closed.

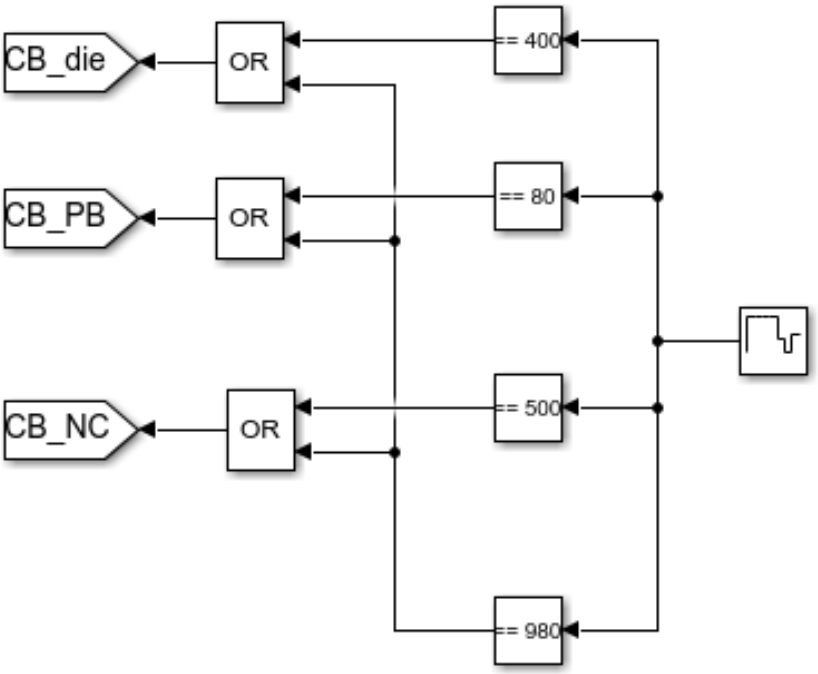

Figure 5.10. Simulink model of the load profile.

The Simulink model of the fault control system is shown in Figure 5.11. In this Simulink model, RMS value of the fault lines are compared with rated value. If the actual voltage is less than the rated value, trip signal is sent to corresponding circuit breaker to isolate from the remaining healthy system.

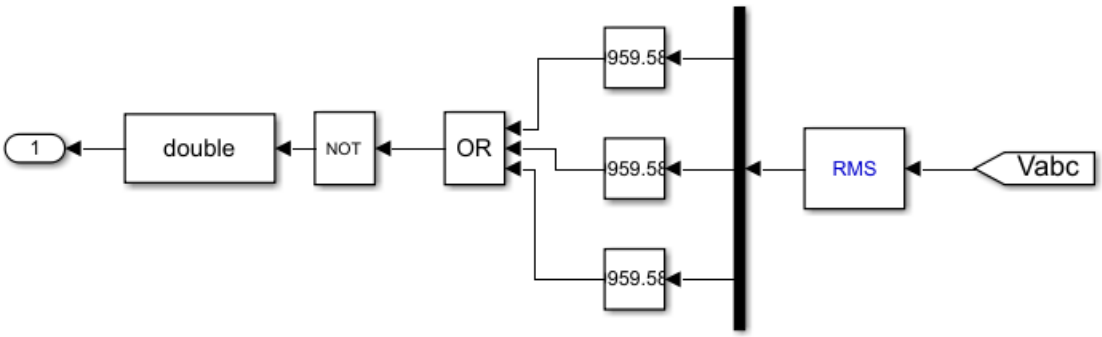

Figure 5.11. Simulink model of the fault control system.

The load profile settings for open and close conditions of the critical and non-critical loads circuit breakers are demonstrated in Figure 5.12. From this figure we can see how the load profile results change when circuit breakers of critical load 1, critical

load 2 and non-critical load disconnected and connected from power sources. The connected load from sec to 2 sec is 980 kW, from 2 Sec to 2.5 sec is 400 kW, from 2.5 sec to 3 sec is 80 kW, from 3 sec to 3.5 sec is 500 kW and 3.5 sec to 4 sec is 980 kW.

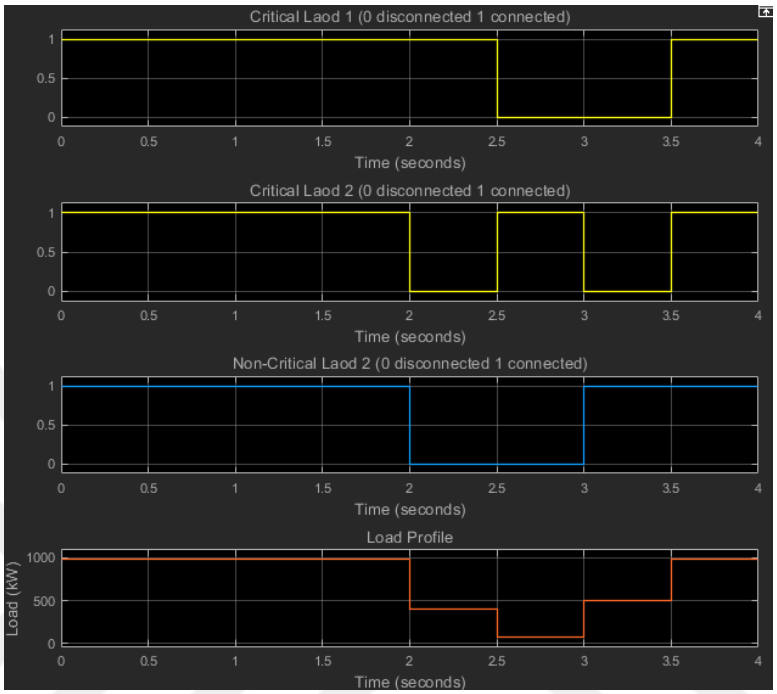

Figure 5.12. Load profile and circuit breaker signal for different loads.

In order to verify the effectiveness of the system, the following test cases have been taken for analyses:

- Three phase faults at grid line conditions;
- Optimal load sharing conditions.

The active power characteristics of grid, solar PV, battery and diesel generator are illustrated in Figure 5.13. Also, island mode and grid connected mode of the MG system is presented in the Table 5.2, and this table provide the sharing of the active power of the grid and distributed energy sources such as PV, battery and diesel generator.

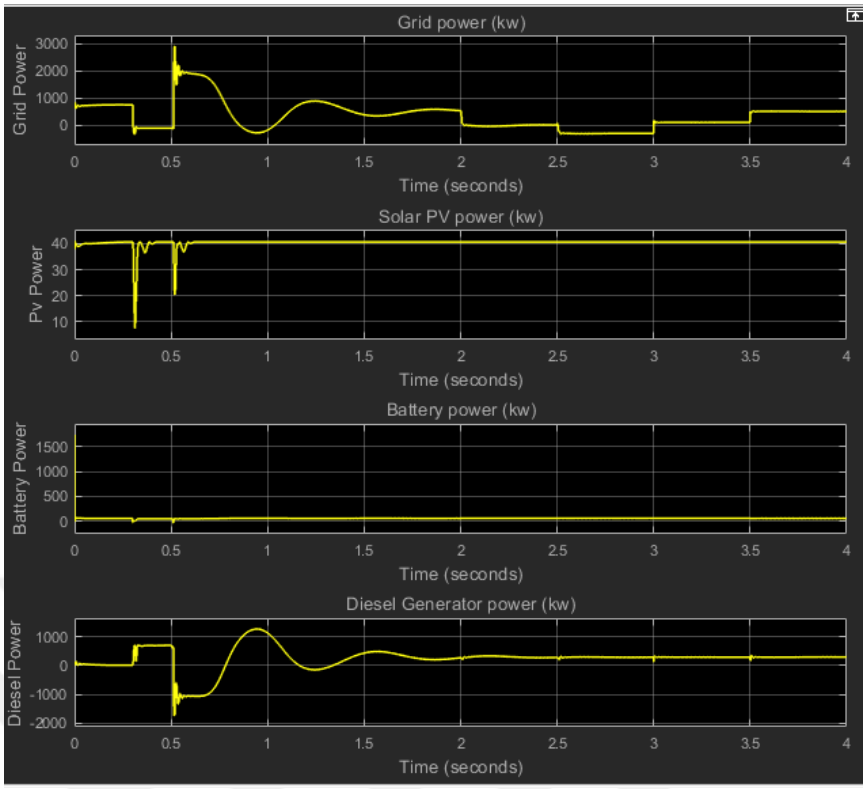

Figure 5.13. Power characteristics of grid, solar PV, battery and diesel generator.

Table 5.2. Active power sharing of KBU MG system.

Time (Sec)	**0 to 0.3 sec.**	**0.3 - 0.5 sec.**	**0.5-2 sec.**	**2 -2.5 sec.**	**2.5-3 sec.**	**3-3.5 sec.**	**3.5-4 sec.**
	Load profile (kW)						
	980	500	980	400	80	500	980
Power Source (kW)	Grid (901)	Grid (-10)	Grid (470)	Grid (-110)	Grid (-430)	Grid (-10)	Grid (470)
	PV-Battery (79)	PV-Battery (80)	PV-Battery (80)	PV-Battery (80)	PV-Battery (80)	PV-Battery (80)	PV-Battery (80)
	Diesel (0)	Diesel (430)	Diesel (430)	Diesel (430)	Diesel (430)	Diesel (430)	Diesel (430)
Operation mode	Grid Connected	Island	Grid Connected	Grid Connected	Grid Connected	Grid Connected	Grid Connected

The fault simulation status and RMS voltage in fault of the system are demonstrated in Figure 5.14. The fault event is occurred at 0.3 sec in main grid and resets at 0.5 sec. During the fault RMS voltage is less than rated value and due to that open command is given to corresponding circuit breaker to isolate the system.

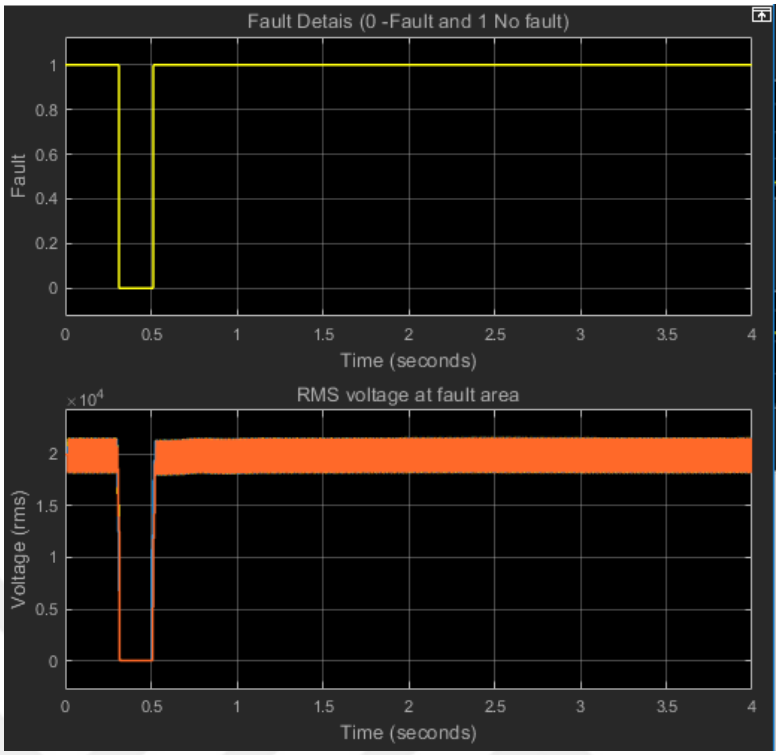

Figure 5.14. Fault details and fault voltage at area.

The critical and non-critical load profiles while the fault in main grid are illustrated in Figure 5.15.

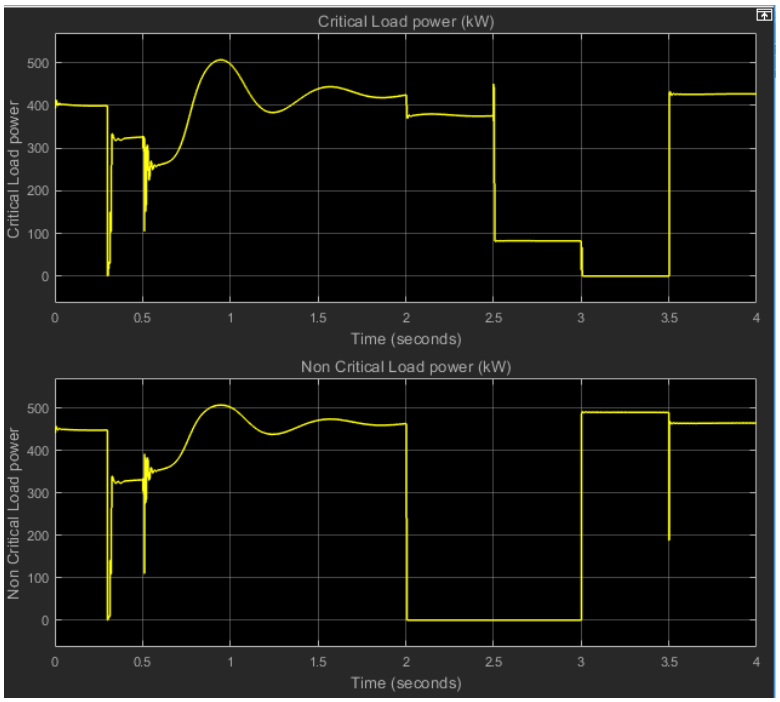

Figure 5.15. Critical and non-critical load profiles while the fault.

The voltage and current variations at HV side of utility grid, LV side of grid, diesel generator bus, PV-battery bus, and load bus are demonstrated from Figure 5.16 to Figure 5.22, respectively. Variation of the voltage and current are follow the load profile settings. The system effective work in both cases such fault control case and optimal load sharing case.

The Figure 5.16 shows the voltage and current of the primary transformer of the grid system. The primary voltage is maintaining at 19.4 kV during 0-0.3 sec. and 0.5 – 4 sec. during fault conditions, primary voltage is equal to 230 V and fault current is increased to 4000 A.

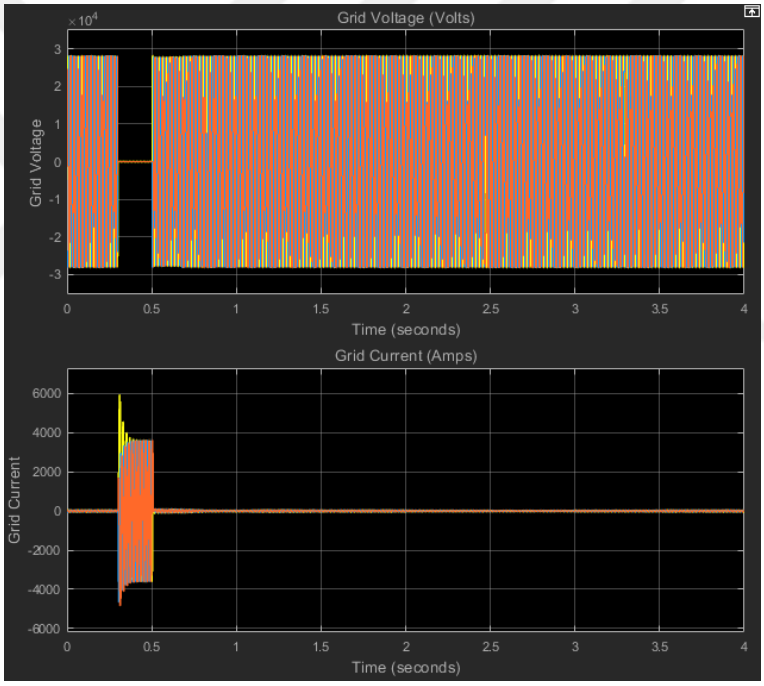

Figure 5.16. Grid voltage and current at the primary transformer.

Figure 5.17 shows the voltage and current of the secondary transformer of the grid system. Secondary of the transformer is maintained at 230 V at intervals 0 – 0.3 sec. and 0.5 – 4 sec. during fault conditions, voltage is slightly reduced to 230 V. The current of the system is vary according with load conditions and fault conditions.

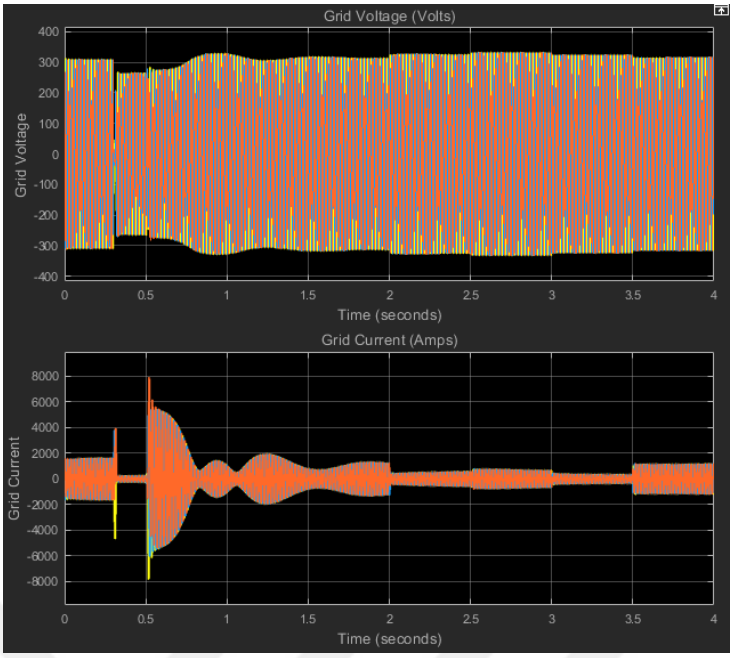

Figure 5.17. Grid voltage and current at the secondary transformer.

Figure 5.18 shows the voltage and current of the PV Battery bus. This bus is maintained at 230 V at intervals 0 – 0.3 sec. and 0.5 sec. – 4 sec. during fault conditions, voltage is slightly reduced to 230 V. The current of the system is varying according with load conditions and fault conditions.

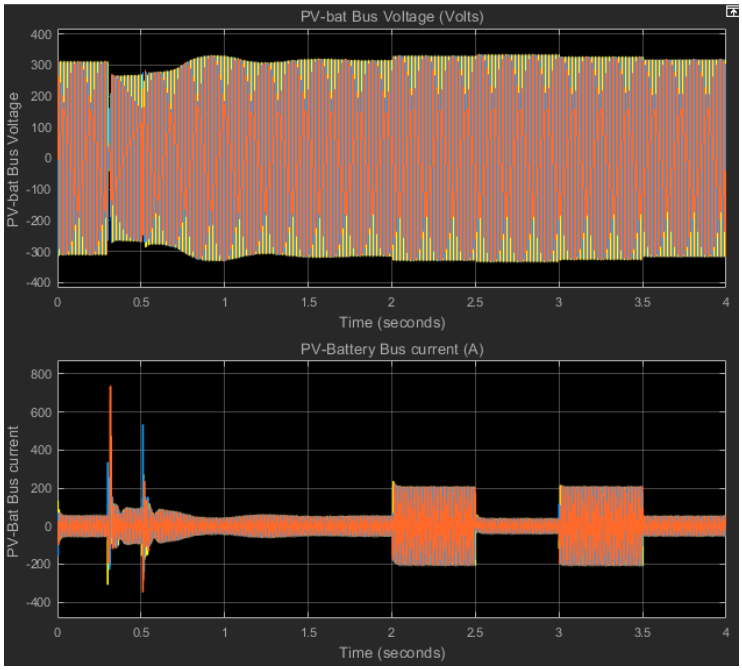

Figure 5.18. Voltage and current of PV-battery bus.

The voltage and current of the diesel generator bus are given in Figure 5.19. This bus is maintained at 230 V at intervals 0 – 0.3 sec. and 0.5 sec. – 4 sec. during fault conditions, voltage is slightly reduced to 230 V. The current of the system is varying according with load conditions and fault conditions.

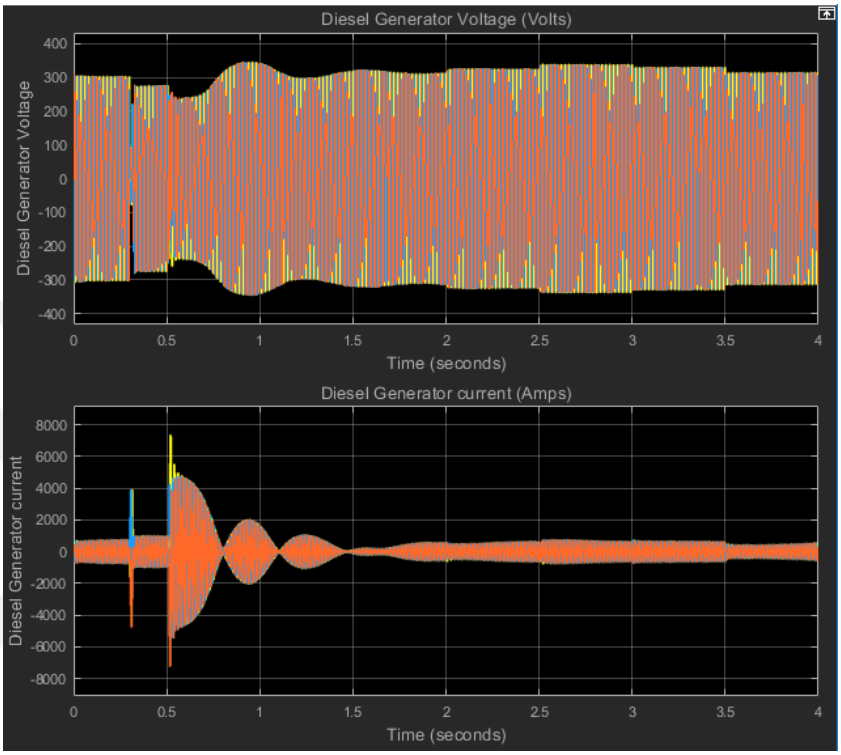

Figure 5.19. Voltage and current of diesel generator.

The voltage and current of the load at diesel generator bus are shown in Figure 5.20. Load is maintained of 230 V at intervals 0 – 0.3 sec. and 0.5 sec. – 4 sec. during fault conditions, voltage is slightly reduced to 230 V. The load is disconnected during 2.5 – 3.5 sec. based on load profile settings. The current of the system is varying according with load conditions and fault conditions.

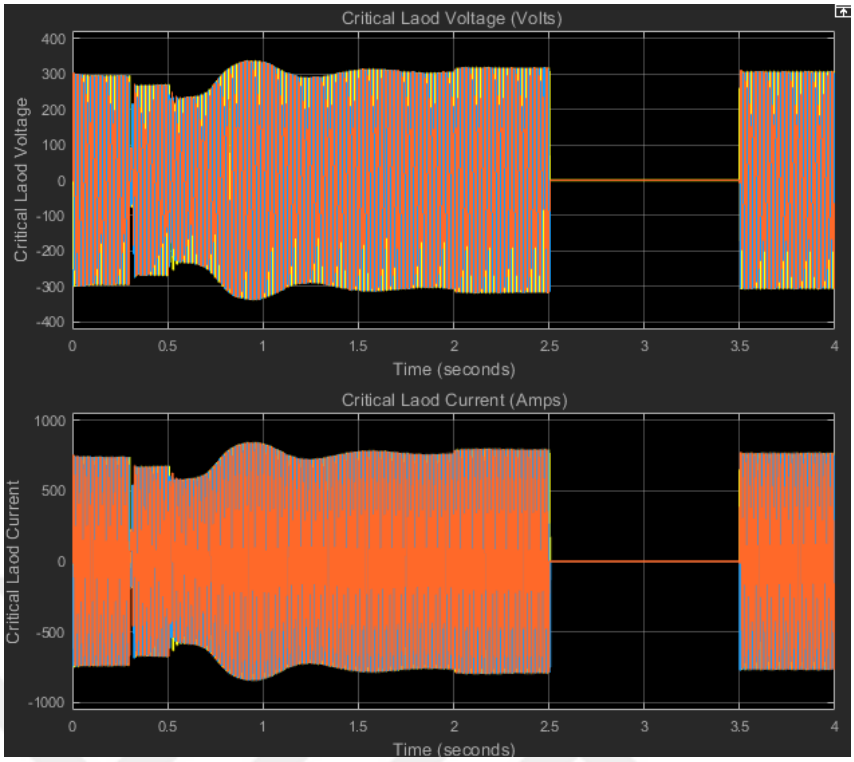

Figure 5.20. Load voltage and current at diesel generator.

The voltage and current of the load at PV-Battery bus are demonstrated in Figure 5.21. The load is maintained of 230 V at the following intervals: 0 – 0.3 sec.; 0.5 sec. – 2 sec.; 2.5 sec. – 3 sec.; 3.5 sec. – 4 sec. while faults occur. The voltage is slightly reduced to 230 V. Load is disconnected during 2 sec to 2.5 sec and 3 sec to 3.5 sec based on load profile settings. The current of the system is varying according with load conditions and fault conditions.

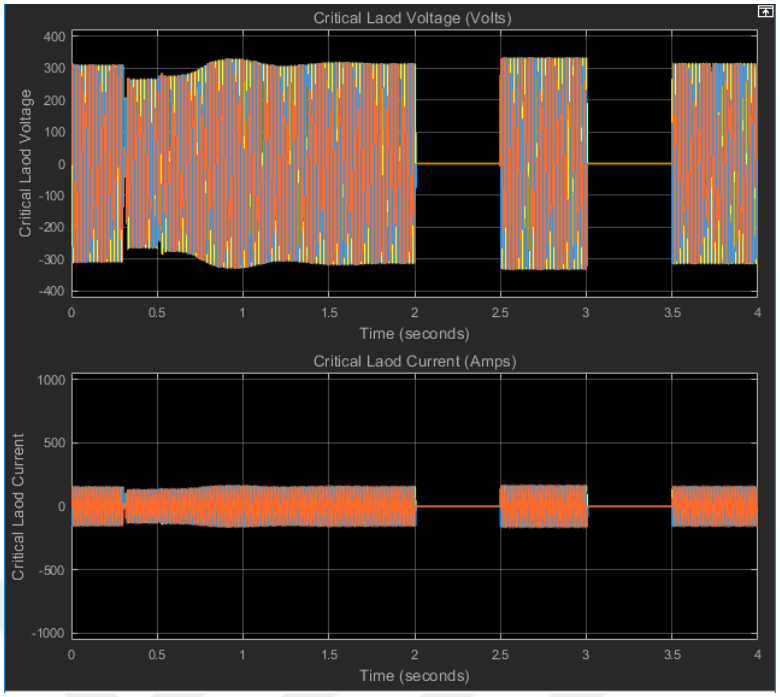

Figure 5.21. Load voltage and current at PV-battery bus.

The voltage and current of the load at secondary transformer of the grid system are shown in Figure 5.22. Load is maintained of 230 V at intervals: 0 – 0.3 sec.; 0.5 sec. to 2 sec.; 3 sec. – 4 sec. while faults occur, we can see how the voltage is slightly reduced to 230 V. Load is disconnected during 2 sec. to 3 sec. based on load profile settings. The current of the system is varying according with load conditions and fault conditions.

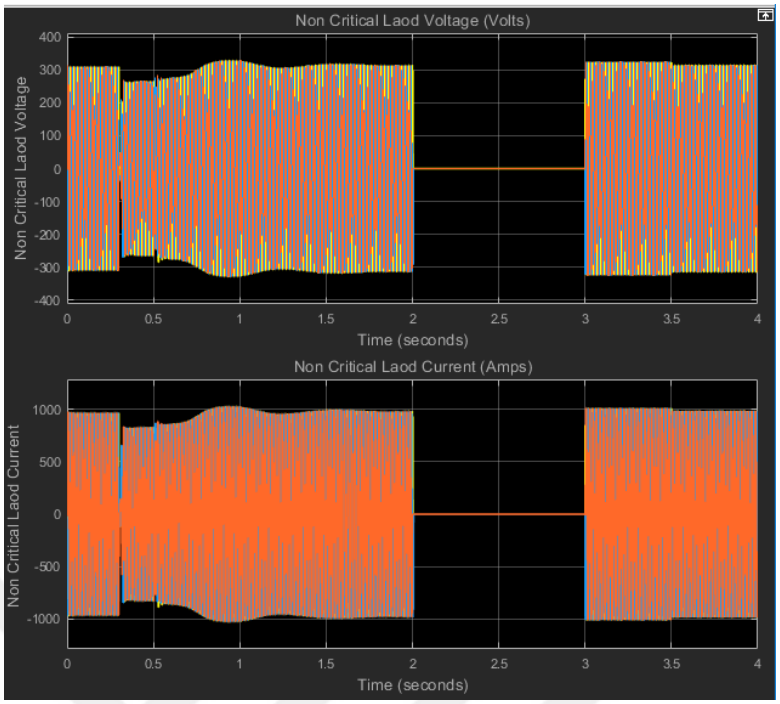

Figure 5.22. Load voltage and current at secondary of the transformer.

The frequency analysis of the microgrid system is shown in Figure 5.23. From 0 to 0.3 sec, the frequency of the system is maintained of 50 Hz. When fault occur during 0.3 to 0.5 sec, the frequency is reduced to 48 Hz. After fault cleared, the frequency of the system is restored to 50 Hz after 2 seconds. After fault it takes 1.7 seconds to restore to rated frequency.

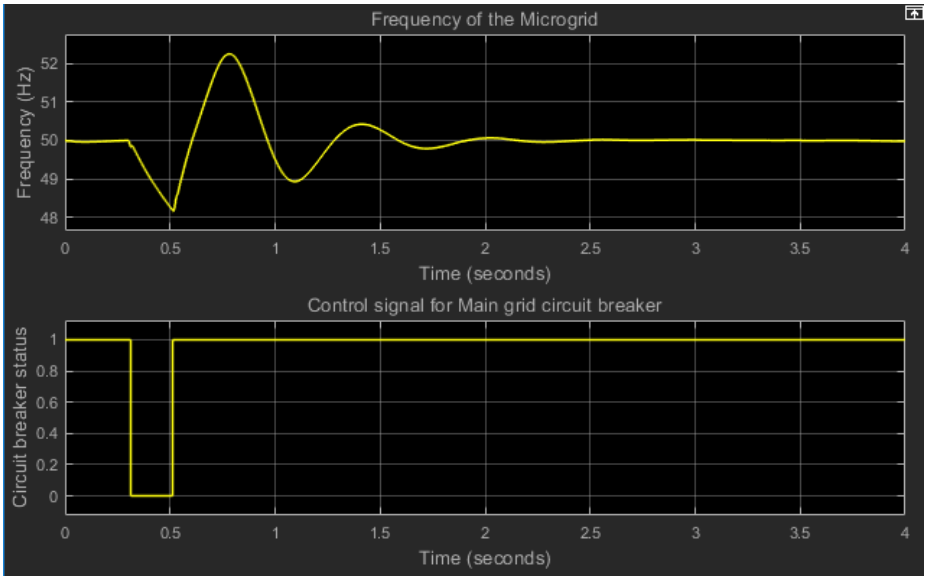

Figure 5.23. Frequency response on grid-connected and island modes.

PART 6

TECHNO-ECONOMIC ANALYSIS OF MICROGRID IMPACT TO KARABUK UNIVERSITY CAMPUS

6.1. INTRODUCTION

Techno-economic analysis of the MG can be carried out using advanced modeling tools that should ensure the reliability of obtained results instead of complex and time-consuming algorithms and costly physical experiments. The survey related to software application for optimization and economic analysis showed that HOMER software has been widely applied and more popular tool than another applied tools [156-163].

In this part of the thesis, MG simulation, optimization, sensitivity, and demand response in addition are performed on the example of Karabuk University (KBU) Engineering faculty. KBU campus has over 53,000 people including students, staff, and academic personnel; so, its power consumption is significant. There are some issues such as increasing utility bills, indirect carbon emissions, and cost of maintaining a complex distribution infrastructure that provides electricity to the large university community. Another problem related to the metering of electricity consumption at each building. Hence, there is only one meter installed at input of university to calculate of power flow. The management of Karabuk university has intended to reduce energy consumption and power managing costs by integrating solar photovoltaic (PV) panels at the university campus. Nowadays, PV panels are installed at five of eight educational buildings of KBU campus. Therefore, our objective is to determine techno-economic and environmental performance of MG and show the effectiveness application of microgrid system in KBU campus.

6.2. METHODOLOGY OF TECHNO-ECONOMIC ASSESSMENT

In this chapter, the results for simulation, technical-economic assessment (optimization, sensitivity analysis, demand response) of KBU Microgrid is utilized by licensed HOMER Grid version 1.6.1 software tool. This software developed by the National Renewable Energy Laboratory (NREL) and implements the following analysis: simulation, optimization, sensitivity and demand response. The following input data are required to process these analyses in Homer: load profile, equipment characteristics, meteorological data, economic and technical data, search space [163,164].

In Figure 6.1 is presented flow chart of the methodology steps utilized for completely analysis. These steps consist of pre-HOMER and post-HOMER analysis. Pre-HOMER analysis is collecting and preparing required initial data for simulation in HOMER program. Then in Post-HOMER analysis, the software executes the simulation of studied MG, analyses for optimization, demand response and sensitivity of MG.

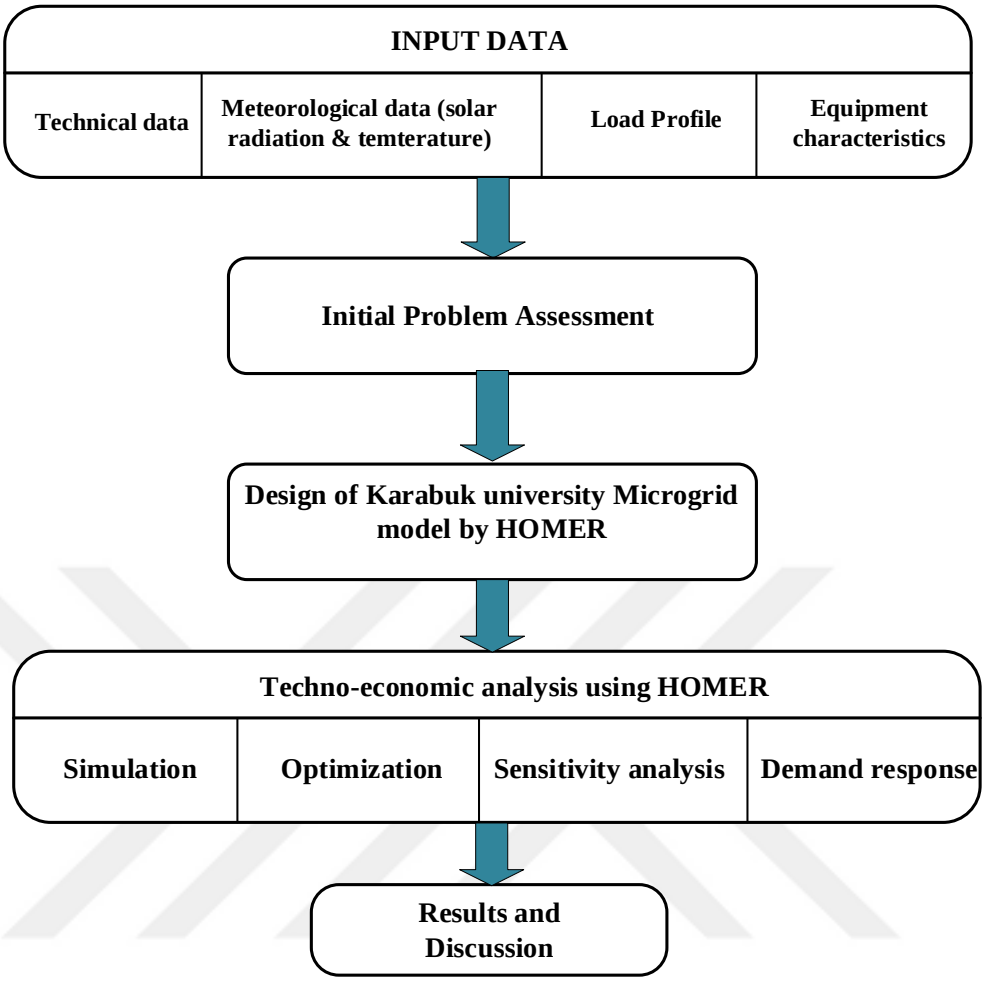

Figure 6.1. Flow chart of the methodology steps for KBU MG analysis.

In the pre-HOMER analysis, we firstly have determined the largest electricity building of KBU consuming electricity. Then KBU MG system is designed on the example of Engineering faculty as biggest electricity consumer of university. Generally, in pre-HOMER input data are collected to perform techno-economic assessment in post-HOMER phase. The detailed load profile of Engineering faculty, equipment characteristics, technical data and meteorological data are carried out in pre-HOMER phase.

The reasonability of basic renewable energy sources, such as wind and solar energy utilizing in Karabuk province is explored according to the research works [165,166] and Turkish solar and wind maps [167]. Research investigation results in [168] show that wind energy utilizing in KBU campus is not effective and rational due to the

insufficient wind speed around Karabuk province. Therefore, the wind system hasn't included to MG design in this work. Meteorological data (solar radiation and temperature), load profile, technical data and equipment characteristics of Engineering faculty building have collected as input data for techno-economic processing in HOMER. Temperature and solar radiation data for Karabuk province is obtained from database of Turkish State Meteorological Service (TSMS) [169].

The optimal designing, sizing and planning of KBU MG system are implemented based on technical characteristics and components, and life-cycle cost of the system. Techno-economic assessment is conducted for both islanded and grid-connected modes of MG system operation. Optimization of system design configurations is performed by minimizing the objective function to the constraints. The objective function in this analysis is total net present cost (NPC), which is the present cost of system excluding the sum of revenues. The constraints are charging and discharging of batteries, power balance and other technical constraints. HOMER simulates the system configurations by making energy balance for each hour and takes the electric loads per hour that a system can supply. Studied system characteristics, i.e. Engineering faculty single line diagram and technical data of components have been represented in Part 4 of this research.

6.3. LOAD PROFILES

KBU MG configurated in HOMER Grid software is illustrated in Figure 6.2. the proposed system consists of utility grid, PV-system with integrated inverter, diesel generator, battery storage, critical and non-critical loads. Utility grid, diesel generator and PV-inverter system are connected to AC-bus, also critical and non-critical loads are power supplied from AC-bus. The battery storage unit is connected to DC-bus. HOMER using initial load profile data calculates average daily energy consumption and peak of critical and non-critical loads.

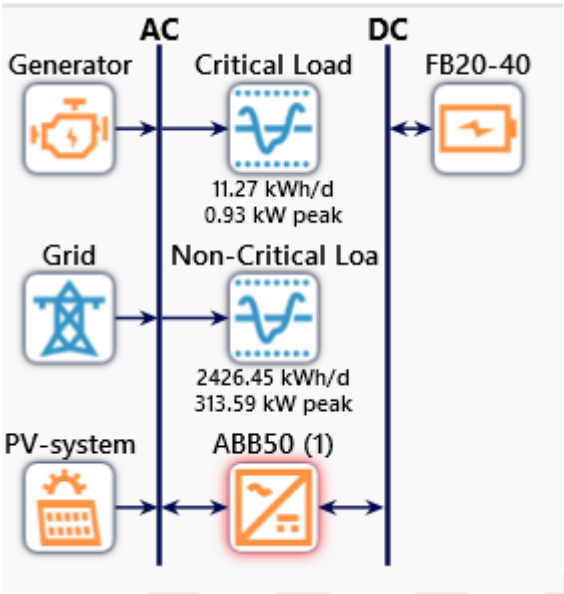

Figure 6.2. System architecture of KBU MG in Homer Grid.

6.3.1. Critical and Non-critical Loads Profile

There was problem accurately calculate the electric consumption loads in the building, because there is not electric meter installed on the faculty. Therefore, the daily, monthly load averages are to obtain load profiles. As mentioned above, load profile of Engineering faculty is given in *Appendix C* and list of critical loads is given in *Appendix D.*

The loads of studied faculty building are divided into critical and non-critical loads (Figure 6.2). MG can be operated in grid-connected mode (MG connected to distribution network) or in islanded mode (MG operates autonomously). By the reason of shortage of distributed energy resources within MG critical loads should be first served. Therefore, loads of Engineering faculty classified into critical and non-critical load. Daily and seasonal profile of critical loads calculated by HOMER are illustrated in Figure 6.3 and Figure 6.4, respectively. In the same way, daily and seasonal profile of non-critical loads calculated by HOMER are illustrated in Figure 6.5 and Figure 6.6, respectively. If there are some outages, failures in utility grid, MG disconnect from grid and the power for critical loads provides by PV-system and diesel generator.

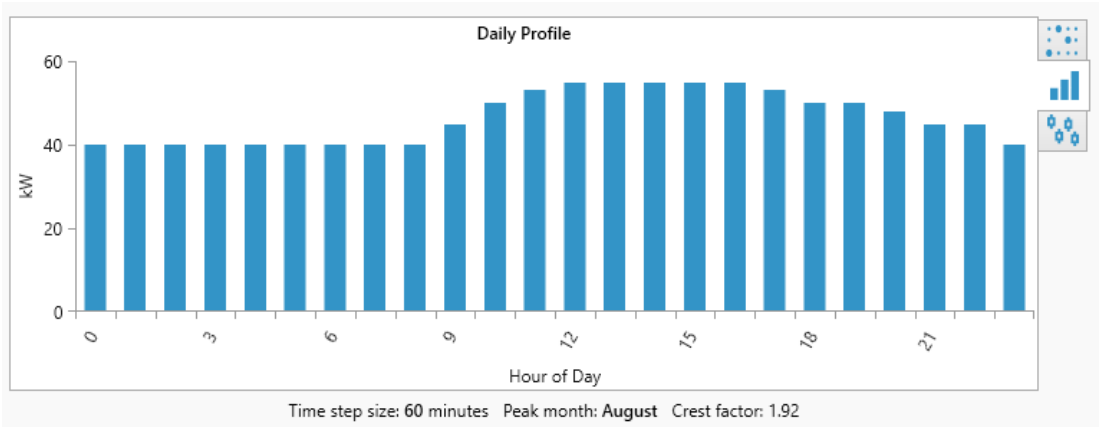

Figure 6.3. Daily profile of critical loads.

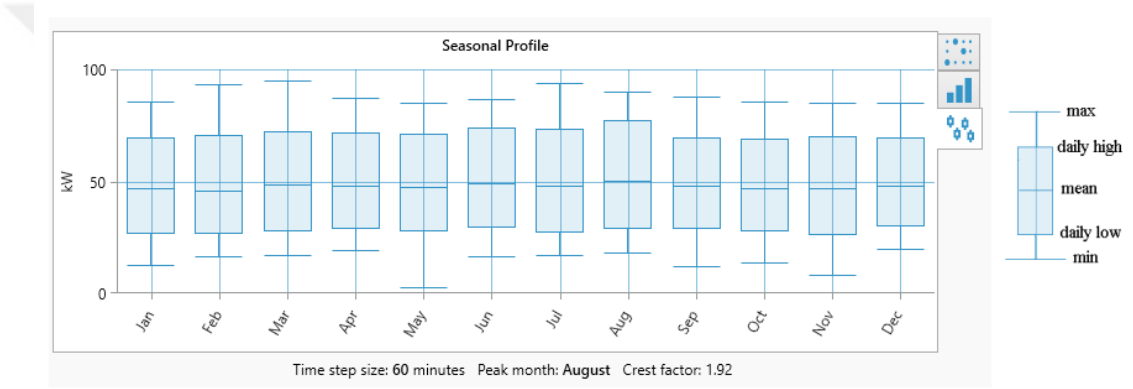

Figure 6.4. Seasonal profile of critical loads.

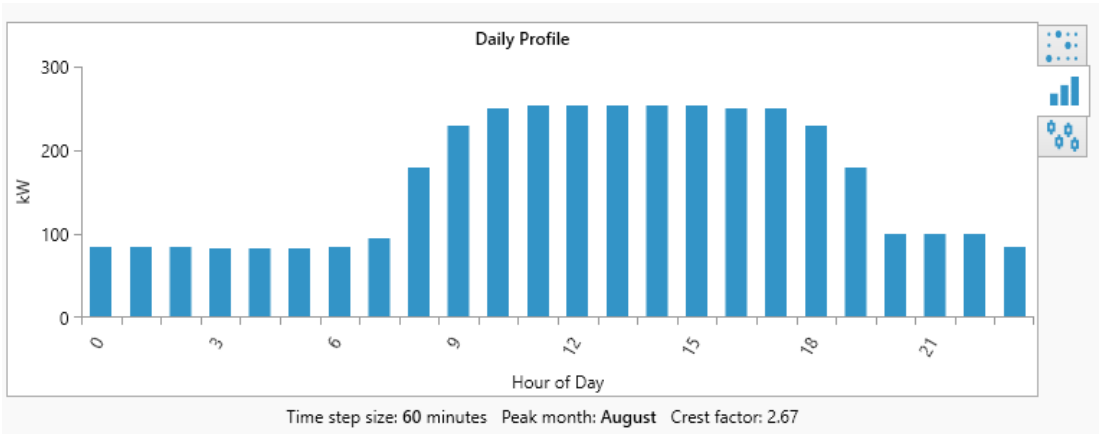

Figure 6.5. Daily profile of non-critical loads.

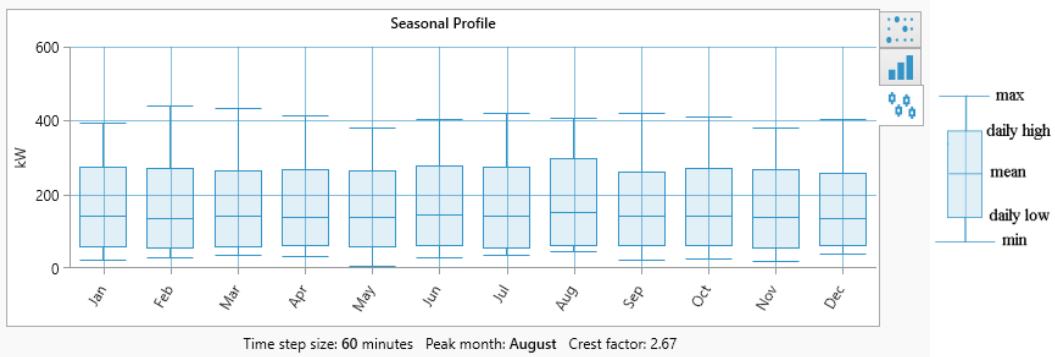

Figure 6.6. Seasonal profile of non-critical loads.

Maximum load of critical loads occurred in March 2018 as 94.78 kW. Maximum demand of non-critical loads was 439.99 kW in February 2018. However, peak month of critical and non-critical loads was in August including minimum and maximum average day, minimum and maximum monthly loads and average per month.

6.3.2. PV-System and Diesel Generator Load Profiles

The annual load profiles of PV-system and diesel generator are given in Figure 6.7 and Figure 6.8, respectively.

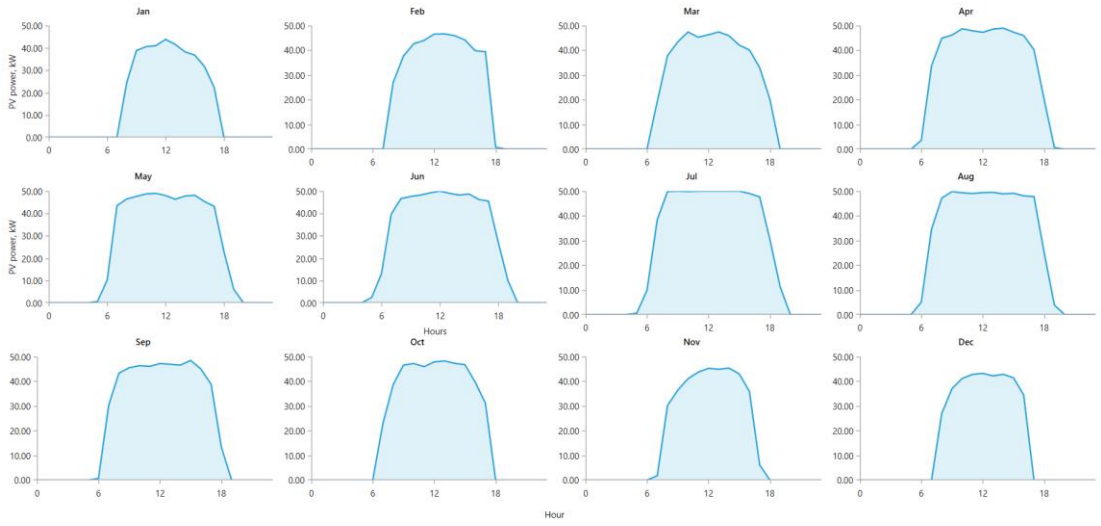

Figure 6.7. PV loads profile consumption (kW) of months with respect to hours.

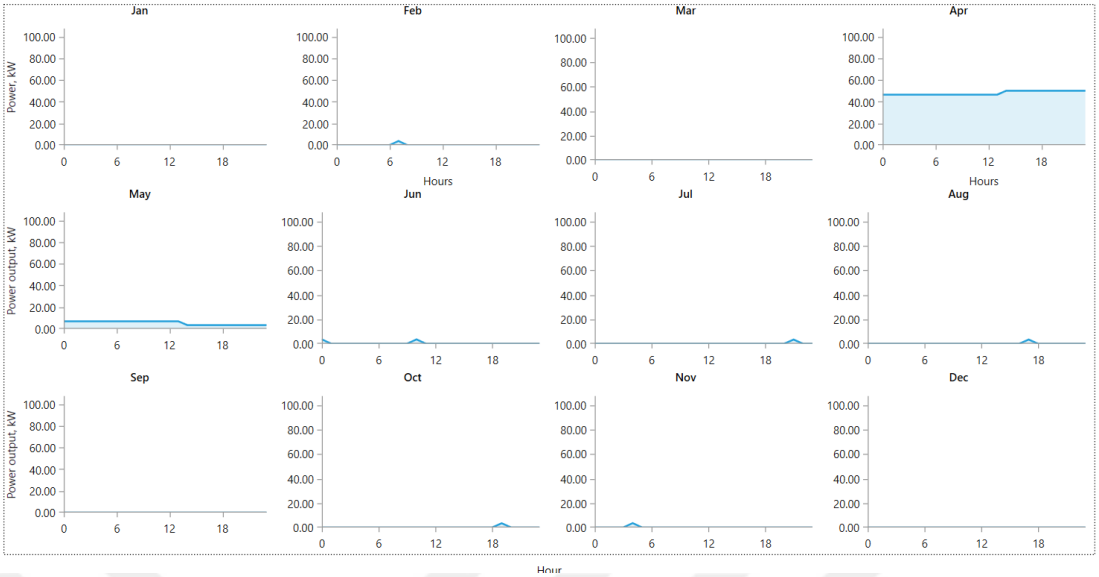

Figure 6.8. Generator loads profile consumption of months with respect to hours.

6.3.3. Solar Resource

Solar resource indicates the amount of global solar radiation that strikes earth's surface. As mentioned above, the temperature and solar radiation data for Karabuk province are obtained from Turkish State Meteorological Service (TSMS). Monthly temperature changing graphic of Karabuk province is given in Figure 6.9. According to TSMS data an average solar radiation in Karabuk is 4.1 kWh/m2/day and a clearness index is 0.520. The clearness index is a measure of the clearness of the atmosphere and which is expressed by the fraction of the solar radiation that is transmitted through the atmosphere to strike the surface of the Earth. The solar irradiation and global horizontal radiations for Karabuk are shown in Figure 6.10. In order to account the degrading factors caused by temperature, soiling, tilt, shading etc. a derating factor of 80% is applied to each panel.

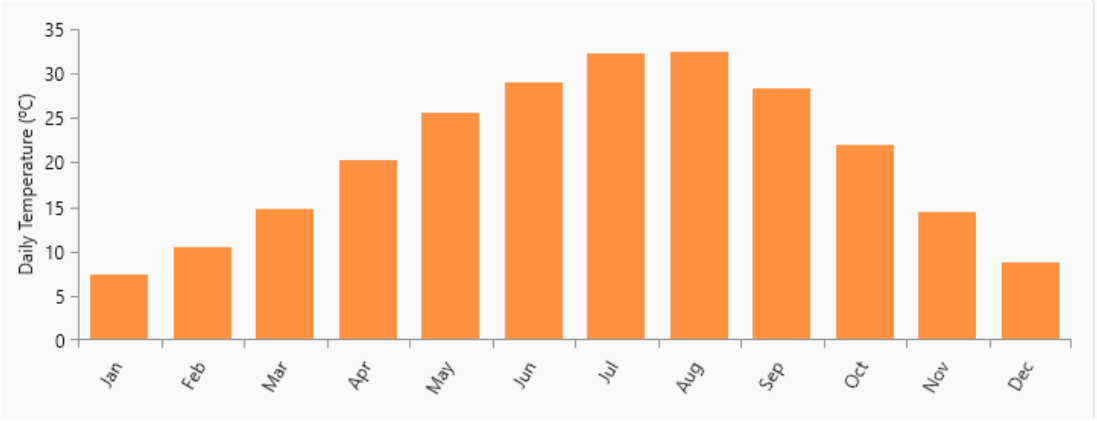

Figure 6.9. Monthly temperature graphic of Karabuk province.

Figure 6.10. Solar global horizontal irradiation.

6.4. OPTIMIZATION ANALYSIS

Techno-economic analysis of the system that calculated by HOMER consists of optimization, sensitivity and demand response analysis.

HOMER using input data processes and simulates multiple system configurations results, and finally determine the best configuration that satisfies the technical restrictions at the lowest life-cycle cost.

NPC and levelized cost of energy (COE) are main indicators to determine economic metrics of energy systems by software tool. The life-cycle cost of the system that is

represented in HOMER as NPC summarizes installing, operating, maintenance, replacement and fuel costs of all component during the project lifetime, also cost of purchasing electricity from the grid. The total NPC reduces if there are any incomes from sale of electricity to the grid. In HOMER the total NPC is calculated using the following equation [170].

$$C_{NPC} = \frac{C_{ann,tot}}{CRF(i,R_{proj})} \tag{6.1}$$

where: $C_{ann,tot}$ – total annualized cost of the system [$/yr]; i – the annual real discount rate [%]; R_{proj} – the project lifetime [year]; *CRF* (·) is a function returning the capital recovery factor, which is given by the formula:

$$CRF(i,N) = \frac{i(1+i)^N}{(1+i)^N-1} \tag{6.2}$$

where:

N – number of years.

Levelized COE is calculated with the following equation:

$$COE = \frac{C_{ann,tot}-c_{boiler}H_{served}}{E_{served}} \tag{6.3}$$

where: c_{boiler} – boiler marginal cost [$/kWh]; H_{served} – total thermal load served [kWh/yr]; E_{served} – total electrical load served [kWh/yr]. In our case study: $c_{boiler} = 0$, H_{served}=0. Therefore, COE is described by the equation:

$$COE = \frac{C_{ann,tot}}{E_{served}} \tag{6.4}$$

Another economic metrics of considered system are the internal rate of return (IRR) and return on investment (ROI). IRR is a discount rate at which net present value (NPV) of all cash flows is equal to zero. IRR is defined from the following equation [171]:

$$0 = NPV = \sum_{t=0}^{T} \frac{CF_t}{(1+IRR)^t} \tag{6.5}$$

where:

CF_t – cash flow during the period *t* (years)
T – the life (years) of the system;
NPV – the net present value of all cash flows from a particular project equal to zero.

ROI introduces yearly cost savings relative to the initial investment. ROI calculation is given by HOMER as follows [172]:

$$ROI = \frac{\sum_{i=0}^{R_{proj}} C_{i,ref} - C_i}{R_{proj}(C_{cap} - C_{cap,ref})} \tag{6.6}$$

where: $C_{i,ref}$ – nominal annual cash flow for base (reference) system; C_i – current system nominal annual cash flow; R_{proj} – project lifetime in years; $C_{cap,ref}$ – base system capital cost; C_{cap} – current system capital cost.

A financial metric for cash flow analysis is defined as payback period (PB). The PB can be calculated as:

$$PB = \left(\frac{Initial\ Investment}{Cash\ flow\ per\ period}\right) \tag{6.7}$$

Renewable fraction (RF) is the fraction of energy that generated from renewable sources and supplied to loads. In can be calculated as follows:

$$RF = 1 - \frac{E_{nonren} + H_{nonren}}{E_{served} + H_{served}} \quad (6.8)$$

E_{nonren} – non-renewable electrical production [kWh/year];
H_{nonren} – non-renewable thermal production [kWh/year];
E_{served} – total electrical load served [kWh/year];
H_{served} – total thermal load served [kWh/year].

6.5. SENSITIVITY ANALYSIS

In the sensitivity process HOMER analyze optimization of the system for uncertainty variables such as global solar, wind speed and diesel fuel price which entered by modeler.

HOMER executes sensitivity analysis of multiple values for each input variable. These multiple values specified for input assumptions is called sensitivity variable. User can designate one, two or more sensitivity variables for each input variable and sensitivity analysis can be one, two-dimensional and so on depending on the quantity of sensitivity variables.

In this process, the program evaluates the influences of uncontrolled parameters or changes. Finally, a list of various hybrid system configurations will be presented in the table, considering total NPC, COE and operating cost of each configuration from lowest to highest value and HOMER will show the optimal configuration system with lowest total NPC, COE and operating cost. In HOMER, random number generator is also used to select the times of outages and demand response events. The “seed” is some number used by the random number generator. Random seed affects random outages and random demand response events.

6.6. DEMAND RESPONSE

As fined in the literature demand response (DR) is the process to reduce or shift of intentional energy usage by costumers while peak time in response in market prices [173,174]. DR is also an effective way to shave of peak demand, to manage of risk and reliability, to reduce of energy cost and carbon emission [175].

DR programs are significant and valued resource of power systems. Over the last few decades, with integration of large fraction of renewable generation into power systems, demand response programs become more functionable tool enabling to provide not only peak load reductions, and also enhance efficient price formation in electricity market, improve reliable operation of power systems. [176,177].

DR resources have connection with energy markets in the following ways: either as dispatchable system operator, or non-dispatchable system operator. Dispatchable system operators interface directly with wholesale market to bid and get reduced payment for DR. Non-dispatchable system operator takes part in price-based demand response programs that provide customers with updated price information by promoting them lower energy consumption while peak load time. These resources are not “steady”, because they are not dispatchable, and system operators do not sure about feedback users’ responses. Non-dispatchable price-based programs can be used by residential and small customers with smart meters.

DR can be employed in MGs for loads managing and to distribute the consumption among hours. If in grid-connected mode DR is used to get economic benefit, while in islanded mode DR can be utilized to provide the security of power supply [178].

HOMER Grid using the electricity production data of all generation units simulates the demand response model [179].

The program calculates the amount of baseline load reduction based on the measures and records of customer baseline load. HOMER demand response program also

supplies how much customers should bid to reduce and what battery/generator capacity they should invest in to reduce grid purchases during DR event.

6.7. SIMULATION RESULTS AND DISCUSSION

Simulation is performed with specified data through HOMER to obtain the optimal result for grid-connected KBU microgrid. After simulation HOMER proposes the best option of NPC, legalized COE, operation cost, reduced electricity bill, and other economic parameters by compare different cases.

There are four cases with following components:

- Case 1 – Utility and generator (base case);
- Case 2 – Utility, PV-system and generator;
- Case 3 – Utility, PV-system, battery storage and generator;
- Case 4 – Utility, battery storage and generator.

HOMER processes optimization and sensitivity analysis, and then presents results for various configuration of hybrid system in table form. HOMER also presents optimization results for all architecture options of KBU MG systems.

In Table 6.1 are given optimization results for various cases of KBU MG. In this Table, we see that the most effective cost and economic metric results are obtained for Case 2 with the smallest electricity price of $0.292 per kWh.

Table 6.1. Case-wise comparison of optimization results.

	Case 1 Base case (Utility, generator)	**Case 2 Proposed system (Utility, PV-system and generator)**	**Case 3 (Utility, PV-system, battery storage and generator)**	**Case 4 (Utility, battery storage and generator)**
Initial capital ($)	$645,000	700,871	758,821	700,000
Net Present Cost ($)	2.03M	1.81M	1.87M	2.09M
LCOE (per kWh)	$0.329	$0.292	$0.302	$0.338
Operating cost ($/year)	190,901	152,618	153,946	191,637
IRR (%)	N/A	68.0	31.0	N/A
Return of investment (%)	0	59.0		-11.3
Renewable fraction (%)	N/A	14.8	15.1	N/A
Annualized utility bill savings ($)	0	38,200	38,617	14.56
Demand charge savings ($/yr)	0	13.51	13.51	13.51
Annualized energy charge savings ($)	0	38,186	38,604	1.05

The comparison results of yearly electricity production and consumption data for all cases of system configuration are presented in Table 6.2. Again, these analysis show that the systems with solar PV configuration (Case 2 and Case 3) have more electricity production than other systems (Case 1 and Case 4). The share of electricity production by solar PV for Case 2 and Case 3 are 19.3% and 19.5%, respectively. Because there are only AC loads in LV bus, the electricity consumption is the same for all cases. The surplus yearly electricity sold to grid by systems with solar PV configurations are 1,964 kWh and 2,015 kWh for Case 2 and Case 3, respectively.

Table 6.2. Comparison of electricity production and consumption.

Component	**Case 1**	**Case 2**	**Case 3**	**Case 4**
Production (kWh/year)				
PV-system	–	174,205 (19.3%)	176,077 (19.5%)	
Generator	39,452 (4.4%)	39,452 (4.38%)	39,452 (4.38%)	39,452 (4.4%)
Grid Purchase	851,793 (95.6%)	687,843 (76.3%)	686,075 (76.1%)	851,789 (95.6%)
Total	891,245	901,500	901,604	891,241
Consumption (kWh/year)				
AC Primary Load	851,962 (100%)	851,962 (99.8%)	852,086 (99.76%)	852,086 (100%)
Grid sales	–	2,076 (0.243%)	2,015 (0.24%)	–
Total	851,962	854,038	854,101	852,086
Excess electricity (kWh/year)	39,284	303,284	324,189	39,284

In Table 6.3 are given the case-wise comparison of yearly emissions. As can be observed from this Table, the value of carbon monoxide and particulate matter emissions have not changed for all simulation cases. There are differences of carbon dioxide, sulfur dioxide and nitrogen oxides emissions between the systems with solar PV (Case 2 and Case 3) and without solar PV (Case 1 and Case 4) configurations.

In difference from optimization results the best emissions reduction belongs to Case 3. This is due to the fact, that solar energy generated by Case 3 was greater than in the Case 2, and battery storage system was used in addition. It should be noted that by installing solar PV systems 18% of CO2 can be prevented to compared with the systems without solar PV.

Table 6.3. Case-wise comparison of yearly emissions.

Quantity	**Case 1**	**Case 2**	**Case 3**	**Case 4**
Emissions (kg/year)				
Carbon Dioxide	561,691	458,074	456,956	561,688
Carbon Monoxide	77.7	77.7	77.7	77.7
Unburned Hydrocarbons	0	0	0	0
Particulate Matter	2.19	2.19	2.19	2.19
Sulfur Dioxide	2,334	1,885	1,880	2,334
Nitrogen Oxides	1,304	1,085	1,082	1,304

Further, the results of Case 2 are analyzed as lowest cost (proposed) system. In Figure 6.11 is presented the comparison of NPC between the base case (Case 1) and proposed (Case 2) configuration system. In the graphic of cumulative cash flow versus project lifetime we can see how the system saves money over the project by comparing winning system and base case system. Simple payback of 1.5 years occurs when two lines intersect with each other (Figure 6.11).

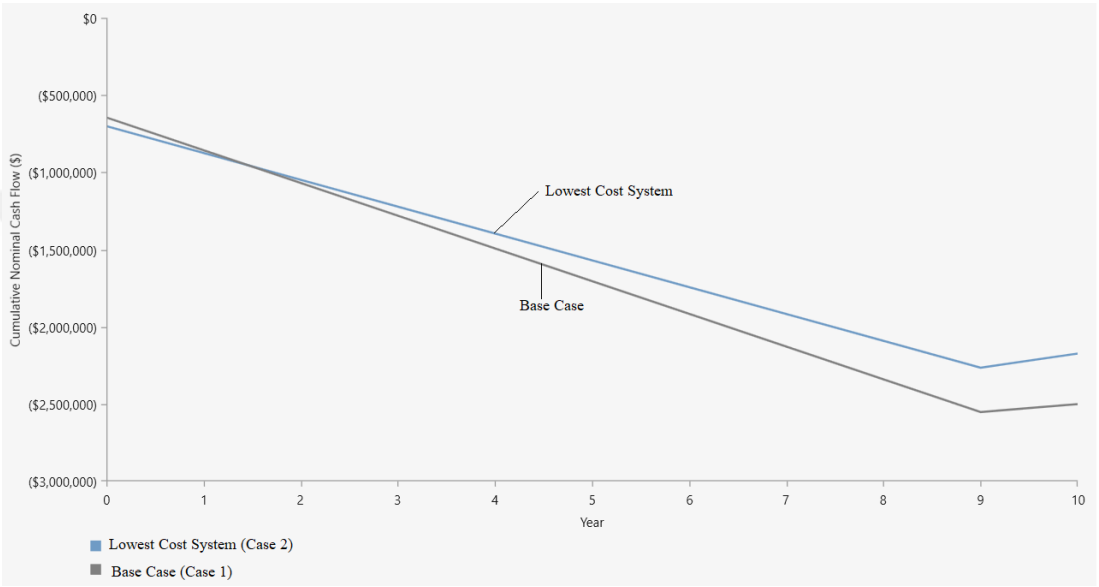

Figure 6.11. Comparison of NPC between base case and lowest cost system configuration.

In Figure 6.12 is summarized down estimated annual savings by the categories for proposed system.

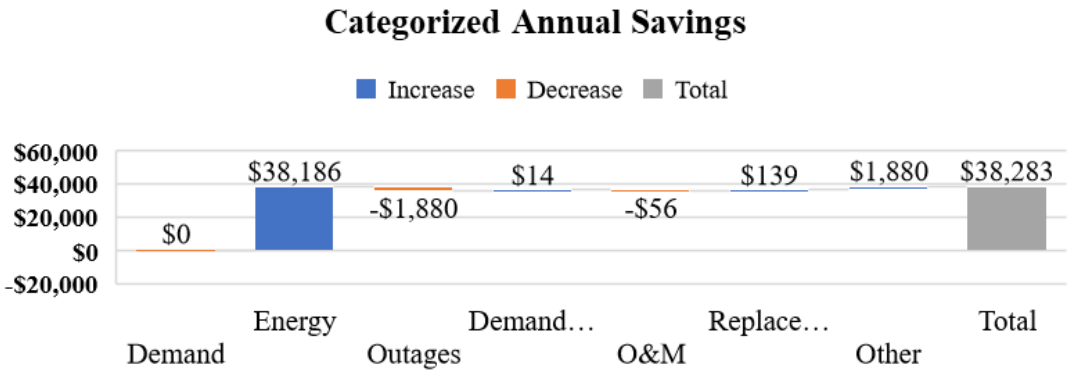

Figure 6.12. Annual savings of the proposed (winning) system by categories.

The annual utility bill of Engineering faculty is reduced to $153,488 by adding PV-system of 279 kW to LV distribution network. The investment has a payback of 1.47 years and an IRR of 67.90%.

The comparison of utility monthly summary between current system and proposed system is given in *Appendix E*.

The share of monthly average electricity production of the Case 2 (utility grid – PV-system – diesel generator) is illustrated in Figure 6.13. Form this figure, we can see that diesel generator mostly is operated during outages in grid, in April and May months, while PV-system generation cannot provide the system electricity demand.

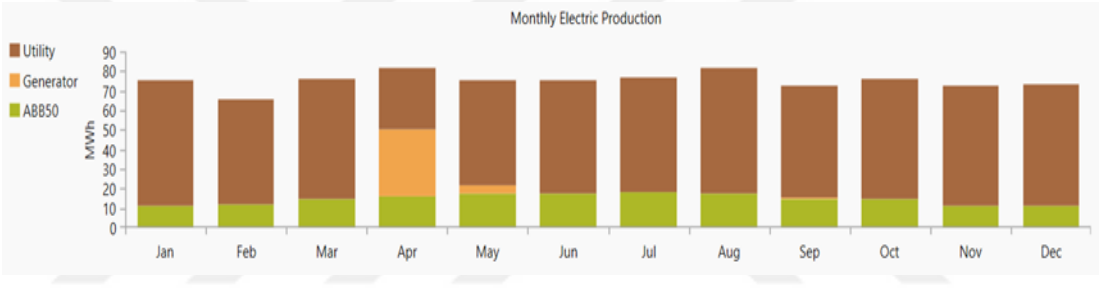

Figure 6.13. Monthly average electricity production for proposed system.

Generator set statistics are given in Table 6.4. It is observed that while eight starts – operation the efficiency of generator was 33% with capital cost of $645000. Power output from the generic generator system, rated at 108 kW using diesel as fuel, is 39,452 kWh/year. Generally, generator has utilized while outages to provide microgrid reliability. The quantity results of diesel generator in outages, failures events are given in Table 6.5.

Table 6.4. Generator statistics.

Characteristics	**Value**
Capacity	108 kW
Operational Life	54.5 year
Number of starts	8 starts/year
Capital Cost	$645,000
Generator Fuel	Diesel
Generator Fuel Price	1.30 $/m³
Maintenance Cost	3,156 $/year
Fuel Consumption	12,098 m³
Hours of Operation	367 hrs./year
Electrical Production	39,452 kWh/year
Mean electrical output	108 kW
Mean electrical efficiency	33%

Table 6.5. Generator quantities during outage.

Quantity	**During outage**
Runtime (hours/day)	24
Operating and maintenance cost ($/day)	206
Fuel consumption (m^3/day)	791
Fuel cost ($/day)	1028
Capacity shortage hours	0

In demand response program Karabuk EDAŞ offers an incentive of $3.00 for every kW reduced. During the notification by the utility KBU should reduce the electric consumption for one hour. Signing up for this program KBU gets a total revenue of $4,239. In the demand response events that occur in a year, and the revenue incurred by reducing Engineering facility's peak during each one of them are given in Table 6.6. One of these events that occurred on January 30 is illustrated in Figure 6.14. According to the demand response program the revenue was $841 for optimized demand reduction bid of 280 kW.

Table 6.6. Demand response and revenue.

Event Date	Reduction (kW)	Revenue ($)
30 Jan 17:00	280	$841.00
01 Apr 18:00	71.7	$215.00
08 May 13:00	195	$585.22
03 Jul 16:00	148	$445.22
24 Jul 11:00	232	$696.15
12 Sep 10:00	230	$691.27
12 Nov 12:00	255	$765.43
Total	1411.7 kW	$4239.29

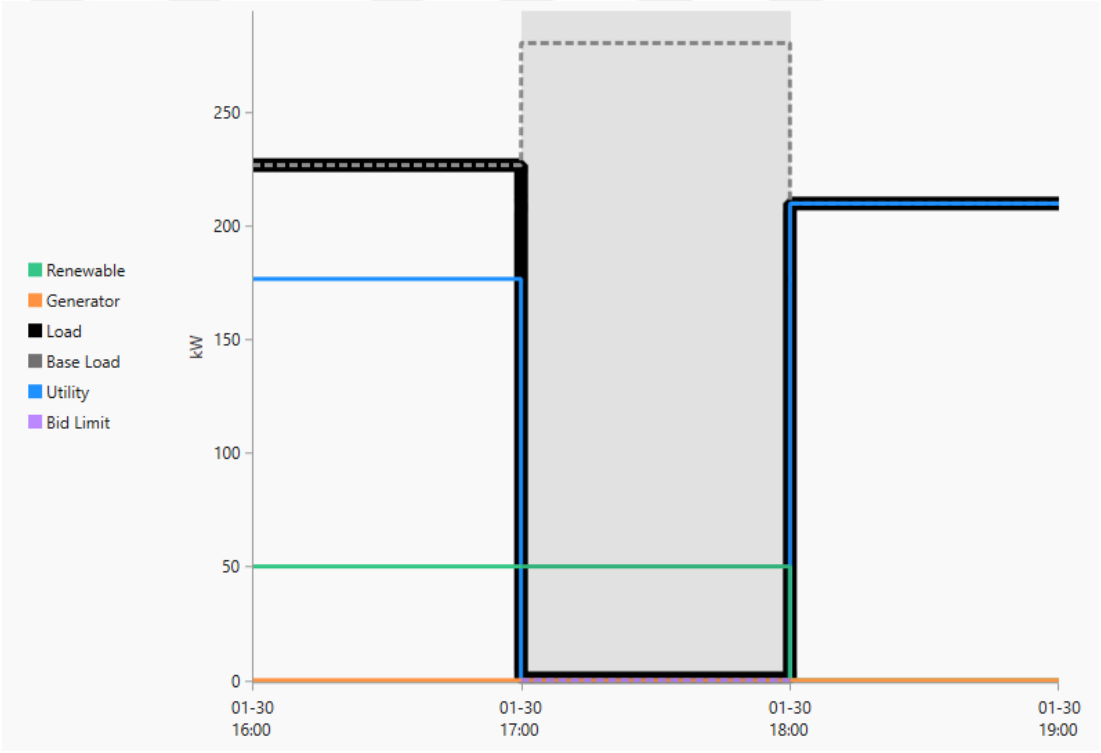

Figure 6.14. Demand reduction during DR program.

PART 7

CONCLUSION AND FUTURE WORKS

Hydrocarbons are the main sources to generate electricity. However, the limited availability of fossil fuels, rising fuel prices and environmental pollution from burning fossil fuels have cast doubt on the future viability of human civilization, which depends on traditional energy sources. In recent year, in many countries the share of renewable energy sources in the energy generation has been increasing due to their positive impact on addressing environmental concerns as a clean energy source, low expenses for operation and maintenance, easy setup.

MG is an interconnection of distributed generation such as microturbines, wind turbines, photovoltaics (PV), and storage devices and interior loads which operate at low-voltage (LV) and/or medium-voltage (MV) distribution network. Such a single system gives a new problem, such as provide a stability while intermittency of renewable energy sources, power quality, etc. These issues should be resolved by applying advanced technologies at LV/MV distribution network of power systems.

7.1. GENERAL CONCLUSIONS

In this thesis the following works have carried out:

- Microgrid system has planned and designed for one substation of Karabuk university (KBU) distribution network. This microgrid system of KBU is considered as AC-microgrid and includes a diesel generator and solar PV systems with battery storages.

- KBU microgrid system dynamics have represented and modeled. Dynamic modeling is generally conducted for all components of KBU microgrid to analyze the stability (small-signal stability) of microgrid system.
- Control strategies of KBU microgrid in grid-connected and island modes have proposed. Such control systems allowed the microgrid system to balance the demand and supply of electric power and to simultaneously control the state of KBU's power network.
- Simulation of microgrid in both grid-connected and isolated operation modes has implemented on MATLAB/Simulink. From the simulation results, the developed control mechanisms provide stable operation in the microgrid system.
- Load sharing control of distributed energy sources has carried out. The distributed energy sources have been supplying the energy to load based load profile settings.
- Fault control of KBU microgrid system has conducted. The fault control and optimal power flow control has been implemented to effectively manage the energy in the microgrid system. The system is effectively disconnecting the microgrid from main grid within a microsecond after fault conditions.
- Techno-economic and environmental analyzing of KBU microgrid have accomplished. It has been observed that applying MG at Engineering faculty of Karabuk University is significantly decreased net present cost and cost of energy. According to the simulation results on HOMER the optimized case solution has been determined with sensitivity parameters from four cases.

7.2. SPECIFIC CONTRIBUTIONS OF THE THESIS

In this dissertation we delivered our contributions towards microgrid designing, planning, modeling and optimization of Karabuk university. The contribution aims to make determined efforts to deal with applying microgrid system of KBU campus. The specific contributions of this thesis are following:

- Karabuk MG system has planned, designed and modeled on the example of Engineering faculty.

- Analysis on applying of distributed energy resources have conducted. According to the research analysis [117,118] we identified that potential of wind energy in Karabuk region is low with 2.4 m/s annual average wind speed and 21.3 W/m^2 annual average wind density. Therefore, designing and installation wind turbine at Karabuk university is not proper. It should be noted that the utilizing wind turbine as distributed generation at other buildings of KBU campus is not effective.
- Developed MG system of KBU can operate either in connection with utility grid or autonomous mode if there are faults or outages in main grid. Therefore, MG can operate in autonomous mode to prevent trouble power trip events and provide power supply of critical loads, such as data center, water and heating pumps, fire alarm system during 24 hours in day.
- Optimization, sensitivity, demand response and environmental assessments of KBU microgrid have implemented for various configuration. The comparison results show that the best case for KBU MG comprises utility, PV-system and diesel generator. For this case we have obtained the smallest electricity price of $0.292 per kWh, with net present cost of $1810000 and operating cost of $152618 per year.
- In the best configuration system of microgrid the share of electricity generation by PV-system was 19.3% of total electricity production. The surplus yearly electricity sold to grid was 1,964 kWh.
- The annual utility bill of Engineering faculty is reduced to $153,488 and saved $38200 by applying the utility grid – PV – diesel generator system. The investment has a payback of 1.47 years and an IRR of 67.90%.
- Systems configuration with solar PV-systems have reduced the emissions (carbon dioxide, sulfur dioxide and nitrogen oxides) than systems configuration without PV-system. So, CO2 emission has minimized to 18% in solar PV system.
- According to the demand response program of Karabuk EDAŞ Karabuk university can get a total revenue of $4,239 for demand reduction bid of 1411.7 kW.

7.3. RECOMMENDATION FOR FUTURE WORKS

Based on the research contributions the following suggestions can be proposed for future works:

- Implementation and development of multi-agent systems for secondary and tertiary control levels of microgrid. Discussing and evaluating simulation findings in this study serves as an introductory step towards the development and hardware execution of decentralized agent-based management for microgrid operation effectively. The suggested multi-agent system-based model for decentralized microgrid control is required further testing through an actual experimental setup study and evaluation.
- For integrated distributed energy resources to main grid to supply power for microgrids.
- For better energy storage, additional distributed energy resources and batteries could be incorporated into the system. The available energy could be stored for later use especially during times when the demand for power is low.
- Merging more distributed energy resources needs further work on specifying new tasks for a distributed energy resource agent.

REFERENCES

1. Azmi, W. H., Sharif, M. Z., Yusof, T. M., Mamat, R., and Redhwan, A. A. M., "Potential of nanorefrigerant and nanolubricant on energy saving in refrigeration system – a review", ***Renew. Sustain. Energy Rev.***, 69: 415–428 (2017).

2. ***International Renewable Energy Agency*** (IRENA), "Renewable energy statistics" (2019).

3. Lasseter, R. H., "MicroGrids", ***Power Engineering Society Winter Meeting, IEEE***, 1: 305–308 (2002).

4. Ackermann, T., Andersson, G., and Soder, L., "Distributed generation: a definition", ***Electric Power Systems Research*** 57: 195–204 (2001).

5. Lasseter, R. H., "Integration of distributed energy resources: The CERTS MicroGrid concept," ***California Energy Commission,*** (2003).

6. Hatziargyriou, N., Asano, H., Iravani, R. and Marnay, C., "An overview of ongoing research, development, and demonstration projects," ***IEEE power & energy magazine***, 78–94 (2007).

7. Chowdhury, S. P., Crossley, P. and Chowdhury S., "Microgrids and active distribution networks", ***Institution of Engineering and Technology,*** London, United Kingdom, 321 (2009).

8. Hatziargyriou, N., "Microgrids: architectures and controls", ***Wiley-IEEE Press***, Chichester, United Kingdom, 341 (2014).

9. Jiayi, H., "A review on distributed energy resources and Microgrid", ***Renewable and Sustainable Energy Reviews***, 12: 2472–2483 (2008).

10. Barnes, M., Kondoh, J., Asano, H., Oyarzabal, J. and Green, T., "Real-World MicroGrids: An Overview," ***IEEE International Conference***, 1–8, (2007).

11. Mahmoud, M., Rahman, M. and A.L.-Sunni F., "Review of microgrid architectures – a system of systems perspective", ***IET Renew. Power Gener.***, 9 (8): 1064–1078 (2015).

12. Martin-Martínez, F., "A literature review of Microgrids: A functional layer based classification" ***Renewable and Sustainable Energy Reviews***, 62: 1133–1153 (2016).

13. Olivares, D., "Trends in Microgrid Control," ***Smart Grid, IEEE Transactions***, 5 (4): 1905–1919 (2014).

14. Katiraei, F., "Microgrids management," ***IEEE Power Energy Mag.***, 6 (3): 54–65 (2008).

15. Alibhai, Z., Gruver, W., E., Kotak, D. B., and Sabaz, D., "Distributed coordination of MicroGrids using bilateral contracts", ***IEEE International Conference Systems, Man Cybernetics***, 1990–1995 (2004).

16. Patra, S. B., Mitra, J., and Ranade, S. J., "MicroGrid architecture: a reliability constrained approach", ***IEEE Power Eng Soc Gen Meet***, 2372–2377 (2005).

17. Ghiani, E., Mocci, S. and Pilo, F., "Optimal reconfiguration of distribution networks according to the MicroGrid paradigm", ***International Conference Future Power Systems***, 1–6 (2005).

18. Jackson, J. J., Francis, M., Ju, L., and Jin-Woo, J., "AC-microgrids versus DC-microgrids with distributed energy resources: A review", ***Renewable and Sustainable Energy Reviews***, 24: 387–405 (2013).

19. Arif, E., Hossen, J., Ramana, G., Bhuvaneswari, T., Velrajkumar, P. and Venkataseshaiah, C., "A survey on neuro-fuzzy controllers for solar panel tracking systems", ***Far East Journal of Electronics and Communications***, 18: 981–1003 (2018).

20. Faisal, M., Hannan, M. A., Ker, P. J., Hussain, A., Mansor, M. B. and Blaabjerg, F., "Review of energy storage system technologies in microgrid applications: Issues and challenges", ***IEEE Access***, 6: 35143-35164 (2018).

21. Guerrero, J. M., Member, S., Vasquez, J. C., Matas, J., Vicuña, L. G. and Castilla, M., "Hierarchical control of droop-controlled AC and DC Microgrids – A general approach toward standardization", ***IEEE Trans. on Industrial Electronics,*** 58 (1): 158–172 (2011).

22. Cagnano, A., De Tuglie, E. and Mancarella, P., "Microgrids: Overview and guidelines for practical implementations and operation", ***Appl Energy***, 258 (2020).

23. Kroposki, B., Pink, C., Basso, T. and DeBlasio, R., "Microgrid standards and technology development", ***Power Engineering Society General Meeting***, ***IEEE***, 1–4 (2007).

24. Unamuno, E. and Barrena, J. A., "Hybrid ac/dc microgrids - Part I: Review and classification of topologies", ***Renew Sustain Energy Rev***, 52 (C): 1251–1259 (2015).

25. Unamuno, E. and Barrena, J. A., "Hybrid AC/DC microgrids - Part II: Review and classification of control strategies", ***Renew Sustain Energy Rev***, 52: 1123-1134 (2015).

26. Mariam, L., Basu, M. and Conlon, M. F., "Microgrid: Architecture, policy and future trends", ***Renew Sustain Energy Rev***, 64: 477–489 (2016).

27. Microgrids: Large Scale Integration of Micro-Generation to Low Voltage Grids", ***ENK5-CT-2002-00610***. 2003–2005 (2005).

28. Bevrani, H., Ghosh, A. and Ledwich, G. "Renewable energy sources and frequency regulation: survey and new perspectives", ***IET Renewable Power Generation***, **4** (5): 438–457 (2010).

29. Mariam, L., Basu, M. and Michael, F., "A Review of Existing Distributed network," ***Architectures Journal of Engineering***, 1–8 (2013).

30. Li, F., Li, R. and Zhou, F., "Microgrid Technology and Engineering Application", ***Elsevier Science***, 198 (2015).

31. Lasseter, R. H. and Piagi, P., "Control and design of microgrid components", Final report, ***University of Wisconsin-Madison, PSERC Publication***, 13–47 (2006).

32. Bevrani, H. "Frequency control in microgrids. Robust Power System Frequency Control", 2nd edition, ***Springer***, Switzerland, 277–301 (2014).

33. Wang, X., Guerrero, J. M., Blaabjerg, F. and Chen, Z., "A Review of Power Electronics Based Microgrids", ***International Journal of Power Electronics***, 12 (1): 181–192 (2012).

34. Byeon, G., Lee, H., Yoon, T., Jang, G., Chae, W., and Kim, J., "A research on the characteristics of fault current of DC distribution system and AC distribution system", ***8th International conference on power electronics. ECCE***, 543–550 (2011).

35. Planas, E., Gil-de-Muro, A., Andreu, J., Kortabarria, I. and Martínez de Alegría, I., "General aspects, hierarchical controls and droop methods in microgrids: a review", ***Renew Sustain Energy Rev***; 17: 147–159 (2013).

36. Hossain, E., Kabalci, E., Bayindir, R., and Perez, R., "Microgrid testbeds around the world: state of art", ***Energy Convers Manage***, 86: 132–153 (2014).

37. Teodorescu, R., "Industrial PhD course on Microgrids "Microgrid Overview", ***Alborg University***, http://www.et.aau.dk (2007).

38. Ding, G., Gao, F. and Zhang, S. "Control of hybrid AC/DC microgrid under islanding operational conditions", ***J. Mod. Power Syst. Clean Energy***, 2: 223–232 (2014).

39. Li, Y. W. and Kao, C. N., "An accurate power control strategy for power-electronics – interfaced distributed generation units operating in a low-voltage multibus microgrid", ***IEEE Transactions on Power Electronics*** 24 (12): 2977–2988 (2009).

40. Alfares, A., Niapour, S. A. and Amirabadi, M., “High frequency AC microgrid based on a highly reliable single-stage converter”, ***IEEE Energy Convers. Congr. Expo***., 2361–2367 (2015).

41. Takahashi, I. and Su, G., “A 500 Hz power system-applications,” ***IEEE IAS***, 996–1002 (1989).

42. Li, X., Ai, X. and Wang, Y., “Study of single-phase HFAC microgrid based on Matlab/Simulink”, ***4th International Conference on Electric Utility Deregulation and Restructuring and Power Technologies (DRPT)***, 1104–1108 (2011).

43. Chakraborty, S., Weiss, M. D. and Simoes, M. G., “Distributed intelligent energy management system for a single-phase high-frequency AC microgrid”, ***IEEE Trans. Ind. Electron.***, 54 (1): 1–13 (2007).

44. Hirose, K., Takeda, T. and Fukui, A., “Field demonstration on multiple power quality supply system in Sendai, Japan,” ***in Proc. EPQU***, 1–6 (2007).

45. Bui, D. M., Lien, K.Y., Chen, Sh. L., Cheng, X. Y. and Lin, M. Sh. “Standards Commonly Used for Microgrids – A Research Project to Develop an Industry Microgrid Standard in Taiwan”, ***Electric Power Components and Systems***, 44: (19) 2143–2160, (2016).

46. Ren, Y. M. and Cao, F. M. “New development and new application of IEC 61850”, ***Proc. Autom. Electr. Power Syst.***, 37: 1–6 (2013).

47. ***IEC 61850-5:2013***. Communication networks and systems in substations – Part 5: Communication requirements for functions and device models (2013).

48. ***IEC 61850-6:2010***. Communication networks and systems for power utility automation – Part 6: Configuration language for communication in electrical substations related to IEDs (2010).

49. ***IEC 61850-8-1:2011***. Communication networks and systems for power utility automation – Part 8-1: Mappings to Specific communication service mapping (SCSM) - Mappings to MMS (ISO 9506-1 and ISO 9506-2) and to ISO/IEC 8802-3 (2011).

50. Ustun, T. S., Ozansoy, C. R. and Zayegh, A., “Modeling of a centralized microgrid protection system and distributed energy resources according to IEC 61850-7-420”, ***IEEE Trans. Power Syst.***, 27: 1560–1567 (2012).

51. Underwriters Laboratories (UL), “UL Standard for Safety for Inverters, Converters, Controllers and Interconnection System Equipment for Use with Distributed Energy Resources”, ***Standard UL 1741***, 2nd ed., (2010).

52. Hawaiian Electric Companies Source Requirement Document Version 1.1 For Certification To UL 1741 ***Supplement SA***, SRD-UL-1741-SA-V1.1 (2017).

53. Dimeas, A., Tsikalakis, A., Kariniotakis, G., and Korres, G., “Microgrids control issues,” ***Wiley-IEEE Press,*** Chichester, 241–307 (2013).

54. Justo, J. J., Mwasilu, F., Lee, J. and Jung, J. W., “AC-microgrids versus DC-microgrids with distributed energy resources: A review”, ***Renew Sustain Energy Rev***, 24: 387–405 (2013).

55. Bidram, A. and Davoudi, A., “Hierarchical structure of microgrids control system”, ***IEEE Trans Smart Grid***; 3 (4): 1963–1976 (2012).

56. Lu, X., Guerrero, J. M., Sun, K., Vasquez, J. C., Teodorescu, R. and Huang, L., “Hierarchical control of parallel AC–DC converter interfaces for hybrid microgrids”, ***IEEE Trans Smart Grid***, 5 (2): 683–692, (2014).

57. Yazdanian, M., and Mehrizi-Sani, A., “Distributed control techniques in microgrids”, ***IEEE Trans Smart Grid,*** 5 (6): 2901–2909 (2014).

58. Vasquez, J., Guerrero, J., Miret, J., Castilla, M., and Vicuna, L., “Hierarchical control of intelligent microgrids”, ***IEEE Ind Electron Mag***, 4 (4): 23–39 (2010).

59. Vandoorn, T. L., Vasquez, J. C., De Kooning, J., Guerrero, J. M., and Vandevelde, L., “Microgrids: hierarchical control and an overview of the control and reserve management strategies,” ***IEEE Ind Electron Mag***, 7 (4): 42–55 (2013).

60. Guerrero, J. M., Chandorkar, M., Lee, T., and Loh, P. C., “Advanced control architectures for intelligent microgrids – Part I: decentralized and hierarchical control,” ***IEEE Trans Ind Electron***, 60 (4): 1254–1262 (2013).

61. Palizban, O. and Kauhaniemi, K., “Hierarchical control structure in microgrids with distributed generation: island and grid-connected mode”, ***Renew Sustain Energy Rev***, 44: 797–813, (2015).

62. Bouzid, A. M., Guerrero, J. M., Cheriti, A., Bouhamida, M., Sicard, P. and Benghanem, M., “A survey on control of electric power distributed generation systems for microgrid applications”, ***Renew Sustain Energy Rev,*** 44: 751–766 (2015).

63. A. Mehrizi-Sani and R. Iravani, “Potential-function based control of a microgrid in islanded and grid-connected models”, ***IEEE Trans. Power Syst.***, 25: 1883–1891 (2010).

64. Rocabert, J., Luna, A., Blaabjerg, F. and Rodríguez, P., “Control of power converters in AC microgrids,” ***IEEE Trans Power Electron***, 27 (11): 4734–4749 (2012).

65. Blaabjerg, F., Teodorescu, R., Liserre, M. and Timbus, A. V., “Overview of control and grid synchronization for distributed power generation systems”, ***IEEE Trans Ind Electron***, 53 (5): 1398–13409 (2006).

66. Green, T. and Prodanović, M., "Control of inverter-based micro-grids", ***Electr Power Syst Res***, 77: 1204–1213 (2007).

67. Palizban, O., Kauhaniemi, K., and Guerrero, J. M., "Microgrids in active network management – Part I: hierarchical control, energy storage, virtual power plants, and market participation", ***Renew Sustain Energy Rev***, 36: 428–439 (2014).

68. Vandoorn, T. L., De Kooning J. D. M., Meersman, B. and Vandevelde, L. "Review of primary control strategies for islanded microgrids with power-electronic interfaces", ***Renew Sustain Energy Rev***, 19: 613–628 (2013).

69. Khadem, S. K., Basu, M. and Conlon, M. F., "Parallel operation of inverters and active power filters in distributed generation system – a review," ***Renew Sustain Energy Rev,*** 15 (9): 5155–5168 (2011).

70. Guerrero, J. M., Hang, L. and Uceda, J., "Control of distributed uninterruptible power supply systems", ***IEEE Trans. Ind. Electron***, 55: 2845–2859 (2008).

71. Cheng, Y. J. and Sng, E. K. K., "A novel communication strategy for decentralized control of paralleled multi-inverter systems," ***IEEE Trans. Power Electron***, 21: 148–156 (2006).

72. S. Sun, L. K. Wong, Y. S. Lee and D. Xu, "Design and analysis of an optimal controller for parallel multi-inverter systems," ***IEEE Trans. Circuit Syst****. II*, 52: 56–61 (2006).

73. Wu, T., Sir,i K. and Banda, J., "The central-limit control and impact of cable resistance in current distribution for parallel-connected DC–DC converters", ***IEEE power electronics specialists conference, PESC'94***, 694–702 (1994).

74. Banda, J. and Siri, K., "Improved central-limit control for parallel-operation of DC-DC power converters", ***The 26th annual IEEE power electronics specialists conference, PESC'95 Record***, 1104–1110 (1995).

75. Kawabata, T. and Higashino, S., "Parallel operation of voltage source inverters", ***IEEE Trans Ind,*** 24: 281–287 (1988).

76. Emadi, A., Nasiri, A. and Bekiarov, S., "Uninterruptible power supplies and active filters", ***CRC Press,*** 272 (2004).

77. Cai, N. and Mitra, J., "A decentralized control architecture for a microgrid with power electronic interfaces", ***Proceedings of the North American power symposium (NAPS)***, 1–8 (2010).

78. Pascual, M., Garcera, G., Figueres, E. and Gonzalez-Espin, F., "Robust model-following control of parallel UPS single-phase inverters", ***IEEE Trans Ind Electron,*** 55: 2870–2883 (2008).

79. Chen, C., Wang, Y., Lai, J., Lee, Y. and Martin, D., "Design of parallel inverters for smooth mode transfer microgrid applications. ***IEEE Trans Power Electron***, 25: 6–15 (2010).

80. Mark, C. and Bolster, L., "Bus-tie synchronization and load share technique in a ring bus system with multiple power inverters", ***IEEE Applied Power Electron. Conf., APEC***, 871–874, (2005).

81. Wu, D., Tang, F., Dragicevic, T., Vasquez, J. C., and Guerrero, J. M., "A Control Architecture to Coordinate Renewable Energy Sources and Energy Storage Systems in Islanded Microgrids", ***Smart Grid, IEEE Transactions on***, 6 (3): 156–1166 (2015).

82. Lee, C., Chu, C. and Cheng, P., "A new droop control method for the autonomous operation of distributed energy resource interface converters", ***IEEE Trans Power Electron***, 28 (4): 1980–1993 (2013).

83. Zhang, M., Du, Z., Lin, X. and Chen, J., "Control strategy design and parameter selection for suppressing circulating current among SSTs in parallel", ***IEEE Trans Smart Grid***, 6 (4): 1602–1609 (2015).

84. De Brabandere, K., Bolsens, B., Vanden Keybus, J., Woyte, A., Driesen, J. and Belmans, R., "A three-phase voltage and frequency droop control scheme for parallel inverters", ***IEEE Trans Power Electron***, 22 (4): 1107–1115 (2007).

85. Vandoorn, T. L., Guerrero, J. M., de Kooning D. M., Vasquez J. C., and Vandevelde L., "Decentralized and centralized control of islanded microgrids including reserve management", ***IEEE Ind Electron Mag,*** 1–14 (2013).

86. Pogaku, N., Prodanovic, M. and Green, T. C., "Modeling, analysis and testing of autonomous operation of an inverter-based microgrid", ***IEEE Trans Power Electron***, 22: 613–625 (2007).

87. Diaz, G., Gonzalez-Moran, C., Gomez-Aleixandre, J. and Diez, A. "Scheduling of droop coefficients for frequency and voltage regulation in isolated microgrids", ***IEEE Trans Power Syst,*** 25: 489–496 (2010).

88. Lopes, J. A. P., Moreira, C. L. and Madureira, A. G., "Defining control strategies for microgrids islanded operation", ***IEEE Trans Power Syst***, 21: 916–924 (2006).

89. Sao, C. K. and Lehn, W. "Control and power management of converter fed microgrids", ***IEEE Trans Power Syst,*** 23: 1088–1098 (2008).

90. Rokrok, E. and Golshan, M. E. H., "Adaptive voltage droop method for voltage source inverters in an islanded multibus microgrid," ***IET Gen Trans Dist*** 4 (5): 562–578 (2010).

91. Borup, U., Blaabjerg, F. and Enjeti, P. N., “Sharing of nonlinear load in parallel-connected three-phase converters,” ***IEEE Trans Ind Appl***, 37: 1817–1823 (2001).

92. Zhong, Q. C., “Harmonic droop controller to reduce the voltage harmonics of inverters”, ***IEEE Trans Ind Electron***, 60: 936–945 (2013).

93. Madureira, A., Moreira, C. and Lopes, J., “Secondary load-frequency control for microgrids in islanded operation,” ***Proc ICREPQ***, 1–5 (2005).

94. Yuen, C., Oudalov, A. and Timbus, A., “The provision of frequency control reserves from multiple microgrids,” ***IEEE Trans Ind Electron***, 58 (1): 173–83 (2011).

95. Zamora, R. and Srivastava, A. K., “Controls for microgrids with storage: review, challenges, and research needs,” ***Renew Sustain Energy Rev***, 14 (7): 2009–2018 (2010).

96. Jovcic, D., “Phase locked loop system for FACTS,” ***IEEE Trans Power Syst***, 18: 1116–1124 (2003).

97. Tsikalakis, A. G. and Hatziargyriou, N. D., “Centralized control for optimizing microgrids operation”, ***IEEE Power Energy Soc. Gen. Meet***, 1–8 (2011).

98. Vaccaro, A., Popov, M., Villacci, D. and Terzija, V., “An integrated framework for smart microgrids modeling, monitoring, control, communication, and verification”, ***Proc IEEE***, 99: 119–32 (2011).

99. Shafiee, Q., Guerrero, J. M. and Vasquez, J., “Distributed secondary control for islanded MicroGrids – A Novel Approach”, ***IEEE Trans Power Electron***, 29: 1018–1031 (2014).

100. Liang, H., Choi, B. J., Zhuang, W., Shen, X., Awad aSa and Abdr A., “Multiagent coordination in microgrids via wireless networks”, ***IEEE Wirel Commun,*** 19: 14–22 (2012).

101. Shafiee, Q., Dragicevic, T., Andrade, F., Vasquez, J. C., and Guerrero, J. M., “Distributed consensus-based control of multiple DC-microgrids clusters”, ***IEEE industrial electronics society***, 2056–2062 (2014).

102. Simpson-Porco, J., Shafiee, Q., Dorfler, F., Vasquez, J.C., Guerrero, J., and Bullo, F., “Secondary frequency and voltage control of islanded microgrids via distributed averaging”, ***IEEE Trans Ind Electron***, 0046: (no.c) (1–1) (2015).

103. Huang, P., Liu, P., Xiao, W., and El Moursi, M. S., “A novel droop-based average voltage sharing control strategy for DC microgrids”, ***IEEE Trans Smart Grid,*** 6 (3): 1096–2106 (2015).

104. Lu, X., Guerrero, J.M., Sun, K., and Vasquez, J. C., "An improved droop control method for DC microgrids based on low bandwidth communication with DC bus voltage restoration and enhanced current sharing accuracy", ***IEEE Trans Power Electron***, 29 (4): 1800–1812 (2014).

105. Guo, F., Wen, C., Mao, J. and Song, Y-D., "Distributed secondary voltage and frequency restoration control of droop-controlled inverter-based microgrids", ***IEEE Trans Ind Electron***, 0046 (no.c) (1–1) (2014).

106. Chandorkar, M. C., Divan, D. M. and Adapa, R., "Control of parallel connected inverters in standalone AC supply systems", ***IEEE Trans Ind***. 29 (1): 136–43 (1993).

107. Diaz, N. L., Dragicevic, T., Vasquez, J. C. and Guerrero, J. M., "Intelligent distributed generation and storage units for DC microgrids – a new concept on cooperative control without communications beyond droop control", ***IEEE Trans Smart Grid,*** 5 (5): 2476–2485 (2014).

108. Katiraei, F., and Iravani, M.R., "Power management strategies for a microgrid with multiple distributed generation units", ***IEEE Trans Power Syst***, 21 (4): 1821–1831 (2006).

109. Ahn, C. and Peng, H., "Decentralized voltage control to minimize distribution power loss of microgrids", ***IEEE Trans Smart Grid***, 4 (3): 1297–1304 (2013).

110. De Brabandere, K., Vanthournout, K., Driesen, J., Deconinck, G., and Belmans, R., "Control of microgrids," ***IEEE power engineering society general meeting (PES)***, 1–7 (2007).

111. Lasseter, R. H. and Paigi, P., "Microgrid: A Conceptual Solution", ***Proceedings of the 2004 Power Electronics Specialists Conference (PESC'04)***, 4285–4290 (2004).

112. Mahmoud, M., Hussain, S. A. and Abido, M., "Modeling and control of microgrid: an overview", ***Journal of Franklin Institute***, 351 (5): 2822–2859 (2014).

113. Majumder, R., "Some aspects of stability in microgrids", ***IEEE Trancactions on Power Systems***, 28 (3): 3243–3252 (2003).

114. Jiayi, H., Chuanwen, J. and Rong, X., "A review on distributed energy resources and MicroGrid", ***Renewable and Sustainable Energy Reviews***, 12: 2472–2483 (2008).

115. Tang, X., Deng, W. and Qi, Z, "Investigation of the dynamic stability of microgrid", ***IEEE Transactions on Power Systems***, 29 (2): 698–706 (2014).

116. Bevrani, H., Francois, B. and Ise, T., "Microgrid dynamics and control", ***John Willey and Sons, Inc.***, 220–238 (2017).

117. Erdogdu, E., “On the wind energy in Turkey”, ***Renewable and Sustainable Energy Reviews***, 13: 1361–1371 (2009).

118. Ilhan, A. and Bilgili, M. “An Overview of Turkey’s Offshore Wind Energy Potential Evaluations”, ***Turkish Journal of Scientific Reviews***, 9 (2): 55–58 (2016).

119. Li, P., “Design and control of a PV active generator with integrated energy storages: application to the aggregation of producers and consumers in an urban micro smart grid”, PhD thesis, ***Ecole Centrale de Lille***, France, 97-105 (2010).

120. Fathima, A. H., Prabaharan, N., Palanisamy, K., Kalam, A., Mekhilef, S. and Justo, J. J.,_”Hybrid-renewable energy systems in microgrids”, ***Woodhead Publishing***, 267 (2018).

121. Park, R. H., “Two-reaction theory of synchronous machines”, ***American Institute of Electrical Engineers, Transactions of the***, 48: 716–727 (1929).

122. Anderson, P. M., and Fouad, A. A., “Power System Control and Stability”, Second Edition, ***John Wiley and Sons, Inc.***, New York, 553 (2003).

123. Xiao, W., Dunford, W.G., and Capel, A., “A Novel Modeling Method for Photovoltaic Cells”, ***IEEE Power Electrics Specialists Conference***, 1950–1956 (2004).

124. Saadat, S. H., Shawn, R. and Spyker R. M., “A method for predicting PV module and array performance at other than standard reporting conditions”, ***IEEE Transactions on Aerospace and Electronic Systems***, 36 (4): 527–569 (1999).

125. Jordehi, A. R., “Maximum power point tracking in photovoltaic systems: A review of different approaches”, ***Renewable and Sustainable Energy Reviews***, 65: 1127–1138 (2016).

126. Freeman, D., “Introduction to Photovoltaic Systems Maximum Power Point Tracking”, ***Texas Instruments Application Report SLVA446*** (2010).

127. Singh, S., Mathew, L. and Shimi, S. L., “Design and simulation of intelligent control MPPT technique for PV module using MATLAB/SIMSCAPE”, ***International Journal of Advanced Research in Electrical, Electronics and Instrumentation Engineering (IJAREEIE)***, 2 (9): 4554–4565 (2013).

128. Durr, M., Cruden, A., Gair, S. and McDonald, J. R., “Dynamic model of a lead acid battery for use in a domestic fuel cell system”, ***J. Power Sour.***, 161: 1400–1411 (2006).

129. Barsali, S., and Ceraolo, M., “Dynamical models of lead-acid batteries: implementation issues”, ***IEEE Trans. Energy Conv.***, 17 (1): 16–23 (2002).

130. Gergaud, O., Robin, G., Multon, B., and Ahmed, B. “Energy modelling of a lead-acid battery within hybrid wind/photovoltaic systems”, ***SATIE – Brittany Branch, EPE*** (2003).

131. Vasquez, J. C., Guerrero, J. M., Savaghebi, M., Eloy-Garcia, J. and Teodorescu, R., “Modeling, analysis, design of stationary-reference-frame droop-controlled parallel three-phase voltage source inverters”, ***IEEE Trans. Ind. Electron***, 60 (4): 1271–1280 (2013).

132. Ding, F., Li, P., Huang, B., Gao, F., Ding, C. and Wang, C., “Modeling and simulation of grid-connected hybrid photovoltaic/battery distributed generation system”, in ***Proceedings of the China International Conference on Electricity Distribution (CICED ’10)***, 1–10 (2010).

133. Zhong, Q. C. and Zeng, Y., “Universal Droop Control of Inverters with Different Types of Output Impedance”, ***IEEE Access***, 4: 702–712 (2016).

134. Saeedimoghadam, M. and Dehghani, M., “Static switch in microgrids”, ***International Research Journal of Applied and Basic Sciences***, 7 (2): 95–99 (2013).

135. Sannino, A., “Static transfer switch: analysis of switching conditions and actual transfer time”, ***IEEE Power Engineering Society Winter Meeting***, 1: 120–125 (2001).

136. Piagi P. and Lasseter, R. H., “Autonomous control of microgrids,” ***IEEE Power Engineering Society General Meeting***, 8–13 (2006).

137. Meng, L., Savaghebi, M., Andrade, F., Vasquez, J. C., Guerrero, J. M. and Graells, M., “Microgrid central controller development and hierarchical control implementation in the intelligent microgrid lab of Aalborg University,” ***IEEE Applied Power Electronics Conference and Exposition (APEC)***, 2585–2592 (2015).

138. He, L., Wei, Z., Yan, H., Xu, K.-Y., Zhao, M. and Cheng, S., “A Day-ahead Scheduling Optimization Model of Multi-Microgrid Considering Interactive Power Control,” ***4th International Conference on Intelligent Green Building and Smart Grid (IGBSG)***, 666–669 (2019).

139. Che, L., Shahidehpour, M., Alabdulwahab, A. and Al-Turki, Y., “Hierarchical coordination of a community microgrid with AC and DC microgrids,” ***IEEE Trans. Smart Grid***, 6 (6): 3042–3051 (2015).

140. Ni, K., Wei, Z., Yan, H., Xu, K.-Y., He, L. J. and Cheng, S., “Bi-level Optimal Scheduling of Microgrid with Integrated Power Station Based on Stackelberg Game,” ***4th International Conference on Intelligent Green Building and Smart Grid (IGBSG)***, 278–281 (2019).

141. Mírez, J., “A modeling and simulation of optimized interconnection between DC microgrids with novel strategies of voltage, power and control,” ***IEEE Second International Conference on DC Microgrids (ICDCM)***, 536–541 (2017).

142. Jin, Z., Savaghebi, M., Vasquez, J. C., Meng, L. and Guerrero, J. M., “Maritime DC microgrids-a combination of microgrid technologies and maritime onboard power system for future ships,” ***IEEE 8th International Power Electronics and Motion Control Conference (IPEMC-ECCE Asia)***, 179–184 (2016).

143. Abu-Elzait S. and Parkin, R., “Economic and Environmental Advantages of Renewable-based Microgrids over Conventional Microgrids”, ***IEEE Green Technologies Conference (GreenTech)***, 1–4 (2019).

144. “IEEE Draft Standard for the Specification of Microgrid Controllers”, ***IEEE P2030.7/D11***, 1–42 (2017).

145. Saleh, M. S., Althaibani, A., Esa, Y., Mhandi, Y. and Mohamed, A. A., “Impact of clustering microgrids on their stability and resilience during blackouts”, ***International Conference on Smart Grid and Clean Energy Technologies (ICSGCE)***, 195–200 (2015).

146. Li, B., Bao, H. and Guo, L., “Strategy of energy storage control for islanded microgrid with photovoltaic and energy storage systems”, ***Autom. Electr. Power Syst.*** 34 (3): 8–15 (2014).

147. Zhang, Y., Guo, L., Jia, H. and Wang, C., “An energy management method of hybrid energy storage system based on smoothing control”, ***Autom. Electr. Power Syst.***, 36 (16): 36–41 (2012).

148. Ozel, O., Shahzad, K. and Ulukus, S., “Optimal energy allocation for energy harvesting transmitters with hybrid energy storage and processing cost”, ***IEEE Trans. Signal Process***, 62 (12): 3232–3245 (2014).

149. Shim, J. W., Cho, Y., Kim, S.-J., Min, S. W. and Hur, K., “Synergistic control of SMES and battery energy storage for enabling dispatchability of renewable energy sources”, ***IEEE Trans. Appl. Supercond***, 23 (3): 3547–3552 (2013).

150. Taj, T. A., Hasanien, H. M., Alolah, A. and Muyeen, S. M., “Transient stability enhancement of a grid-connected wind farm using an adaptive neuro-fuzzy controlled-flywheel energy storage system”, ***IET Renew. Power Gener***., 9 (7): 792–800 (2015).

151. Goncalves de Oliveira, J., Schettino, H., Gama, V., Carvalho, R. and Bernhoff, H., “Study on a doubly-fed flywheel machine-based driveline with an AC/DC/AC converter”, ***IET Electr. Syst. Transp***. 2 (2): 51–57 (2012).

152. Xiong, Q., Liao, Y. and Yao, J., "Active power smoothing control of direct-driven permanent magnet synchronous wind power generation system with flywheel energy storage unit", ***Autom. Electr. Power Syst***. 33 (5): 97–105 (2013).

153. Liu, S., Sun, H., Gu, M. and Wen, J., "Novel structure and operation control of a flywheel energy storage system associated to wind generator connected to power grid", ***Trans. China Electrotech. Soc***. 27 (4): 248–254 (2012).

154. Dragicevic, T., Sucic, S., Vasquez, J. C. and Guerrero, J. M., "Flywheel-based distributed bus signalling strategy for the public fast charging station", ***IEEE Trans. Smart Grid*** 5 (6): 2825–2835 (2014).

155. Zhang, Y., Xu, Y., Guo, H., Zhang, X., Guo, C. and Chen, H., "A hybrid energy storage system with optimized operating strategy for mitigating wind power fluctuations", ***Renew. Energy*** 125: 121–132 (2018).

156. Bracco, S., Dentici, G. and Siri, S., "Economic and environmental optimization model for the design and the operation of a combined heat and power distributed generation system in an urban area", ***Energy***, 55 (0): 1014–1024 (2013).

157. Bahramara, S., Moghaddam, M. P. and Haghifam, M. R., "Optimal planning of hybrid renewable energy systems using HOMER: a review", ***Renew Sustain Energy Rev***, 62: 609–20 (2016).

158. Hafez, O. and Bhattacharya, K., Optimal planning and design of a renewable energy based supply system for microgrids, ***Renew. Energy***, 45: 7–15 (2012).

159. Ismail, M. S., Moghavvemi, M. and Mahlia, T. M. I., "Techno-economic analysis of an optimized photovoltaic and diesel generator hybrid power system for remote houses in a tropical climate", ***Energy Convers. Manag***. 69: 163–173 (2013).

160. Baneshi, M. and Hadianfard, F., "Techno-economic feasibility of hybrid diesel/PV/ wind/battery electricity generation systems for non-residential large electricity consumers under southern Iran climate conditions", ***Energy Convers. Manag***. 127: 233–244 (2016).

161. Halabi, L. M., Mekhilef, S., Olatomiwa, L. and Hazelton, J., "Performance analysis of hybrid PV/diesel/battery system using HOMER: a case study Sabah, Malaysia", ***Energy Convers. Manag***. 144: 322–339 (2017).

162. Shahzad, M. K., Zahid, A., Rashid, T. M., Rehan, A., Ali, M. and Ahmad, M., "Techno-economic feasibility analysis of a solar-biomass off grid system for the electrification of remote rural areas in Pakistan using HOMER software", ***Renew. Energy***, 106: 264–273 (2017).

163. Akhtari, R. M., Shayegh I. and Karimi, N., "Techno-economic assessment and optimization of a hybrid renewable earth-air heat exchanger coupled with electric boiler, hydrogen, wind and PV configurations", ***Renew Energy***, 148: 839–851 (2020).

164. Al Garni, H. Z., Awasthi A. and Ramli, M. A. M., "Optimal design and analysis of grid-connected photovoltaic under different tracking systems using HOMER", ***Energy Conversion and Management*** 155: 42–57 (2018).

165. Anderson, W., Kobold, K. and Yakimenko, O., "Tools for Analysis and Optimization of Standalone Green Microgrids", World Academy of Science, ***Engineering and Technology International Journal of Energy and Power Engineering,*** 12 (6): 398–405 (2018).

166. Sen, R., and Bhattacharyya S. C., "Off-grid electricity generation with renewable energy technologies in India: An application of HOMER", ***Renewable Energy,*** 62: 388–398 (2014).

167. Erdogdu, E., "On the wind energy in Turkey", ***Renewable and Sustainable Energy Reviews***, 13 (6-7): 1361–1371 (2009).

168. İlhan, A., and Bilgili, M., "An Overview of Turkey's Offshore Wind Energy Potential Evaluations", ***Türk Bilimsel Derlemeler Dergisi***, (2): 55–58 (2016).

169. http://www.yegm.gov.tr

170. Tabak A., Ozkaymak, M., Guneser, M. T. and Erkol, H. O., "Optimization and evaluation of hybrid PV/WT/BM system in different initial costs and LPSP conditions", ***International Journal of Advanced Computer and Science***, 8 (11): 123–131 (2017).

171. Web site of Turkish State Meteorological Service. **https://www.mgm.gov.tr/veridegerlendirme/il-ve-ilceler-istatistik.aspx?m=KARABUK** (2018).

172. Lambert, T., Gilman, P. and Lilienthal, P., "Micropower system modelling with HOMER, *In: FA Farret, and M. Godoy Simões editors*. Integration of alternative sources of energy. ***Wiley-IEEE Press***, United States, 379–418 (2006).

173. Parra, D., Gillott, M., Norman, S. A. and Walker, G. S., "Optimum community energy storage system for PV energy time-shift", ***Appl Energy,*** 137: 576–87 (2015).

174. HOMER Energy, NREL. Available from: ***http://www.homerenergy.com*** (2019).

175. ***Federal energy regulatory commission***. Assessment of demand response & advanced metering (2012).

176. Xiang, Y., Cai, H., Gu, Ch., Shen, X., “Cost-benefit analysis of integrated energy system planning considering demand response”, ***Energy***, 192: 1–15 (2020).

177. Yan, X., Hu, Y., Hu, Z., “A review on price-driven residential demand response”, ***Renew Sustain Energy Rev,*** 96: 411–419 (2018).

178. Doug, H., Peterson, P., “Demand Response as a Power System Resource. Program Designs, Performance, and Lessons Learned in the United States”, ***Whited, Melissa***, Edited by RAP (2013).

179. Issi, F., and O. Kaplan, ”Determination of Load Profiles and Power Consumptions of Home Appliances”, ***Energies***, 11 (3): 1–18 (2018).

APPENDIX A.

TECHNICAL SPECIFICATIONS OF KBU SUBSTATION AND DISTRIBUTION CENTER TRANSFORMERS

Table A.1. Technical specification of the KBU substation transformer TR 6.

Power of Transformer, S_{rQT}	75 MVA
Primary Voltage of Transformer, U_{nQ}	154 kV
Secondary Voltage of Transformer, U_{rQTLV}	34.5 kV
Short circuit power, S_k	7256 MVA
Relative Short circuit voltage, $\%U_k$	11.33
Relative Ohmic Short circuit voltage, $\%U_r$	0.7
Nominal Voltage, U_n	34.5 kV

Table A.2. Technical specification of the distribution center transformer.

Transformer Power of Distribution center, S_{rT1}	7600 kVA
Primary Voltage of Transformer in Distribution center, U_{rT1HV}	34.5 kV
Secondary Voltage of Transformer in Distribution center, U_{rQTLV}	0.4 kV
Relative Short circuit voltage, $\%U_{krT}$	3.9
Copper Loss on Load, P_{krT}	8 kW
Nominal Voltage, U_n	0.4 kV

APPENDIX B.

TECHNICAL CHARACTERISTICS OF PV SYSTEM, BATTERY AND DIESEL GENERATOR

Table B.1. Technical specifications of PV panel CWT300-72M.

Electrical Performance							
Model type	CWT300-72M						
Power output	P_{max}	W	300	310	320	330	350
Modul effectivity		%	15.39	15.90	16.42	16.93	17.96
Voltage at P_{max}	Vmpp	V	36.5	37.1	37.7	38.1	38.7
Current at P_{max}	Impp	A	8.22	8.36	8.49	8.67	9.05
×Open-circuit Voltage	Vdc	V	44.6	45.4	44.9	45.5	47.5
Short-circuit current	Idc	A	8.74	8.89	9.04	9.24	9.53
Power output tolerance	ΔPmax	W	0 – 5				
Max. system DC voltage	V_{dc}	V	1000				
Operating temperature range	T_{op}	C^0	-40$C^0$to 85C^0				
Limiting reverse current	$I_{max.res}$	A	15				

Mechanical characteristics	
Front cover (material /thickness)	Low-iron tempered glass /3.2mm
Back shell (color)	White
Cell (quantity /material/dimensions)	72 /polycrystalline silicon /156 mm x 156 mm
Junction box (protection degree)	IP67
Cables &Plug connectors	900mm/400mm^2& MC4 compatible/IP67
Module Dimensions (L/W/H)	1959 mm × 995 mm ×40 mm
Module Weight	25.5Kg

TERMAL characteristics			
Nominal operating cell tempreture	N_{OCT}	℃	45±2
Temperature Coefficient of Pmax	λ	%/℃	-0.45
Temperature Coefficient of Voc	β_{Voc}	%/℃	-0.34
Temperature Coefficient of Isc	α_{Isc}	%/℃	0.06
Temperature Coefficient of Vmpp	β_{Vmpp}	%/℃	-0.40

Table B.2. Technical specification of battery MUTLU 6OPzS-300.

U=1.83 V/Cell
Discharge Current (A)

15 min	30 min	1 h	2 h	3 h	4 h	5 h	6 h	8 h	10 h
185	158	124	88.5	68	56.4	48	42.3	34.4	28.2

U=1.80V/Cell
Discharge Current (A)

15 min	30 min	1 h	2 h	3 h	4 h	5 h	6 h	8 h	10 h
218	180	146	92	71	58	50	44	36	30

U=1.75 V/Cell
Discharge Current (A)

15 min	30 min	1 h	2 h	3 h	4 h	5 h	6 h	8 h	10 h
220	207	155	100	76	62	53.5	46	36.8	31

U=1.70 V/Cell
Discharge Current (A)

15 min	30 min	1 h	2 h	3 h	4 h	5 h	6 h	8 h	10 h
289	225	160	105	79	64	55	47	37	31.2

Table B.3. Technical Data of Inverter ABB TRIO-50.

Input side	
Absolute maximum DC input voltage ($V_{max.abs}$)	1000 V
Start- up DC input Voltage (V_{start})	420…700 V (Default 420 V)
Operating DC input Voltage rang (V_{dcmin}…V_{dcmax})	0.7xV_{start}… 950 V (min 300 V)
Rated DC input voltage (V_{dcr})	610 V_{DC}
Number of independent MPPT	1
MPPT input DC Voltage range ($V_{MPPTmin}$…$V_{MPPTmax}$) at P_{dcr}	480 – 800 V_{DC}
Maximum DC input current (I_{dcmax})	108 A
Maximum input short circuit current	160 A
Number of DC input pairs	12 (-SX/-SY); 16 (-SX)
Input protection	
Reverse polarity protection	Yes; from limited current source
Input over voltage protection for each MPPT – varistor	Yes; 2

Table B.4. Technical Data of Inverter ABB TRIO-50 (continued).

Input over voltage protection for each MPPT – plug in modular surge arrester	Type; 2 (-SX version)/ Type +2 (-SY version)
Photovoltaic array isolation control	According to local standard
DC switch rating for each MPPT	200 A/ 1000 A
Fuse rating (version with fuses)	15 A / 1000 A
Output side	
AC grid connection type	Three-phase (3W+PE or 4W+PE)
Rated AC power (P_{acr} @$\cos\emptyset = 1$)	50000 W
Maximum AC output power (P_{acmax} @$\cos\emptyset = 1$)	50000 W
Maximum apparent power (S_{max})	50000 VA
Rated AC grid voltage ($V_{ac.r}$)	400 V
AC Voltage range	320…480 V
Maximum AC output current ($I_{ac.max}$)	77A
Contributory fault current	92 A
Rated output frequency range ($f_{.r}$)	50Hz/ 60Hz
Output frequency range ($f_{min…}f_{max}$)	47…53 Hz/ 57…63 Hz
Nominal power factor and adjustable range	> 0.995; 0 ... 1 inductive /capacitive with maximum S_{max}
Total current harmonic distortion	$< 3\%$
Operating performance	
Maximum efficiency (η_{max})	98.3%
Weighted efficiency (EURO/CE C)	98.0 %
Communication	
Remote monitoring	VSN300 Wi-fi logger card
Wireless local monitoring	VSN300 Wi-fi logger card
User interface	LEDs Display (option)
Communication interface	2(RS485)
Physical	
Environmental protection rating	IP65 (IP54 for cooling section)
Cooling	Forced air
Dimension (H x W x D)	750 mm x 1491 mm x 315mm

APPENDIX C.

LOAD PROFILE OF ENGINEERING FACULTY

Table C.1. Load profile of Engineering faculty.

-2.Floor		
Electric panel	**Demand power, kW**	**Total power, kW**
1	**2**	**3**
BBKP	6.51	9.31
BBKUP	3.40	4.85
DBKP	7.96	11.38
Total	**17.87**	**25.53**
A Block (-1. Floor)		
BZAKP	6.87	9.81
BZAKUP	3.40	4.85
FZKAP	17.51	25.02
DZAKP	7.67	10.95
Total	**35.44**	**50.63**
Decanoate (-1.Floor)		
DZKP	25.34	36.20
DZKUP	7.70	11.00
BZKP	6.20	8.86
AZKP	30.25	43.21
AZKUP	55.76	79.65
CZKP	24.99	35.71
CZKUP	11.52	16.45
Total	**161.75**	**231.08**
First Floor		
C1KP	28.64	40.92
C1KUP	13.16	18.80
A1KP	17.44	24.91
A1KUP	7.00	10.00
B1KP	5.15	7.36
D1K1P	15.52	22.17
D1K1UP	6.83	9.75
D1K2P	15.06	21.51
D1K2UP	7.39	10.55
Total	**116.18**	**165.97**
Second Floor		
A2KP	6.06	8.65
A2KUP	7.00	10.00
B2KP	5.87	8.38
C2KP	17.05	24.36
C2KUP	7.00	10.00

Table 1 Appendix C. Load profile of Engineering faculty (cont.).

1	2	3
D2K1P	15.52	22.17
D2K1UP	6.83	9.75
Third Floor		
A3KP	7.56	10.80
A3KUP	7.00	10.00
B3KP	5.87	8.38
C3KP	17.05	24.36
C3KUP	7.00	10.00
D3K1P	15.52	22.17
D3K1UP	6.83	9.75
D3K2P	14.64	20.91
D3K2UP	7.39	10.55
Total	**88.84**	**126.92**
Fourth Floor		
A4KP	17.95	25.64
A4KUP	8.68	12.40
B4KP	6.70	9.56
C4KP	17.74	25.34
C4KUP	8.68	12.40
D4K1P	8.67	12.38
D4K1UP	4.83	6.90
D4K2P	9.74	13.91
D4K2UP	5.08	7.25
Total	**88.05**	**125.79**
Student's Refectory (with electric meter)		
Monthly average	34.06	48.66
Personal's Refectory (with electric meter)		
Monthly average	28.75	41.07
Total for Engineering Faculty	**657.94**	**939.91**

APPENDIX D.

CRITICAL LOADS OF ENGINEERING FACULTY

Table D.1. Critical loads list of Engineering faculty.

Name	**Power, kW**	**Pieces**	**Total power, kW**	**Daily hours**	**Working hours in a year**	**Consumption, kWh**
Heating pump	10	1	10	24	4872	48720
Booster pump	5.5	3	16.5	24	4872	80388
Circulation pump	1.4	2	2.8	24	4872	13642
VRF pump	18	1	18	5	345	6210
Outdoor lighting	0.07	20	1.4	11	4015	5621
Indoor lighting	0.05	10	0.5	24	8760	4380
Data Center	0.5	1	0.5	24	8760	4380
Fire-alarm system	0.3	1	0.3	24	8760	2628
Wi-Fi modems	0.05	7	0.35	24	8760	3066
Total	**35.87**		**50.35**			**169 035**

APPENDIX E.

UTILITY MONTHLY SUMMARY COMPARISON

Table E.1. Utility monthly summary comparison.

Current system.

Month	Energy Purchased (kWh)	Energy Sold (kWh)	Net Energy Purchased (kWh)	Peak Load (kW)	Energy Charge	Total
January	74,940	0	74,940	282	$17,236	$17,236
February	65,228	0	65,228	314	$15,002	$15,002
March	75,370	0	75,370	312	$17,335	$17,335
April	39,962	0	39,962	295	$9,191	$8,411
May	70,354	0	70,354	272	$16,181	$16,181
June	75,075	0	75,075	290	$17,267	$17,267
July	76,394	0	76,394	302	$17,571	$17,571
August	81,644	0	81,644	292	$18,778	$18,778
September	72,025	0	72,025	300	$16,566	$16,566
October	75,383	0	75,383	293	$17,338	$16,080
November	72,388	0	72,388	272	$16,649	$16,153
December	73,155	0	73,155	289	$16,826	$16,426
Annual	851,918	0	851,918	314	$195,941	$193,007

Proposed system.

Month	Energy Purchased (kWh)	Energy Sold (kWh)	Net Energy Purchased (kWh)	Peak Load (kW)	Energy Charge	Total
January	64,040	243	63,797	282	$14,673	$14,673
February	53,839	235	53,604	314	$12,329	$12,329
March	60,984	103	60,882	312	$14,003	$14,003
April	31,545	92.3	31,453	295	$7,234	$6,452
May	54,237	158	54,079	272	$12,438	$12,438
June	58,114	190	57,924	290	$13,323	$13,323
July	58,398	196	58,202	302	$13,386	$13,386
August	64,495	112	64,383	292	$14,808	$14,808
September	57,206	81.3	57,125	300	$13,139	$13,139
October	61,329	228	61,101	293	$14,053	$12,792
November	61,371	186	61,185	272	$14,073	$13,575
December	62,383	140	62,243	289	$14,316	$13,915
Annual	687,941	1,964	685,978	314	$157,775	$154,833

APPENDIX F.

PUBLISHED PAPERS

ESCI-indexed Journal

Issa, Z. Yusupov, N. Almagrahi, "Development of MAS based distributed intelligent control strategy for microgrid," *Ciência e Técnica Vitivinícola*, pp. 167-180, 2019.

International Coferences

1. Arifjanov, A., Zakhidov, R., and Almagrahi, N., "Comparative Analysis of the Distributed Energy Resources Connections to Distribution Network", *International Conference on Advanced Technologies, Computer Engineering and Science (ICATCES'18),* May 11-13, 2018 Safranbolu, Turkey, pp.276-281 (2018)
2. Yusupov, Z., Izzatillaev, J., Almagrahi, N., "The deployment of smart grid as an emerging power system in Uzbekistan", 1st International Conference on Energy System Engineering (ICESE-2017) (2017)
3. Yusupov, Z., Guneser, M. T., Almagrahi, N., "The Deployment of Microgrid as an Emerging Power System in Uzbekistan", International Conference on Advanced Technologies and Sciences (ICAT'16), Konya, pp. 889 – 892 (2016)

RESUME

Nuri Almargani Ali ALMAGRAHI was born in Tripoli (Libya) in 1960 and he graduated first and elementary education in this city. He completed high school education in Ben Gasher. He graduated Master program in High University Department of Electric-Electronics in Odessa (Ukraine), 1986. Then in 1988, he started working at Electronic Research Center in Libya Research Assistant. From 2000 he teched at High Education institute at Department of Electric-Electronics. He started his Ph.D education program at Karabük University in Department of Electrical-Electronics.

CONTACT INFORMATION

Address: Karabük University
Graduate School of Natural & Applied Science
Demir-Çelik Campus/KARABUK
E-mail : nuri_almagrhy@yahoo.com
Tel. : +90-5445373207